Characterization of emerin LEM-domain missense mutations present in patients with exclusive atrial cardiac defects

Nada Essawy

Characterization of emerin LEM-domain missense mutations present in patients with exclusive atrial cardiac defects

Submitted by: Nada Essawy

July 2018

A thesis submitted in the fulfilment of the requirements for the degree of
Doctor of Philosophy

In agreement with the co-tutelle between
Ecole Doctorale 515 "Complexité du Vivant", Université Pierre et Marie Curie
Department of Biology, Chemistry and Pharmacy, Freie Universität

Thesis defense committee:

Dr Catherine Coirault (Thesis co-supervisor)	Institut de Myologie, Paris
Prof Simone Spuler (Thesis co-supervisor)	Freie Universität, Berlin
Dr Vincent Gache (Reviewer)	Université Claude Bernard Lyon 1, Lyon
Dr François Lallemand (Reviewer)	Institut Curie, Paris
Prof Sigmar Stricker (Reviewer)	Freie Universität, Berlin
Dr Maria Reichenbach (FU Postdoc)	Freie Universität, Berlin
Prof Katherine Wilson (Examiner)	John Hopkins School of Medicine, USA
Dr Sophie Zinn-Justin (Invited member)	Commissariat à l'Energie Atomique
CEA, Paris-Saclay	
Prof Onnik Agbulut (Head of committee)	Université Pierre et Marie-Curie, Paris

Defended: October 19, 2018

Table of contents

List of figures

List tables

List abbreviations

ACD: Atrial Cardiac Defect

AD: Autosomal dominant

ADLD: Autosomal Dominant Leukodystrophy.

APC: Adenomatous polyposis coli

AR: Autosomal recessive

AV: Atrioventricular

BAF: Barrier-to-auto-integration factor

BAF/Banf1: Barrier-to-auto-integration factor

BOS: Buschkle-Ollendorf

CK: Casein kinase

CM: Cardiomyocytes

CMT2: Charcot-Marie-Tooth type 2

CRX: Cone-Rod homeobox

CTRT46: Cataract 46

Cul4: Cullin 4

DAD: Deacetylase activation domain

DamID: DNA adenine methyltransferase identification

DCM: Dilated Cardiomyopathy

DDB2: Damage-specific DNA binding protein 2

Dvl: Dishevelled

ER: Endoplasmic reticulum

FHL1: Four and a half LIM domains protein1

Fz: Frizzled

GCL: Germ cell-less

GSK: Glycogen synthase kinase

HDAC: Histone Deacetylase

HDF : Human dermal fibroblasts

HEH: Helix-Extension-Helix

HGNC: Human Gene Nomenclature Database

HGPS: Hutchinson-Gilford Progeria Syndrome

hiPSC: Human induced pluripotent stem cells

HIV-1: Human immunodeficiency type 1

ICD: Intercalated discs

IGF: Insulin-like growth factor

INM: Inner nuclear membrane

KASH: Klarsicht, ANC-1, Syne Homology

LADs: Lamina-associated domains

LAP: lamina-associated protein

LBR: Lamin B receptor

LEM: LAP2, emerin, and Man1

LINC: Linker of Nucleoskeleton and Cytoskeleton

Lmo7: Lim-domain-only 7

LRP: Low-density lipoprotein receptor related protein

MAP1LC3B: Microtubule-associated protein 1 light chain 3 beta

MAPK: Mitogen-activated protein kinase

MCPH16: Microcephaly 16

MKL1 : Megakaryoblastic leukemia 1

MoMLV: Moloney Murine Leukemia Virus

MSC: Man1/Src1-C-terminal

MTOC: Microtubule organizing center

NCBI: National Centre for Biotechnology Information

NE: Nuclear envelope

NESPRIN: Nuclear envelope spectrin repeat

NET: Nuclear envelope transmembrane

NGPS: Nestor-Guillermo progeria syndrome

NMI : Nuclear myosin I

NMIIA: Non-muscle myosin IIA

NMR: Nuclear magnetic resonance

NPC: Nuclear pore complex

NUPs: Nucleoporins

O-GlcNAc: O-linked β-N-acetylglucosamine

ONM: Outer nuclear membrane

PCNA: Proliferating cell nuclear antigen

PKA: Protein kinase A

PKC: Protein kinase C

PLK1:Polo-like kinase 1

PNS: Perinuclear space

PP1: Protein phosphatase 1

PRKACA: Protein kinase, cAMP-dependent, catalytic, α

RBD: Regulator binding domain

RNA: Ribonucleic acid

SA: Sinoatrial

SFK: Src family kinase

SUN: Sad1p/UNC-84

TA: Tail-anchored

TCF/LEF: T cell factor/lymphoid enhancer factor

TGF-β: Transforming growth factor β

VRK: Vaccina-related kinase

X-EDMD: X-linked Emery Dreifuss Muscular Dystrophy

YT521-B: YTH-domain containing protein 1

αII-spectrin: Spectrin isoform αII

Preamble

Emery-Dreifuss Muscular Dystrophy (EDMD) is among the most widely common human genetic muscular dystrophies. The cardiac involvement in the disease is the most life-threatening symptom and the major cause of mortality. The majority of cases of its X-linked type are due to mutations in a gene encoding for the nuclear envelope protein, emerin. Despite the considerable advances that have been achieved in terms of the characterization of emerin structure, various binding partners, and functions in the human body, the picture is still rather incomplete. Fifty years now after EDMD had been first documented, researchers still fall short of understanding the pathophysiology of the disease. Thereby, it comes as no surprise that, to date, there is no described treatment of EDMD. Accordingly, this thesis is an initial attempt to characterize three emerin LEM-domain missense mutations (P22L, ΔK37, and T43I) present in patients with exclusive cardiac defects. The main objective of this thesis is to investigate the effect of the three mutations on: emerin structure, its self-assembly, and interactions with some of its well-described binding partners.

The presented work highlights that albeit the localization of the three mutations in the only folded region of emerin, the variants show no global defect in their structure, except for the destabilization of the LEM-domain of the variant ΔK37. Importantly, the mutants are able to self-assemble, yet with astonishing fast polymerization kinetics. In addition, the investigations have illustrated that the three variants, despite the presence of the mutations in the BAF-binding domain, are surprisingly capable of binding BAF. The analysis did not reveal any differences in the mutants binding to Ig-fold domain of lamin A/C. Further, there is no defect in ΔK37 phosphorylation by Src kinase. Also, preliminary characterization of the ΔK37 mutation in immortalized human fibroblasts has featured no overt defects in mechanobiology, and in the expression of nuclear envelope or cytoskeletal proteins.

Taken all together, the presented work outlines that the three emerin missense mutations display no defects in several prominent emerin properties, which are questioned in this thesis. On the basis of the results of the conducted research, considerable insight has been gained with regard to the consequences of the mutations of interest. In other words, the presented work lends support to following investigations in order to explore other unquestioned properties or functions of emerin that might be associated with the pathophysiology of EDMD.

Résumé

La dystrophie musculaire d'Emery-Dreifuss (DMED) est l'une des dystrophies musculaires génétiques humaines les plus répandues. L'implication cardiaque dans la maladie est le symptôme qui met le plus la vie en danger et la principale cause de mortalité. La majorité des cas de son type liée à l'X sont dus à des mutations dans un gène codant pour une protéine de l'enveloppe nucléaire, l'émerine. Malgré les progrès considérables qui ont été réalisés en termes de caractérisation de la structure de l'émerine, ses différents partenaires de liaison, et ses fonctions dans le corps humain, le tableau est encore assez incomplet. Cinquante ans après que la DMED ait été documentée pour la première fois, les chercheurs n'ont toujours pas compris la pathophysiologie de la maladie. Il n'est donc pas surprenant qu'à ce jour, il n'existe pas de traitement décrit pour la DMED. Cette thèse est une première tentative pour caractériser trois mutations faux-sens du domaine LEM de l'émerine (P22L, ΔK37, et T43I) présentes chez des patients présentant uniquement des symptômes cardiaques. L'objectif principal de cette thèse est d'étudier l'effet des trois mutations sur la structure de l'émerine, son auto-assemblage, et les interactions avec certains de ses partenaires de liaison bien décrits.

Le travail présenté souligne que malgré la présence des trois mutations dans la seule région repliée de l'émerine, les variants ne présentent aucun défaut global dans leur structure, à l'exception de la déstabilisation du domaine LEM du variant ΔK37. Il est important de noter que les mutants sont capables de s'auto-assembler, mais avec une cinétique de polymérisation rapide. En outre, l'étude a montré que les trois variants, bien que mutés dans le domaine de liaison à BAF, sont étonnamment capables de se lier à la protéine BAF. De plus, l'analyse ne révèle aucune différence dans les interactions des variants avec l'Ig-fold de la lamine A/C. De plus, il n'y a pas de défaut dans la phosphorylation du variant ΔK37 par la kinase Src. La caractérisation préliminaire de la mutation ΔK37 dans des fibroblastes humains immortalisés

n'a pas montré de défauts manifestes en mécanobiologie et dans l'expression des protéines de l'enveloppe nucléaire ou du cytosquelette.

Pris dans son ensemble, le travail présenté souligne que les trois mutations faux-sens de l'émerine ne provoquent aucun défaut dans plusieurs propriétés importantes de l'émerine, qui sont testées dans cette thèse. Sur la base des résultats de la recherche menée, nous avons acquis des connaissances considérables en ce qui concerne les conséquences des mutations d'intérêt. En d'autres termes, le travail présenté montre qu'il faut continuer les recherches sur l'émerine, afin d'explorer d'autres propriétés ou fonctions de cette protéine qui pourraient être associées à la physiopathologie de la DMED.

Zusammenfassung

Die Emery-Dreifuss Muskeldystrophie (EDMD) gehört zu den häufigsten genetischen Muskeldystrophien des Menschen. Die kardiale Beteiligung an der Erkrankung ist das lebensbedrohlichste Symptom und die häufigste Todesursache. Die meisten Fälle seiner X-verknüpften typ sind auf Mutationen in einem Gen zurückzuführen, das für das Kernhüllprotein Emerin kodiert. Trotz der erheblichen Fortschritte, die bei der Charakterisierung die Emerin-Struktur, ihrer verschiedenen Bindungspartner und Funktionen im menschlichen Körper erzielt wurden, ist das Bild noch recht unvollständig. Fünfzig Jahre nach der ersten Dokumentation der EDMD sind die Forscher immer noch nicht in der Lage, die Pathophysiologie der Krankheit zu verstehen. Dabei überrascht es nicht, dass es bis heute keine beschriebene Behandlung der EDMD gibt. Dementsprechend ist diese Arbeit ein erster Versuch, drei emerin der LEM-Domäne Fehlsinn-Mutationen (P22L, K37 und T43I) bei Patienten mit exklusiven Herzfehlern zu charakterisieren. Das Hauptziel dieser Arbeit ist es, die Wirkung der drei Mutationen auf die Emerin-Struktur, ihre Selbstorganisation zu untersuchen, und die Wechselwirkungen mit einigen ihrer gut beschriebenen Bindungspartner.

Die vorgestellte Arbeit hebt hervor, dass, obwohl die drei Mutationen in der einzigen gefalteten Region in emerin, die Mutationen zeigen keinen globalen Defekt in ihrer Struktur, mit Ausnahme der Destabilisierung der LEM-Domäne von die K37. Wichtig ist, dass sich die Mutanten selbst zusammensetzen können, jedoch mit einer erstaunlich schnellen Polymerisationskinetik. Darüber hinaus haben die Untersuchungen gezeigt, dass die drei Mutationen trotz ihres Vorhandenseins im BAF-bindenden Bereich überraschend an das BAF binden können. Darüber hinaus zeigt die Analyse keine Unterschiede in der Bindung der Mutanten an die Ig-Falte des Lamin A/C. Weiterhin gibt es keinen Defekt in der K37-Phosphorylierung durch Src-Kinase. Vorläufige Charakterisierung der K37-Mutation in

unsterblichen menschlichen Fibroblasten hat keine offenen Defekte in der Mechanobiologie und der Expression von Zytoskelett- oder Kernhüllproteinen gezeigt.

Insgesamt zeigt die vorgestellte Arbeit, dass drei emerin Fehlsinn-Mutationen keine Defekte in mehreren prominenten emerin Eigenschaften, die in dieser Arbeit in Frage gestellt werden. Auf der Grundlage der Ergebnisse der durchgeführten Untersuchungen wurden erhebliche Erkenntnisse über die Folgen der interessierenden Mutationen gewonnen. Mit anderen Worten, die vorgestellte Arbeit unterstützt nachfolgende Untersuchungen, um andere unbestrittene Eigenschaften oder Funktionen von emerin zu erforschen.

Outline

The presented doctoral thesis comprises four chapters:

1 Chapter I, "**Introduction**", featuring general introduction to the addressed topic, as well as the hypotheses and work objectives.

2 Chapter II, "**Manuscript**", including the scientific manuscript documenting the scientific work conducted during the doctoral thesis.

3 Chapter III, "**Additional data**", presenting and discussing additional data, that were gathered during the doctoral thesis and not included in the manuscript together with the materials and methods employed in order to obtain them.

4 Chapter IV, "**Discussion**", summarizing the attained outcomes, unanswered questions, and future perspectives.

Chapter I: Introduction

Emery-Dreifuss Muscular Dystrophy (EDMD) is one of the best described muscular dystrophies in humans. The X linked type of EDMD (X-EDMD) is clinically characterized by early contractures, slowly progressive humero-peroneal muscle weakness and atrophy, and cardiac involvement which presents as conduction defects, arrhythmias and dilated cardiomyopathy. If not diagnosed early enough, this cardiac involvement could be life-threatening.

Mutations in EMD gene, encoding for the nuclear envelope protein emerin, are responsible for most of X-EDMD cases. In most patients, mutations lead to an absence of emerin. Thus, EDMD is caused by a loss of function of emerin. Having said that, missense and small deletion EDMD causing mutations were also reported. These mutations are all present in the region comprising amino acid 54 to amino acid 183 of emerin, predicted as nucleoplasmic and intrinsically disordered. More recently, three mutations (P22L, ΔK37, and T43I) were identified in patients with exclusive cardiac defects. These new mutations reside in the N-terminal folded LEM domain of emerin. To date, the structural and functional impacts of these mutations remain elusive. For this reason, the main objective of the presented thesis is to investigate for the first time the effect of the three mutations on emerin structure, self-assembly, and interactions with some of its well-described binding partners.

As an introduction to the subject, the nuclear envelope and the LEM-domain family of proteins, that are anchored at the inner nuclear membrane of most cells, are described in this section. Then the rest of the focus is on the LEM-domain protein emerin, its structure, functions and partners, and its role in EDMD.

1 The nuclear envelope

One of the chief differences between prokaryotic and eukaryotic cells is the presence of membrane bound-organelles, such as the nucleus[1]. Functional eukaryotic nuclei are encompassed by the nuclear envelope (NE) , which outlines the perimeter of nuclei, and partitions nuclear and cytoplasmic activities[2] **(**Figure 1**)**. The NE is made of two lipid bilayer membranes, namely the outer (ONM) and inner nuclear membranes (INM), which weld at sites where nuclear pore complexes (NPCs) are embedded. The ONM is continuous with the endoplasmic reticulum (ER), and is separated from the INM by the perinuclear space (PNS). Regardless of its continuity with the ER, both ONM and INMs contain diversified assortment of proteins that are not commonly enriched in the ER[3]. The NE comprises principally four protein groups that will be briefly described: NPC, ONM, INM and nuclear lamina proteins.

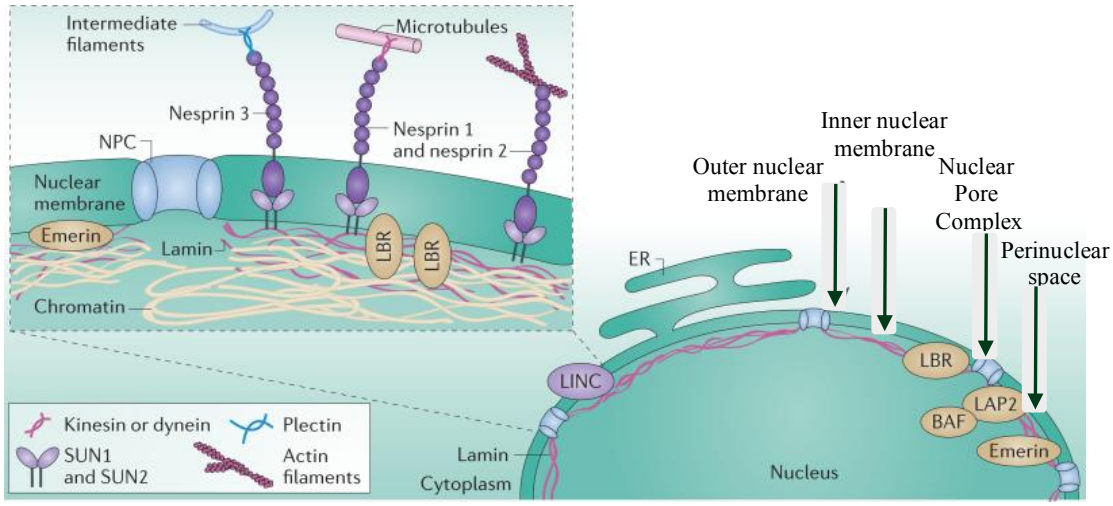

Figure 1. The eukaryotic nucleus and the nuclear envelope (adapted from[197]). The eukaryotic nucleus is encircled by two lipid membranes (outer and inner nuclear envelope membranes) that fuse at the nuclear pore complex (NPC), and they are separated by the perinuclear space (PNS). The outer membrane is continuous with the endoplasmic reticulum (ER). Both membranes are studded with diverse integral proteins. The inner membrane proteins interact with lamins and chromatin, while those at the outer membrane interact with actin, microtubules and intermediate filaments.

The NPC is formed of at least 30 different polypeptides, called nucleoporins (Nups)[4]. It functions as a bidirectional channel for the transport of macromolecules such as ribonucleic acid (RNA), proteins, and ribonucleoproteins between the cytoplasm and the nucleoplasm[5].

The ONM protein group includes a diverse set of integral membrane proteins that shares a KASH (Klarsicht, ANC-1, Syne Homology) domain. Two related members of this group, nuclear envelope spectrin repeat (NESPRIN) -1 and -2, interact with the actin cytoskeleton, thereby, they play important role in nuclear positioning[6].

The INM protein group embodies several integral proteins including lamin B receptor (LBR), emerin, lamina-associated protein (LAP)1, LAP2 and Man1. These proteins are capable of interacting with chromatin. Thus, they contribute in chromatin organization and gene expression[7,8,9]. As shown in Figure 1, SUN (Sad1p/UNC-84) –domain proteins, located as well at the INM, interact with nesprin proteins within the PNS; forming so-called LINC (Linker of Nucleoskeleton and Cytoskeleton) complexes which connect the actin cytoskeleton to the nucleoskeleton[10,6].

Lamins represent the last group of proteins at the NE. They mostly comprise lamin A, B1, B2, and C, which are woven together to form a meshwork of type V intermediate filaments underneath the INM[11]. They are critical for gene expression, as well as nuclear stability during mechanical forces[12,13]. The majority of characterized INM proteins directly bind to A- or B-lamins (or both) and are hence retained at the NE[14]. Lamins together with nuclear lamin associated-proteins are collectively called the nuclear lamina.

Several proteomic approaches have detected the differential expression of nuclear lamina and nuclear envelope transmembrane (NET) proteins across different tissues and cell states. A comprehensive review of differentially expressed NETs across tissues has been put forth by Wong et al.[15]. Schirmer and colleagues provided the first subtractive proteomic study,

using multidimensional protein identification technology (MudPIT), in which they identified 67 uncharacterized putative NETs in the NE isolated from rodent liver[16]. Five of which were detected to be up-regulated during myogenesis of C2C12 myoblasts and of strikingly high abundance in mice skeletal muscles, namely: NET9, NET14a, NET25 (LEM2), NET37 and NET39[17] (Figure 2).

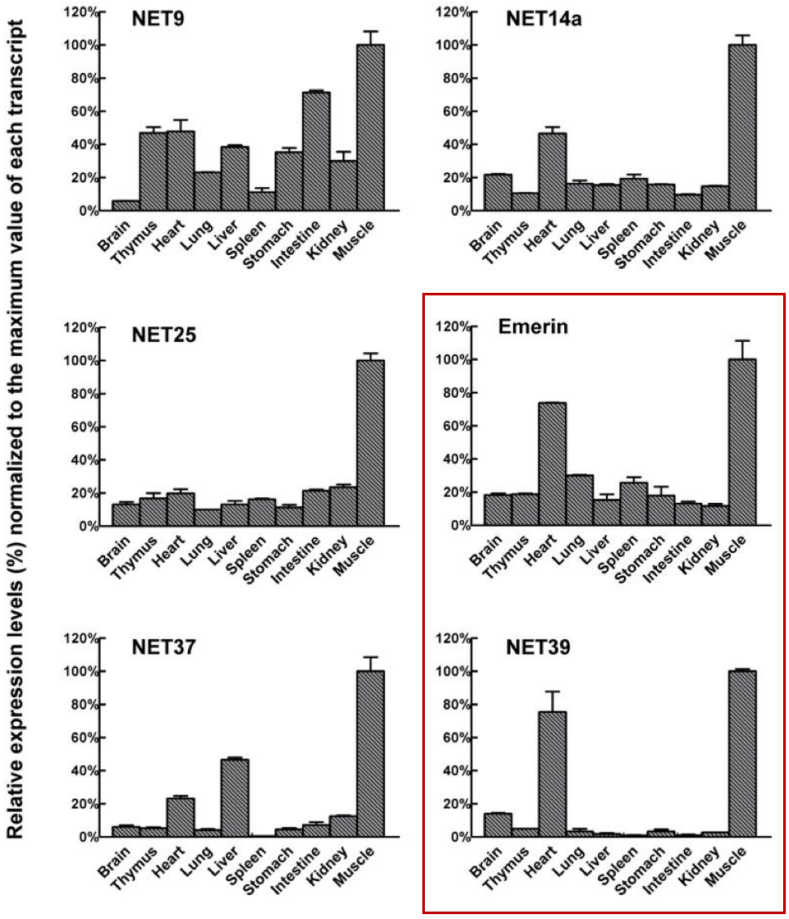

Figure 2. Relative expression levels of the up-regulated NETs during C2C12 differentiation in tissues of adult mice (adapted from[17]). Quantitative real-time PCR of the gene expression levels of NETs that were up-regulated during C2C12 differentiation revealed the high expression of these proteins in the skeletal muscle of adult mice. The relative expression levels of emerin that has the highest expression levels in skeletal and hearts muscles, was added for comparison. Both emerin and NET39 (E. Schirmer, personal communication) are associated with Emery Dreifuss Muscular Dystrophy (EDMD) (boxed in red rectangle).

The NE main function is to shield the nuclear genome from cytoplasmic components and to mediate the nucleocytoplasmic transport. Nevertheless, in view of the diversity of proteins present at the NE, further functions have been reported (an all-embracing summary of the different nuclear envelope functions has been provided by Wilson and Berk[14]). The following paragraphs mount examples for the NE roles in nuclear positioning, cell signaling, and DNA replication.

NETs are implicated in nuclear positioning. The ONM nesprin-4 binds kinesin-1, the plus-end directed microtubule motor, then together they push the nucleus away from the Golgi apparatus and MTOC (microtubule organizing center). Collectively, they are implicated in achieving a basal position in a polarized cell. Further, SAMP, a well-conserved INM protein, tethers the MTOC near the nucleus, which is an important step in repositioning nuclei of motile cells[18].

NETs regulate several signaling pathways. MAN1 tunes transforming growth factor β (TGF-β) signaling, during both embryogenesis and vertebrate development, via binding to receptor-regulated Smads (R-Smads)[19,20]. Also, the INM NET39 binds directly to mTOR resulting in the inhibition of the insulin-like growth factor 2 (IGF2) autocrine signaling and production, together with the inhibition of the AKT signaling pathway[21]. Interestingly, NET37 has a glycosidase activity, which is involved in IGF2 maturation[22].

Lastly, lamins have non-structural roles inside the nucleus, such as the regulation of DNA replication. The highly conserved Ig-fold domain of nuclear lamins binds directly to proliferating cell nuclear antigen (PCNA), which is the processivity factor required for the DNA replication chain elongation phase[23]. The inhibition of DNA replication after excessive addition of lamin Ig-fold and/or its tail domain suggests that the interactions of these regions with PCNA competitively inhibit the interaction of the latter with chromatin[23].

Mutations in nuclear envelope proteins have been associated with a wide range of human diseases in which one or more tissues (nervous, bone, muscle, fat, skin, connective tissue, blood or heart) are affected, brain development is perturbed, or aging is accelerated, as collectively illustrated in Figure 3[24,25,26].

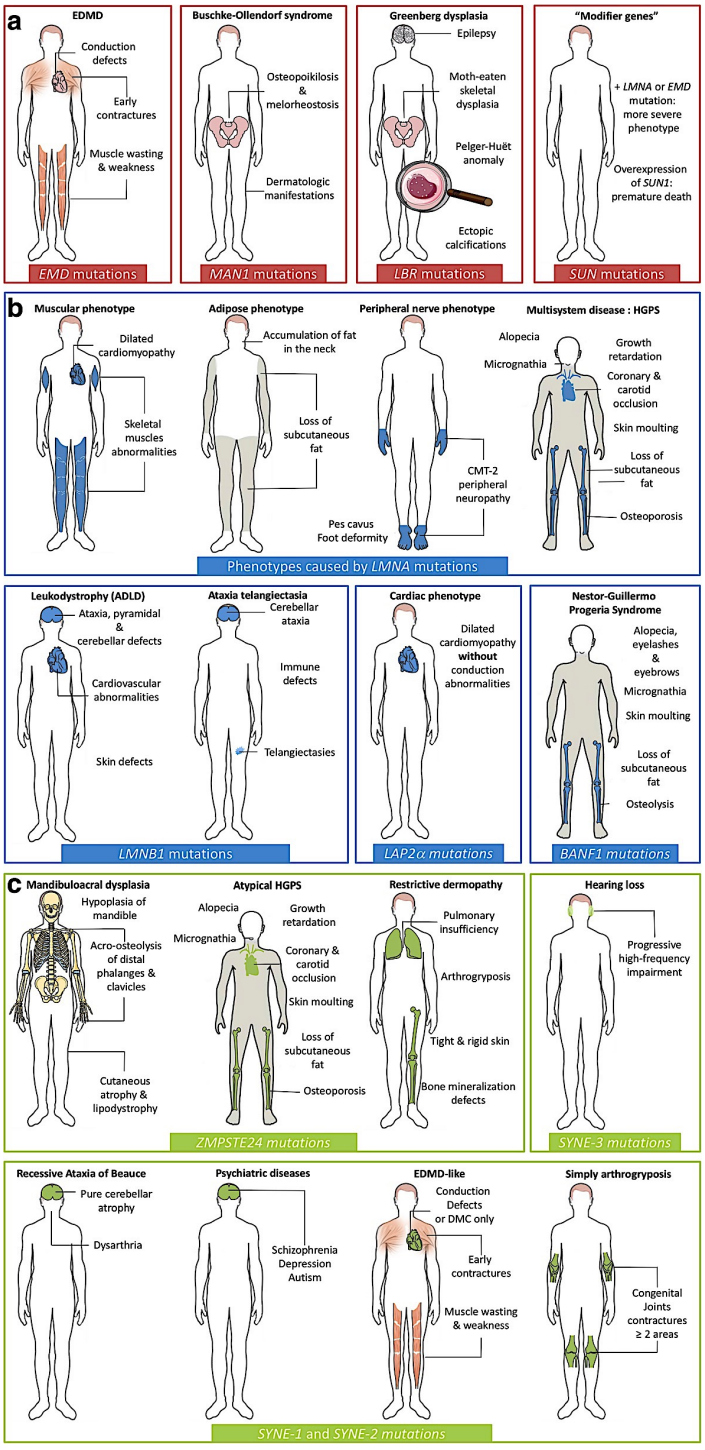

Figure 3. Nuclear envelope proteins and diseases[24]. Comprehensive summary of all known human diseases, their affected tissues and accompanying symptoms caused by mutations in genes encoding for components of (a) the inner nuclear envelope membrane (b) nuclear lamina (c) the outer nuclear envelope membrane. *EMD*: gene encoding for emerin, *MAN1*: gene encoding for Man1, *LBR*: gene encoding for lamin B receptor, SUN: *SUN1* and *SUN2* genes encoding for SUN1 and SUN2 proteins respectively, *LMNA*: gene encoding for prelamin A/C which is cleaved later into lamin A and C, LMNB1: gene encoding for lamin B1, LAP2α: protein encoded by *LAP2* (*TMPO*) gene, *BANF1*: gene encoding for barrier-to-autointegration factor (BAF), *ZMPSTE24*: gene encoding for CAAX prenyl protease 1 homolog (Farnesylated proteins-converting enzyme 1/ Zinc metalloproteinase Ste24 homolog/ Prenyl protein-specific endoprotease 1), *SYNE-3*: gene encoding for nesprin-3, *SYNE-1*: gene encoding for nesprin-1, *SYNE-2*: gene encoding for nesprin-2. EDMD: Emery-Dreifuss Muscular Dystrophy, HGPS: Hutchinson-Gilford Progeria Syndrome, CMT: Charcot-Marie-Tooth Disease, ADLD: Autosomal Dominant Leukodystrophy.

2 LEM-domain proteins

The LEM-domain family of proteins is named after its founding members: LAP2, emerin and Man1[27]. As summarized in Table 1, human LEM-domain proteins are encoded by seven genes[28,29]. These proteins are conserved in both single-celled and multicellular Opisthokonts[30]. For example, the nematode worm *C. elegans* expresses three proteins orthologous to human Ankle1, emerin and LEM domain containing protein 2[31].

***Opisthokonts**: is a group of eukaryotes, comprising animal (Metazoa), fungus, and choanoflagellates kingdoms. Opisthokonts were previously called (Fungi/Metazoa) group. In greek opisthios means posterior or rear and kontos means pole, i.e flagellum. The group acquired that name seeing that its common characteristic is having flagellate cells (sperms or spores) that propel themselves with single posterior flagellum, contrary to flagellate cells in other euokaryotic groups that propel themselves using one or more anterior flagella.*

Table 1. List of human LEM-domain genes and proteins

*Gene symbol, gene full name and gene also known as (gene AKA) source is National Centre for Biotechnology Information (NCBI) provided by Human Gene Nomenclature Database (HGNC). *Protein name(s) source is UniProt.
* 3 more LAP2 isoforms have been identified in mice: ε,Δ, ζ[32]

Gene Symbol*	Gene full name*	Gene AKA*	Protein name(s)*
LEMD1	LEM domain containing 1	*CT50, LEMP-1*	LEM domain containing protein 1 (Isoform 1,2,3,4,5,6)
LEMD2	LEM domain containing 2	*NET25; CTRCT42; dJ482C21.1*	LEM domain containing protein 2
LEMD3	LEM domain containing 3	*MAN1*	Man1
TMPO	Thymopoietin	*TP; LAP2; CMD1T; LEMD4; PRO0868*	Lamina-associated polypeptide 2 (α, β, γ)*
EMD	Emerin	*STA; EDMD; LEMD5*	Emerin
ANKLE1	Ankyrin repeat and LEM domain containing 1	*LEM3; LEMD6; ANKRD41*	Ankyrin repeat and LEM domain containing1 (Isoform 1,2)

ANKLE2	Ankyrin repeat and LEM domain containing 2	*LEM4; LEMD7; MCPH16; KIAA0692*	Ankyrin repeat and LEM domain containing 2 (Isoform 1, 2, 3)

The LEM-domain is a ≈ 40-amino acid domain composed of a three-residue helical turn at its N-terminus, and two large parallel alpha helices interacting through conserved set of hydrophobic amino acids. The two helices are connected by a long loop forming a helix-loop-helix fold[38] (Figure 4).

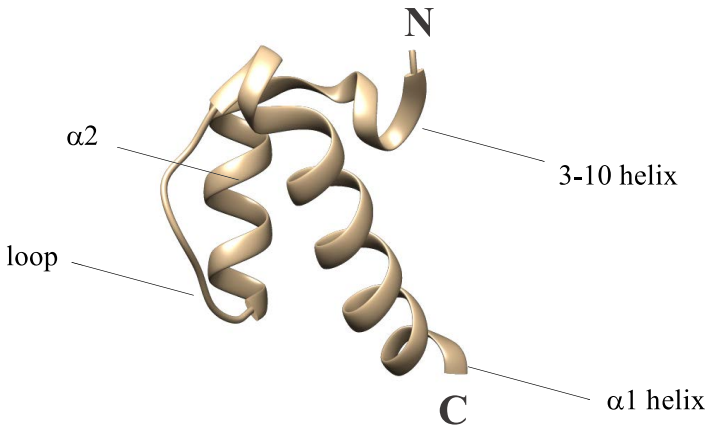

Figure 4. Structure of emerin LEM-domain. Ribbon representation of emerin LEM domain (1-47) (PDB:2ODC) showing the 3-10 helical turn and the two α helices connected by a loop.

Almost all LEM-domain proteins localize at the INM, yet some are present in either the ER or the nuclear interior depending whether they have transmembrane domain(s)[33] (Table 2). To date, the one known function for eukaryotic LEM-domains is to bind to BAF[34–37]. Crystal structures for emerin LEM-domain solely[38,39], or in complex with BAF have been resolved[38]. The crystal structure of BAF bound to DNA has also been determined[40]. Analysis of all these structures suggests that emerin may bind BAF in complex with DNA. LAP2 has a LEM-domain and an additional LEM-like domain that may bind DNA as well[34].

Besides their LEM and LEM-like domains, LEM-domain proteins possess other interacting domains that binds to the nucleoskeleton, and to signaling or gene-regulatory proteins[28,41]. For example, LAP2α self-interacts (to form dimers), binds to lamin A, telomeres and chromatin, and is necessary to organize lamin A in the nuclear interior [42,43,44]; and Man1 binds to lamin A and Smad2/3 which regulates the TGF-β signaling pathway.

Table 2. LEM-domain proteins structure and localization

Protein name	LEM-domain	Transmembrane	Localization
LEM domain containing protein 1	LEM-domain	present; one	INM
LEM domain containing protein 2	LEM-domain	present; two	INM
LAP2α	LEM-domain + LEM-like domain	absent	Nucleus
LAP2β/γ	LEM-domain + LEM-like domain	present; one	INM
Emerin	LEM-domain	present; one	INM
Ankle1	LEM-domain	absent	Nucleus
Ankle2	LEM-domain	absent	ER
Man1	LEM-domain	present; two	INM

It's important to realize that despite the lack of genes encoding for lamins, BAF, LAPs (lamina associated proteins), and their orthologs in yeast[45], LEM-domain proteins are present in lower eukaryotes. As an illustration, yeast express evolutionarily distant relatives of LEM-domain family of proteins, called MSC (Man1/Src1-C-terminal) proteins. Particularly, two MSC proteins exist in budding and fission yeast (Heh1/Scr1 and Heh2 in S Saccharomyces *cerevisiae*; and Lem2 and Man1 in Saccharomyces *pombe*). Similar to LEM-domain proteins in animals, this family of proteins owns a conserved N-terminal HEH (Helix-Extension-Helix)

domain, however this domain directly binds DNA[46]. It is evidenced that in *S. cerevisiae*, Heh1/Src1 enriches with telomeres and represses subtelomeric, telomeric and rDNA genes[47]. Further, in *S. pombe*, Lem2 and Man1 result in the compaction of chromatin near the spindle pole body[48], attesting the competitive release of telomeres from attachment sites at the NE[49]. Taken all together, these findings highlight the significance of LEM-domain proteins for nuclear structure and genomic organization in metazoans independently of both BAF and lamins.

LEM-domain proteins have been associated with several human pathologies portraying their crucial roles in cells. For instance, LEMD2 mutations cause juvenile-onset cataract 46 (CTRT46), which is accompanied by the opacification of the eye's lens resulting in visual impairment or blindness, and associated with sudden cardiac death[50]. As illustrated in Figure 3, mutations in LEMD3 (MAN1) result in Buschkle-Ollendorf syndrome (BOS), a disease characterized by *osteopoikilosis* (skeletal dysplasia with symmetrical but unequal excessive growth or thickening of bone tissue in different skeleton areas), melorheostosis (asymmetric excessive growth or thickening of the cortex of tubular bones) and *disseminated connective-tissue* nevi (a group of benign tumor-like malformations with increased quantities of dermal collagen and diverse changes in elastic tissue). *Elastic-type nevi* (a variant of connective tissue nevus with predominantly increase in dermal elastic tissue) and *collagen-type nevi (*a variant of connective tissue nevus with predominantly increase in dermal collagen) have been described in BOS[51]. Additionally, mutations in LAP2 are associated with familial or idiopathic isolated dilated cardiomyopathy leading to systolic and diastolic dysfunction in left and/or right ventricles[52]. ANKLE2 mutations cause microcephaly 16 (MCPH16), a disease defined by reduced brain weight and disproportionately small cerebral cortex [53]. Mutations in EMD and their link to diseases will be discussed in the following section.

3 Emerin

3.1 Structure

The emerin gene (formerly: STA; renamed: EMD), located on the long arm of the X-chromosome at position 28 (Xq28), consists of 6 exons and 5 introns. EMD encodes a type II integral membrane protein, emerin, which is a 34-kDa serine-rich protein. Emerin is made of 254 amino acids including a 220 amino acid N-terminal nucleoplasmic region, a 23-residue transmembrane segment and an 11-residue luminal domain from the carboxyl terminus[54]. Solution state nuclear magnetic resonance (NMR) analysis of emerin fragment 1-187 revealed that it is composed of a globular LEM domain (illustrated in Figure 4), and a vast intrinsically disordered fragment[55].

Owing to the large disordered fragment, mutations in emerin may not only directly affect the structure of emerin, but they can also alter the platform required for interactions with partners, post translational modifications, and flexibility for emerin to switch between different configurations.

Several biochemical and cellular studies corroborate that emerin is able to self-assemble *in vitro*. First, yeast two-hybrid experiments shed lights on the ability of emerin (residues 1-225) to form homodimers or multimers[56]. Then Berk et al., were the first to offer specific molecular details regarding emerin-emerin interactions at the inner nuclear membrane. Using GST-pulldown experiments of emerin fragment 1-221 and co-immunoprecipitation of full length emerin from HEK293T cells, Berk and colleagues have outlined two mechanisms for emerin self-assembly[57]. Particularly, emerin can exhibit homotypic (R-R) interactions of region 170-220, as well as heterotypic (R-S) interactions between the same region and region 1-132 (Figure 5). Also, they proffer two configurations for the emerin backbone depending on the position of LEM-domain[57]. The “up configuration”, in which the LEM domain is bound to

the emerin backbone; and a "down configuration", in which the LEM-domain binds chromatin for example through the chromatin binding protein BAF[57].

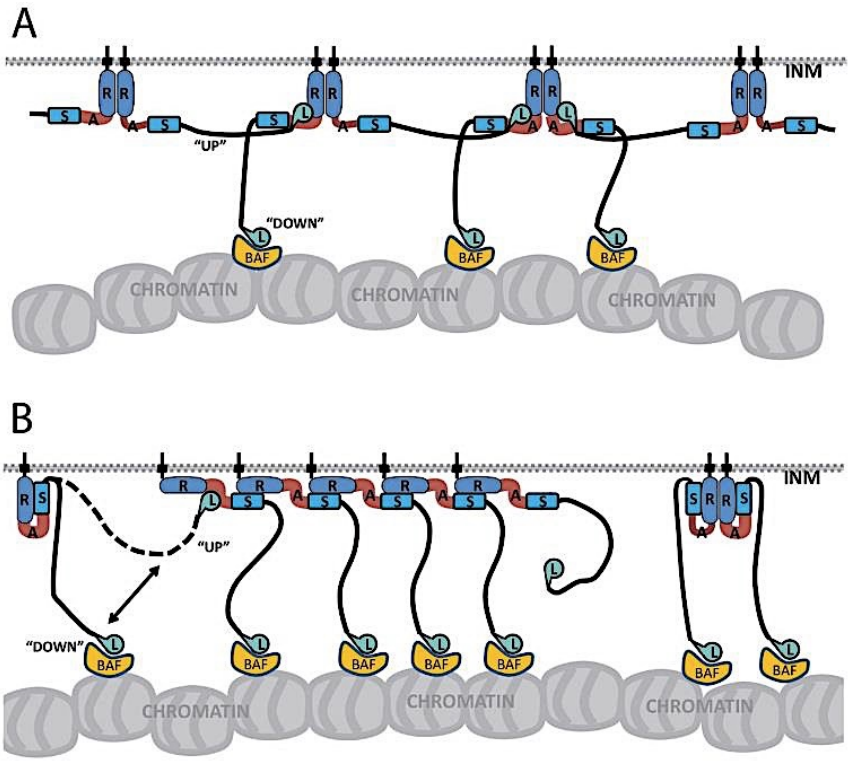

Figure 5. Models of emerin-emerin interactions[57](A) R-R association (B) R-S association. We can see the "up" configuration where the LEM-domain (L) is bound to the backbone, and "down" configuration where the LEM-domain is bound to BAF. INM, inner nuclear membrane; BAF, barrier to auto-integration factor.

Further, Zinn-Justin's group has been engaged in characterizing the oligomerization of emerin *in vitro* using various biochemistry and biophysical techniques. The group has demonstrated that emerin fragment 1-187 is able to self-assemble *in vitro* to form curvilinear filaments, and they followed the formation of these filaments by Thioflavin-T binding and Fourier-transform Infrared spectrometry[55]. Next, they evidenced that emerin fragment 1-132 is sufficient to form curvilinear filaments, which are rich in β-structures, and that the LEM-

domain is involved in the self-assembly, yet not enough on its own[58]. Interestingly, emerin missense mutations (Δ95-99 and Q133H) causing X-EDMD alter the self-assembly capacity of emerin *in vitro* and in HeLa cells. Δ95-99 and Q133H impact the self-assembly capacity (the former completely abolishes it), along with interaction with lamins. Also, Zinn-Justin's group has recently shown that emerin fragment 67-221 was also able to self-assemble *in vitro* (Samson et al., under review). In this region, amino acid proline 183 display immense relevance to emerin's oligomerization and localization. P183H mutation favors emerin aggregation *in vitro*, and P183T evokes the accumulation of emerin in cytoplasmic foci when expressed in HeLa cells[55].

3.2 Synthesis and localization

Prior research had generally agreed that the transmembrane segment of emerin is the key determinant for its nuclear membrane targeting[59], however others have evidenced later that it is the nucleoplasmic amino terminal domain of emerin that is essential and sufficient for its targeting and retention at the inner nuclear envelope membrane[60]. More specifically, studies came to conclusion that residues 110-147 are essential for nuclear transport of emerin, whereas residues 109-175 are responsible for the nuclear envelope localization[60]. It came as no surprise that the latter domain comprises the lamin A binding domain. That's to say that emerin targeting to the inner nuclear membrane follows the "diffusion and retention" model. In this model, proteins synthesized in the ER diffuse to the inner nuclear membrane where they are retained by binding to nuclear ligands, such as nuclear lamins or chromatin[61,62]. Accordingly, upon synthesis in the cytoplasm, (presumably soluble) emerin is inserted post-translationally, by the virtue of its transmembrane segment acting as signal anchor, into the ER membrane with the help of ATP-dependent TRC40/Asna-1 complex[63]. The latter is a mammalian soluble ATPase that interacts with newly synthesized tail-anchored (TA) proteins in the cytoplasm so as to deliver them to the surface of the ER-derived vesicles (microsomes). There the cargo

undergoes ATP-membrane dependent insertion, then diffuses freely throughout the ER, passing by the NPC, till reaching the nuclear envelope membrane[60,64]. Emerin slides smoothly through the NPC for the sake of its small cytoplasmic-exposed domain (25 kDa)[60]. Once inside the nucleus, the binding of emerin to lamins determines its retention at the nuclear membrane. Otherwise, in LMNA-null cells, emerin remains mobile throughout the nuclear envelope and ER[60,65,66,67].

Alternatively, it has been shown that emerin can be present in unconventional sites, such as: outer nuclear envelope membrane, plasma membrane, and intercalated discs (ICD) of cardiomyocytes[59]. The presence of emerin at the outer nuclear membrane might be justified by its interaction with nesprin-1 isoforms[68]. Mechanical stress can as well be implicated in the enrichment of emerin at the outer nuclear envelope[69]. Several hypotheses get across how emerin can reach the other unconventional sites. The first one includes the direct insertion of nascent emerin post-translationally into alternative membranes; the second one postulates its release as ER vesicle membrane in which it is trafficked to the plasma membrane; and the third one presumes a hypothetical mechanism by which the hydrophobic domain of emerin is masked, allowing nascent emerin to associate as soluble protein with partners outside the nucleus [70].

3.3 Distribution of emerin during mitosis

During mitosis, eukaryotic cells undergo extensive rearrangements and molecular changes. Confocal laser scanning immunofluorescence microscopy for labelled emerin in human HEp-2 cells revealed that during prophase, emerin is still located at the nuclear envelope (Figure 6)[71]. In metaphase, after the complete disassembly of the nuclear envelope, emerin is enclosed in vesicles that are dispersed in the cytoplasm. Some of these vesicles are present close to the poles of the mitotic spindle apparatus[71]. During anaphase, emerin accumulates at

poles of the mitotic spindles[71]. Coincidently, the centromere or the core region of chromosomes move as well during this phase to the spindle pole pulling with them the rest of the chromosome[72]. In early telophase, emerin is concentrated in two opposite areas in the nuclear membrane in close proximity to microtubules[71]. During late telophase, emerin is redistributed over the nuclear periphery co-localizing with lamin A/C; and in middle of dividing cells[71].

It is important to realize that at this stage the fate of emerin is similar to lamin A/C, yet different from lamin B and LAP2, as they both lack the telophase focal accumulation of emerin and lamin A/C at opposite regions of nuclear membrane. Seeing that LAP2 is localized in different areas at the nuclear envelope during nuclear assembly favors the idea that integral proteins are managed distinctively during nuclear envelope assembly[71].

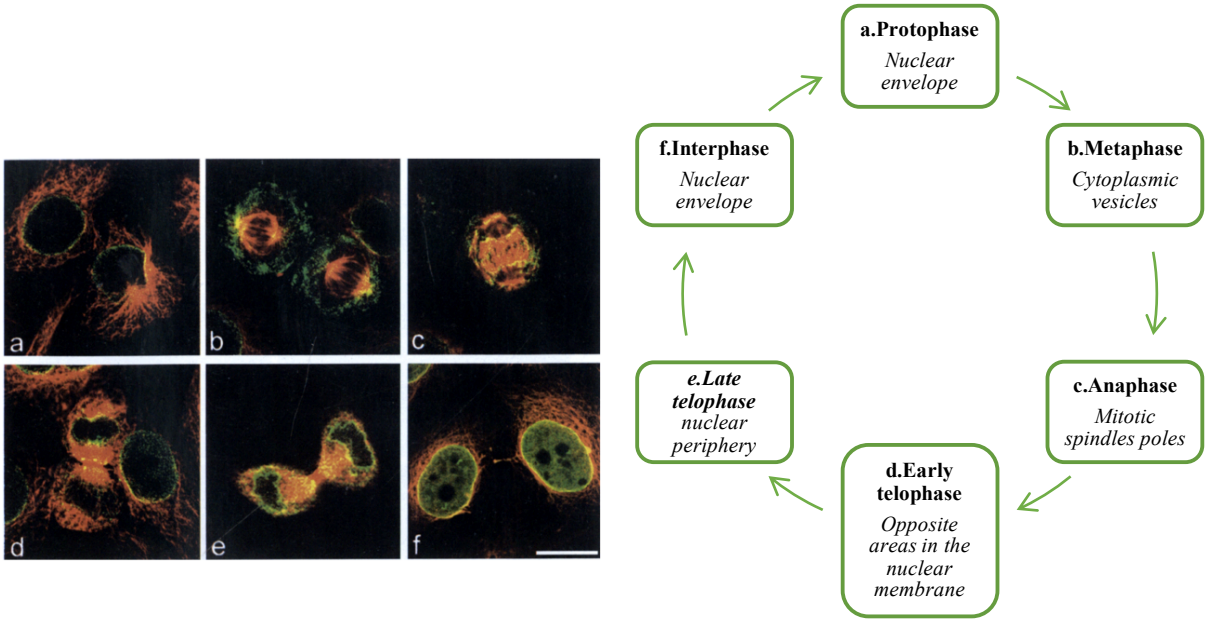

Figure 6 Localization of emerin during mitosis[71]. Left panel: Immunofluorescence images of emerin (in green) and β-tubulin (in red) stainings showing the localization of the former with respect to the latter in unsynchronized HEp-2 cells during mitosis (a) prophase, (b) metaphase, (c) anaphase, (d) early telophase, (e) late telophase, (f) interphase. Scale bar, 10 μm. Right panel: summary of the localization of emerin during mitosis.

3.4 Emerin partners and functions

Owing to its diverse binding partners, emerin has myriad of functions in cells. This section sheds light on emerin's roles in maintaining nuclear architecture, regulation of transcription, signaling, and chromatin architecture. The functions are elucidated in terms of emerin's binding partners.

3.4.1 Nuclear architecture

3.4.1.1 Actin

Accumulating pieces of evidence have revealed how emerin anchors the cortical nuclear actin-myosin networks around the nuclear envelope. Holaska et al. were the first to show that emerin binds and stabilizes the pointed end of growing actin filaments, promoting its polymerization, *in vitro*[73]. Published and unpublished data have shown that the actin-binding region in emerin overlaps with the interacting domains of lamin A[36], nesprin-1α (James M. Holaska and Katherine L. Wilson, unpublished data), GCL, YT521-B[74,75].

In the same line, it has been recently demonstrated that emerin is enriched at the outer nuclear membrane upon the application of force on epidermal stem cells[69]. This enrichment was concomitant with the enrichment of non-muscle myosin IIA (NMIIA) to promote the polymerization of perinuclear F-actin[69]. Accordingly, there is reduced nuclear actin levels [69].

Emerin, together with myosin IIB, polarize actin flow and nuclear movement in migrating fibroblasts[76]. Nuclei of emerin-null fibroblasts either adopted non-directional movement or failed completely to move. Thus, emerin is crucial for cytoplasmic polarity and the directional actin flow[76].

Proteomic studies performed on HeLa cells nuclear lysates have shown that emerin binds directly, *in vitro*, nuclear myosin I (NMI) and nuclear specific spectrin isoform αII (αII-

spectrin). Nuclear myosin I is an isoform of myosin I, which is specifically located in the nucleus. It is involved in rRNA gene transcription and interacts with the nuclear pore basket[77]. Spectrin is a cytoskeleton protein present in eukaryotic cells at the intracellular side of the plasma membrane. It maintains the cytoskeleton structure, plasma membrane integrity, and genomic stability[78].

Taken all together, the aforementioned evidences highlight how emerin contributes to the cell architecture via its roles in anchoring the cortical nuclear actin-myosin network to the nuclear envelope.

3.4.1.2 LINC complex

As mentioned earlier, the LINC complex is considered the bridge that connects the cytoskeleton to the nucleus and relays the mechanical forces from the outside of the nucleus, across the nuclear envelope to the nucleoskeleton[79] (Figure 7).

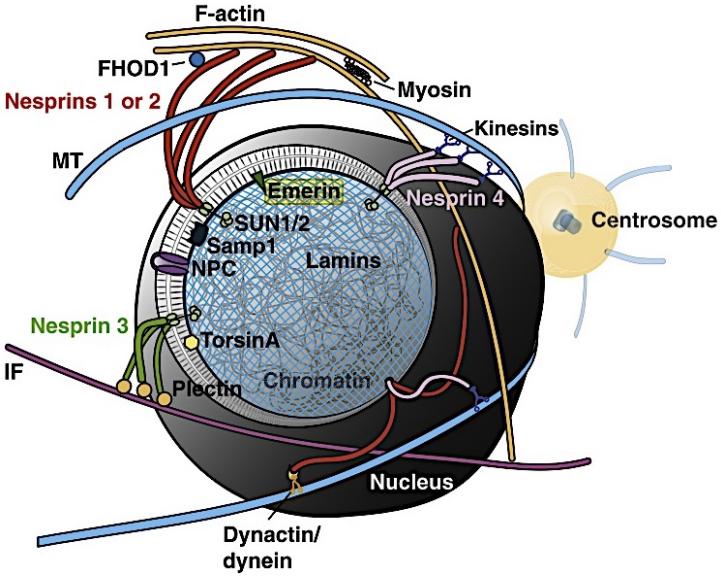

Figure 7. LINC complex and its associated proteins clinging to the nucleus[79]. The nuclear envelope sliced off exposing the nuclear lamina (blue mesh) and chromatin. Inner nuclear envelope proteins SUN1/2, Samp1 and emerin regulate interaction with different isoforms of KASH-domain containing nesprins (1-4). Nesprins, in turn, bind cytoskeleton either directly or indirectly via small adaptor proteins.

The LINC complex has numerous cellular functions, such as cell division, organelle positioning, cytoskeletal organization, and transmission of force. The latter was extensively studied in the context of cell migration, adhesion, cell-matrix and cell-cell interactions. Regarding the model of LINC complex, nesprins localized at the outer nuclear envelope membrane interact, through their N-terminal domain, with the cytoskeletal actin and microtubules; and simultaneously bind, through their C-terminal conserved KASH-domain, SUN1 and SUN2 proteins across the luminal space. In turn, SUN proteins interact with the nuclear lamins, other inner nuclear envelope proteins, and chromatin[80]. Emerin directly binds lamins and nesprins, thus, it owns fundamental roles in mechanostransduction, the process by which cells detect, interpret, and respond to mechanical stimuli.

Numerous studies have shown how several nuclear proteins play key roles in nuclear response to mechanical force, including SUN1/2, lamin A/C, and emerin. Upon application of force on isolated nuclei via nesprin-1, there is an increased rigidity as an adaptation to mechanical force[81]. On the other hand, the isolated nuclei of emerin-null cells have defective response preventing nuclear adaption to stress[81]. In addition, it has been proven that isolated nuclei phosphorylate emerin in response to force, particularly on residues tyrosine 74 and 95[81]. Emerin mutant, which is resistant to phosphorylation on these two residues, fail to adapt to force and show less bundled actin filament polymerization at the nuclear surface. Further, the application of mechanical forces to the plasma membrane or cytoskeleton causes the deformation of the nucleus and triggers the expression of mechanosensitive genes[81]. However, emerin-null fibroblasts show impaired expression of mechanosensitive genes (EGR-1 and IEX-1) in response to mechanical stress, and apoptosis was induced in these cells[82]. In addition, emerin-null cells adopt altered nuclear envelope elastic properties or increased nuclear fragility[83]. Lastly, emerin may be involved in longer term cellular adaptations after mechanical signals via regulating the expression of mechanoresponsive transcription factors, such as

megakaryoblastic leukemia 1 (MKL1). MKL1 is a mechanoresponsive transcription factor important for smooth muscles differentiation with anti-apoptotic and cardiac functions[84]. Upon mechanical stimuli, MKL1 detaches from cytoplasmic G-actin and translocates to the nucleus[85]. Interestingly, LMNA null cells, which have defective translocation and downstream signalling of MKL-1, display normal MKL-1 translocation following ectopic emerin expression. Taken all together, these finding outline emerin's importance in mechanotransduction by mediating nuclear stiffening, cytoskeletal actin polymerization, and gene regulation.

3.4.1.3 β-tubulin

Early confocal images have proffered the interaction between emerin and microtubules when they captured the co-localization of emerin and β-tubulin near mitotic spindles in the middle of mitotic cells[71]. Then live fluorescence imaging evidenced the concentration of emerin at the kinetochores during the nuclear envelope assembly[86]. Contrary to lamin A/C-null mouse embryonic fibroblasts, the absence of emerin in X-EDMD doesn't provoke striking cytoskeletal disorganization. Nevertheless, the detachment of the centrosome characterizes emerin-null cells[87]. In an attempt to justify this observation, the study points out that a fraction of emerin localize at the outer membrane of human dermal fibroblasts (HDF) where it binds tubulin, and they both anchor the centrosomes, henceforth, underlining the linkage between the tubulin cytoskeleton and the outer nuclear envelope membrane through the centrioles[87].

3.4.2 Chromatin architecture

Although it is agreed that members of the nuclear lamina localize and maintain repressed chromatin near nuclear envelope, the question that remains unanswered is how they manage to do that. Rising pieces of evidence that substantiate the roles of emerin in genomic organization are discussed in this section.

DNA adenine methyltransferase identification (DamID) profile of emerin shows nearly identical results to that of DAM-LMNB1 in which that majority of lamina-associated domains (LADs) harbor chromatin modifications (decrease in H3K4me2 and increase in H3K27me3 and H3K9me2) consistent with compaction of chromatin and transcription repression[88].

Emerin, as enumerated earlier, binds directly various transcription regulators. In addition, emerin-null cells are associated with less repressed chromatin and increased gene expression. For example, EDMD patients' fibroblasts and muscle cells display less repressed chromatin both at the nuclear periphery and in the nucleoplasm. In addition, emerin-null myogenic progenitors adopt epigenetic signatures of relaxed chromatin architecture (increased H4K5ac and H3K4me2, decreased H3K27me3). These changes are seen all over the nucleus, and not restricted to the nuclear envelope; highlighting the open conformation of the chromatin in emerin-null cells[89].

Emerin recruits HDAC3, member of the NCoR complex, to the nuclear lamina, localizes it to the nuclear envelope where it binds directly to it with affinity 7.2 μM stimulating its activity 2.5 folds *in vitro* (increasing its Vmax and Km)[89]. For emerin to boost HDAC3 activity, it is suggested that the binding of HDAC3 to emerin may trigger a conformational change in the former or stabilize the binding of HDAC3 to the deacetylase activation domain (DAD) of NCoR complex. Interestingly, emerin missense mutations (Δ95-99, S54F, Q133H and P183H) causing EDMD failed to bind to HDAC3[89].

Another key point is that another LEM-domain protein, LAP2β, binds similarly HDAC3; mediating the acetylation of H4 and tethering the chromatin of chromatin to the nuclear envelope. Thus, it seems that there are overlapping roles for LAP2β and emerin in regulating genomic organization and tissue-specific gene expression[90]. All points considered,

it is suggested that emerin is inevitable for the maintenance of repressed chromatin and the repression of gene expression.

DamID: *A molecular biology technique that identifies the binding sites of DNA- and chromatin binding proteins in eukaryotes. The binding sites are mapped by expressing the DNA-binding protein of interest as a fusion protein with DNA methyltransferase. The binding of the protein of interest approaches the methyltransferase to the DNA. Since methyltransferase does not occur naturally in eukaryotes, hence the DNA methylation signifies the binding of the fusion protein to DNA and identifies the binding region.*

NCoR complex: *Is a repressive chromatin complex composed of TBL1/TBL1R, GPS2, NCoR, and HDAC3. The deacetylase activation domain (DAD) is the binding domain of HDAC3, which is needed for its activation. Next to DAD is the histone interacting domain (HID), which binds the unacetylated H4 N-terminal tails. It is hypothesized the deacetylation of H4 by HDAC3 induce the binding of H4 to TBL1 and HID, thereby the NCoR complex is stably bound to chromatin.*

3.4.3 Regulation of transcription

Emerin binds to several transcription factors or regulators, such as: GCL, Lmo7, β-catenin, BAF, Btf, and SIKE; triggering the expression of their target genes. In the same line, emerin mediates the expression of a number of cardiac and skeletal muscles genes.

3.4.3.1 Germ cell-less (GCL)

GCL is a transcription repressor that is conserved from *Caenorhabditis elegans* to humans. It is not a nuclear envelope integral protein, but rather a nuclear matrix protein, which binds several nuclear structures, such as: lamins, chromatin, and E2F-DP transcription factor[91]. Emerin, as well as other LEM-domain proteins, interacts directly with GCL, with 30 nM affinity, through emerin's regulator binding domain (RBD) -1 and RBD-2[75]. GCL binds to the DP3 subunit of E2F-DP3 heterodimers, repressing the transcription of their target genes. The latter are involved in the transition of cells from G1 to S phase. Hence, GCL acts similar to the well-known p-Rb as a transcription repressor. Downregulation of emerin results in the

mislocalization of GCL to the cytoplasm, together with the stimulation of E2F-orchestrated gene expression. That's to say, emerin restricts the expression of E2F-DP3 mediated genes, and thereby cell proliferation. What goes well with this observation is another study that has documented the augmentation of cell proliferation in emerin KO cells[75].

3.4.3.2 Btf

Bcl-2 associated transcription factor, Btf, is a transcription repressor, which is expressed in various tissues and markedly expressed in skeletal muscles. Biochemical studies have indicated that emerin directly binds Btf with 100 nM affinity. The Btf binding domains were mapped to residues 45-83 and 175-217 on emerin, i.e flanking lamin A/C binding region[92].

In addition, it has been shown that Btf is recruited at the nuclear envelope upon apoptosis. When Btf is overexpressed, it induces cell death by binding to and inhibiting the anti-apoptotic Bcl-2 family. In fact, Bcl-2 and emerin bind to neighboring regions on Btf. That's to say that when Btf receives apoptotic signals, it has to choose whether to bind emerin, and inhibit apoptosis, or bind BCL-2, and promote apoptosis. It is postulated that upon apoptosis, Btf releases Bcl-2 and relocalizes at the nuclear envelope where it binds emerin. The latter will in turn inhibit the pro-apoptotic effects of Btf, thereby it protects the skeletal muscles from apoptosis[92].

In the same line, the S54F emerin missense mutation, which causes EDMD despite normal emerin expression and localization, selectively impedes binding to Btf [92]. What further supports the perception of emerin as a nuclear envelope guard against apoptosis is that in EDMD, when emerin is lost, we see muscle wasting which involves apoptosis. By the same

token, emerin null fibroblasts displayed decreased igr-2 (an anti-apoptotic gene) expression in response to mechanical stimulation[82].

3.4.3.3 Lim-domain-only 7 (Lmo7)

Lmo7 is considered as a shuttling transcription activator between the nucleus and the cell surface. Emerin and Lmo7 act as mutual regulators and emerin, astonishingly, regulates Lmo7 both positively and negatively[93]. As a positive regulator, Holaska et al., have illustrated that emerin is necessary for the nuclear localization and accumulation of Lmo7, possibly by modifying Lmo7's export kinetics or its affinity for nuclear targets, so that Lmo7 can eventually reach its target genes. As negative regulator, emerin directly binds Lmo7 with affinity 125 nM and functionally inhibits it[93].

Two mechanisms have been put forward for this inhibition: the direct sequestration of Lmo7 at the nuclear envelope or the inhibitory post-translational changes of Lmo7 by emerin associated protein complexes. On the other hand, Lmo7 positively regulates the expression of emerin. Ultimately, it seems that Lmo7 acts as a sensitive emerin sensor; when emerin is bound to its partners or limited, Lmo7 stimulates emerin's expression, whereas when emerin is free or unbound, Lmo7 binds to it and gets inhibited[93].

Emerin missense mutation P183H, in spite of having normal emerin protein level and localization, results in classical EDMD. This mutation fails to bind Lmo7, whereas it exhibits normal binding to several other emerin partners (BAF, nesprin-1α, lamin A, GCL, bf, MAN1, YT521 and actin). This result evidently portrays a defective Lmo7 activity as a molecular mechanism for EDMD in patients with P183H mutation[93].

3.4.3.4 β-catenin

β-catenin is a transcriptional co-activator of the canonical Wnt signaling pathway and is involved in several developmental processes. Markiewicz et al., have been the first to identify the interaction between β-catenin and emerin through its conserved adenomatous polyposis coli (APC)-like domain. They have shown that emerin prevents β-catenin nuclear accumulation, and that the correct nuclear localization of emerin is essential for this action[94].

Regarding the mechanism by which emerin could restrict β-catenin to the cytoplasm, it is suggested that the phosphorylation of emerin might promote the nuclear export of β-catenin[94]. To enumerate, it is hypothesized that the binding of β-catenin to emerin would retain the β-catenin at the nuclear envelope and evoke a conformational change in the intrinsically disordered nucleoplasmic region of emerin, where β-catenin binds, that eventually lead to the export of β-catenin via the NPC. This change in conformation may be triggered by phosphorylation of emerin, since major phosphorylation sites (Ser163, Tyr167 and Ser175) of emerin are close to binding domain of β-catenin[94].

In 2002, Lickert et al., have highlighted the importance of Wnt/β-catenin pathway during cardiac development when their β-catenin KO mice grew multiple ectopic hearts[95]. In addition, it has been shown that β-catenin regulates normal (physiological) and stress-induced (hypertrophy) growth of the heart [96]. In view of the involvement of cardiomyopathy in EDMD, the role of emerin as a modifier of Wnt/βcatenin signaling in normal and EDMD heart has been investigated[97]. Indeed, it has been underlined that emerin binds β-catenin at ICD of cardiomyocytes[98], where β-catenin is an important component of adherens junctions and mediates cell-cell contacts.

Lastly, the work of Stubenvoll et al., have divulged how emerin is crucial for regulating Wnt/β-catenin signaling in cardiomyocytes. First, the depletion of emerin during early developmental stages has limited cardiomyocytes differentiation and promoted their

proliferation due to enhanced Wnt/β-catenin activity. Second, emerin was essential for normal cardiac function and response to pressure-induced cardiac overload. Lastly, they were able to restore the emerin-mediated cardiac dysfunction in emerin-null mice by inactivating a single allele of β-catenin[97].

It is important to realize that defects in other LEM domain proteins (Man1 and LAP2α) result in cardiac abnormalities also, which suggests a broad significance of LEM proteins in the regulation of heart function and morphogenesis[20,99].

3.4.3.5 Barrier-to-auto-integration factor (BAF/Banf1)

BAF is a highly conserved metazoan protein, which was first discovered due to its ability to cross-bridge the DNA of Moloney Murine Leukemia Virus (MoMLV) thus blocking its auto-integration, hence the name[100]. It is a small (10 kDa; 89 residues) protein that forms obligate dimer, which binds two dsDNA molecules[101].

BAF is widely diffused in the nuclei, however it can be restricted to certain locations during specific times. For example, BAF concentrates at the telomeres during anaphase likewise, it localizes at chromosome core regions, which are the central regions of the assembling nuclear rim, at telophase. It has several binding partners, such as: all LEM-domain proteins, histones (H3, H4 and H1.1 linker histone)[102], Cone-Rod homeobox (CRX)[103], lamin A, and Vaccinia-related kinase (VRK)[104].

Emerin directly binds BAF in a LEM-domain dependent fashion[36,38]. It is suggested that BAF and LEM-domain proteins co-evolved together seeing their conserved interaction. In cells, BAF is important for post-mitotic nuclear assembly, cell cycle progression and cell viability. Several functions are known for emerin-BAF interactions. First, during telophase, BAF recruits emerin, by binding to its LEM domain, to the core region. This recruitment is fundamental for emerin's nuclear localization during nuclear assembly[105] and the attachment

of chromatin to the inner nuclear membrane[106]. Interestingly, phosphorylation plays pivotal roles in emerin-BAF interactions. On one hand, the dissociation of emerin from BAF is regulated by the M-phase phosphorylation of the former at serine 175[107]. On the other hand, phosphorylation of BAF during interphase, specifically at serine 4, inhibits nuclear localization of emerin and the binding of the latter to lamin A[108]. Accordingly, it is suggested that BAF is phosphorylated in order to export emerin from the nuclear envelope or impede emerin's binding to lamin A, whenever needed. Comparatively, BAF is dephosphorylated to enable recruitment of emerin to the core region during telophase[108]. Mutation A12T in BAF leads to the mislocalization of emerin to cytoplasm and present a premature aging syndrome, called Nestor-Guillermo progeria syndrome (NGPS)[109,110].

Second, emerin proteomic studies performed in HeLa cells have shown that BAF and emerin co-exist in different influential complexes. One of these complexes comprises Histone Deacetylases 1 and 3 (HDAC 1 and 3). Therefore, it is suggested that BAF-emerin interaction may, also, be involved in the repression of chromatin at the nuclear envelope[111].

Third, it is hypothesized that emerin-BAF interaction is important for genomic integrity and that it regulates DNA damage responses. That's because emerin and BAF associate with DNA repair proteins, namely: Cullin 4 (Cul4), member of the Cul4-DDB-ROCI complex; and damage-specific DNA binding protein 2 (DDB2), member of the UV-DNA-damage-binding protein complex UV-DDB, upon exposure to UV light in HeLa cells[101]. Ideally, ionizing radiation provokes the phosphorylation of histone 2 variant, H2AX, which forms nuclear foci at the sites of the radiation-induced DNA double-strand breaks, and correspondingly recruits the repair factors to these nuclear foci[112]. However, lamin A mutations (AD-EDMD disease-causing mutations, G232E, Q294P or R386K), that bind less efficiently to emerin and mislocalize it, impair histone H2AX phosphorylation subsequent to UV light exposure[113].

Lastly, it was shown that, through BAF, emerin binds the cDNA of human immunodeficiency type 1 (HIV-1), thus playing an essential role in the integration of the viral cDNA, and disease infection[114].

3.4.4 Signaling

Investigations have shown that depletion of emerin in mice and humans disrupts the expression of number of genes regulated by retinoblastoma Rb1 and MyoD pathways during muscle regeneration. As a result, both human patient and mice muscle cells lacking emerin suffer from delayed differentiation during regeneration[115,116].

Genome-wide expression profiles have been conducted in hearts from emerin knock out mice. They display activation of the ERK1/2 branch of the mitogen-activated protein kinase (MAPK) pathway, as well as of downstream targets involved in cardiomyopathy[117].

Recently, using RNA sequencing technology, it has been highlighted that mice emerin-null myogenic progenitors exhibit delayed cell cycle exit, upon receiving differentiation signals, which is indispensable for proliferating myogenic progenitors to proceed with differentiation. These cells fail to reorganize their genome, a critical step required for temporal expression of essential differentiation genes, including MyoD, Myf5, Pax3 and Pax7. In other words, loss of emerin caused a defect in a key transcriptional reprogramming step owing to defective genomic reorganization of loci containing myogenic differentiation genes[118].

In the same study, multiple signaling pathways were altered in emerin-null myogenic progenitors, including insulin-like growth factor 1 (IGF-1) signaling, which is involved in the growth of satellite cells; JAK-STAT pathway, which is important for the expansion of satellite cells numbers; Polo-like (PLK) kinase signaling, which is involved in cell cycle withdrawal; transforming growth factor β (TGF-β), Wnt, and Notch pathways, which are all involved in satellite cells activation, myogenic differentiation and skeletal muscle regeneration upon

injury. In accordance with the idea that emerin clutches a repressive signal on the chromatin near the inner nuclear membrane, myogenic progenitors lacking emerin exhibit greater number of expression transcripts signifying the loss of emerin's repressive function[118].

3.5 Post translational modifications

3.5.1 Phosphorylation

Emerin accommodates around 40 possible phosphorylation sites (18 tyrosines, 27 serines/threonines). These sites are modified by well-studied serine/threonine kinases including protein kinase A (PKA), ERK2/MAPK, GSK3β and protein kinase C (PKC) delta. For example, during lentiviral infection, ERK2 phosphorylates emerin directly *in vivo* and the hyper-phosphorylation of emerin, provoked by the virus, results in the mislocalization of emerin to the outer nuclear envelope membrane[119].

Emerin is considered as a tyrosine phosphorylation target for both receptor and non-receptor protein tyrosine kinases. It is phosphorylated *in vivo* by the receptor protein kinase, Her2[120]. Interestingly, Her2 knock-out cardiomyocytes suffered from dilated cardiomyopathy coupled with contractile defects that lead to sudden death[121]. In like manner, mice muscles lacking Her2 showed poor motor. As can be seen, Her2 can offer new mechanism for EDMD.

Two non-receptor protein tyrosine kinases phosphorylate emerin namely, Src and Abl. Both kinases are members of Src family kinase (SFK). There are several sites predicted to be directly phosphorylated by Src, at least three of them (59,74, and 95) represent the majority of Src-regulated sites in emerin *in vitro* and in HeLa cells. Src signaling is of physiological relevance in skeletal and heart muscles, which are the main tissues affected by EDMD. Additionally, LAP2β, whose mutations are associated with cardiac defects, is similarly

phosphorylated by Src *in vitro*[120]. The other non-receptor protein tyrosine kinase is Abl, whose main phosphorylation site on emerin is suggested to be tyrosine 167[120].

Several functions are assigned for emerin phosphorylation. Guilluy et al. demonstrated that isolated nuclei respond to applied force via nesprin-1 by nuclear stiffening and phosphorylating emerin, particularly at tyrosines 74 and 95 by Src kinase[81]. Not only externally applied force but also cell-generated contractility, triggered by plating cells on varying rigidity, increase emerin phosphorylation, showing that it is a response to forces experienced by the whole cell and not only externally applied forces to the nuclei[81]. It is, hence, suggested that cellular pre-stress regulate emerin phosphorylation[81]. Recently, it has been shown that emerin acts as a mechanosensor via the phosphorylation of tyrosine 99 when cells are plated on softer matrices. In the same study, it was underlined that emerin phosphorylation modulates the spatial organization of chromosome 18 and 19 territories in interphase nucleus in the same cells[122].

In addition, it has been elucidated that emerin phosphorylation regulate its binding to one of its partners, BAF. BAF binding to emerin was strikingly reduced in HeLa cells treated with tyrosine phosphatase inhibitor. In the same study, the phosphorylation of tyrosine hydroxyl moieties of LEM-domain (BAF known binding site in emerin) at residues 4, 19, 34; emerin central domain tyrosine residues 59, 74, 95; and membrane proximal residue 161 was shown to affect BAF binding. Particularly, the phosphorylation of the conserved tyrosine 19 and 34 can co-ordinately inhibit BAF binding in HeLa cells. Whereas the phosphorylation of tyrosine 4, by unidentified kinases, leads to the release of bound BAF since this tyrosine demonstrate chief significance for BAF binding. By the same token, the phosphorylation of emerin at serine 175 in Xenopus egg cell-free system lead to the dissociation of emerin from BAF[107].

Moreover, it is suggested that emerin phosphorylation mediate emerin-actin dynamics in muscle cells. Lattanzi et al. have emphasized that λ-phosphatase, a serine/threonine phosphatase, stabilizes the emerin-actin interaction, whereas the dephosphorylation of emerin by protein phosphatase 1 (PP1) reduce the interaction between actin and emerin in differentiating mouse myoblasts. Such contradictory observations drove the hypothesis that the modulation of emerin-actin interaction by phosphorylation may be regulated by different differentiation stimuli[123].

In addition, phosphorylation is known to have principal significance during nuclear disassembly. Emerin is phosphorylated in a cell-cycle-dependent manner in human lymphoblastoid cells lines; it is hyper-phosphorylated during M and early S phases before the nuclear disassembly[124]. In like manner, human emerin is undergoing cell cycle-dependent phosphorylation at five residues in Xenopus egg cell-free system[107]. With all of this in mind, it came with no surprise that emerin missense mutation, Δ95-99 causing X-EDMD, has altered emerin phosphorylation during cell-cycle[124].

3.5.2 O-GlcNAcylation

O-GlcNAcylation is a metazoan post-translational modification, that involves the attachment of O-linked β-N-acetylglucosamine (O-GlcNAc) moiety to proteins. It is implicated in different processes in the cells, including epigenetic regulations, cell signaling, modulation of transcription and acting as stress and nutrient sensor[125].

Emerin owns features that define proteins modified by O-GlcNAc: it is rich in Ser/Thr residues and contains vast intrinsically disordered regions. Berk et al. have highlighed that emerin is highly O-GlcNAcylated in mammalian cells. Eight serine residues have been identified as sites of emerin O-GlnNAcylation, including: S53, S54, S87, S171, and S173[126]. Notably, S54F is mutated in X-EDMD patients[127]. In the same study, Berk's group has

underlined that O-GlcNAc, similar to phosphorylation, regulates binding to BAF. Astonishingly, the different post translational modifications of S173, either by O-GlcNAc or phosphorylation, have opposing effects on BAF binding. To enumerate, phosphorylation of S173 reduces BAF binding, whereas O-GlcNAc of S173 increases BAF binding. BAF is not the only emerin partner affected by O-GlcNAc, lamin B and chromatin (histone H3) show increased binding to emerin after O-GlcNAc[126].

3.6 Emerin in disease

X-linked Emery Dreifuss Muscular Dystrophy (X-EDMD)

EDMD is a rare muscular dystrophy clinically characterized by early contractures, slowly progressive humero-peroneal muscle weakness and atrophy, and cardiac involvement which presents as conduction defects, arrhythmias and dilated cardiomyopathy.

3.6.1 Epidemiology

The data regarding the epidemiology of EDMD is scarce and the overall prevalence of EDMD is unknown. Older studies have estimated EDMD to be the third most common muscular dystrophy after Duchenne and Becker muscular dystrophies with X-EDMD prevalence estimated to range from 1 in 300, 000 to 1 in 100,000[128]. However, more recent studies have promoted X-EDMD prevalence as 0.1-0.20 in 100,000[129]. Be that as it may, there is considerable agreement that AD-EDMD is more common than the X-linked one, and that AR-EDMD is the rarest.

3.6.2 Pathophysiology

X-EDMD belongs to the so-called envelopathies, which is a group of rare genetic human diseases caused by mutations of genes of nuclear envelope proteins. Several genes are

causative of EDMD (*LMNA*, EMD, FHL1, TMEM43, and SYNE1/2) and their mode of inheritance is variable (autosomal dominant AD or recessive AR, X-linked) (Figure 8**).**

There is an on-going dilemma in the muscular dystrophy field concerning the pathophysiology of EDMD. The exact mechanism by which mutations in a single gene, that is almost ubiquitously expressed, cause the tissue-specific clinical features of EDMD, as well as the relationship between changes in a nuclear envelope protein and the observed clinical symptoms in EDMD remain elusive. A point often overlooked is that the different nuclear envelope proteins, of ideally different roles and partners in the cells, cause the same pathological manifestations in EDMD patients. This suggests that the different mutations can cause defects in numerous pathways, but they will all travel down a common road in order to eventually result in the same disease, by pursuing a common general mechanism. Therefore, it comes with no surprise that the molecular signature present in hearts of emerin null mice is similar to that in *LMNA* knock in ones[117]. It must be remembered as well that almost half of EDMD cases are due to unknown causes, which promotes the hypothesis that tissue-specific NETs may be involved in the pathogenesis of EDMD (E. Schirmer, personal communication).

Having said that, there are two pathophysiological hypotheses suggested for EDMD. The first hypothesis, gene regulation one, links EMD mutations and associated defects in the nuclear envelope proteins and the nuclear lamina to consequent disorganization of nuclear chromatin and gene expression. The second hypothesis, structural one, proposes that EMD mutations weaken the nuclear lamina. Consequently, tissues that are steadily subjected to mechanical stress, such as the skeletal muscles and heart, are unable to withstand such stress because of their structural and signaling failings[130].

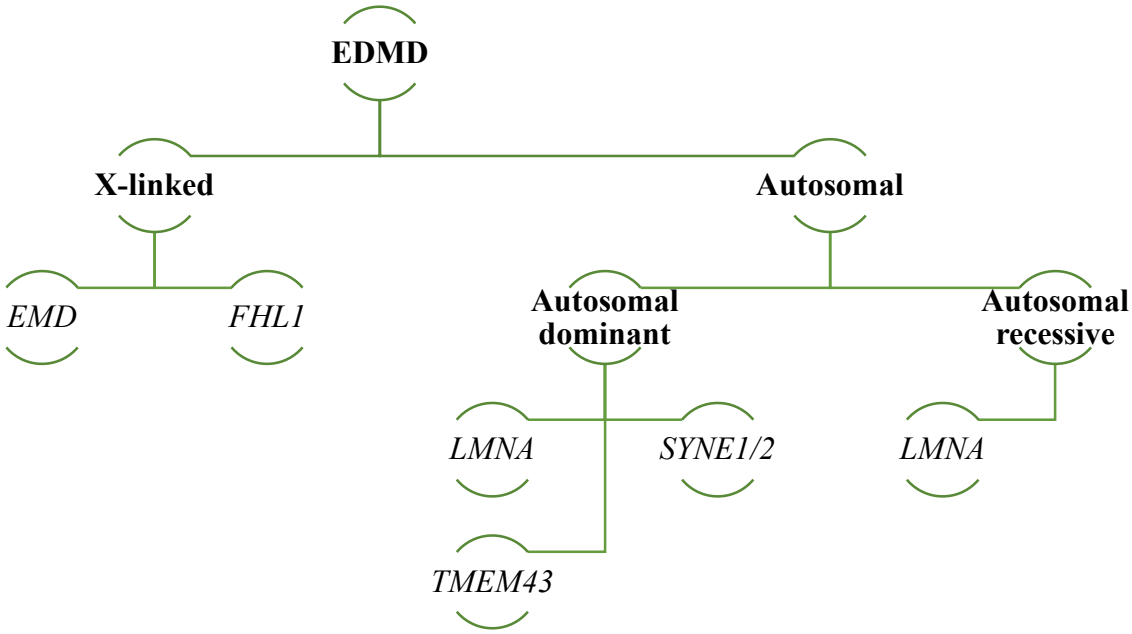

Figure 8. Diagram chart for EDMD causative genes and their modes of inheritance. There are versatile modes of inheritance for EDMD (X-linked, autosomal dominant or recessive). The majority (61%) of X-EDMD cases are due to mutations in EMD gene encoding the inner nuclear envelope protein, emerin. 10% of X-EDMD cases are due to mutations in FHL1 gene encoding for a four and a half LIM domains protein1(FHL1), which is not a nuclear envelope protein but it is expressed in striated muscles and very likely takes part in the assembly of sarcomeres. Concerning the autosomal dominant (AD-EDMD), 45% of the cases are due to mutations in *LMNA* gene, encoding the intermediate filaments lamin A and C. Mutations in genes such as TMEM43, encoding for the nuclear envelope protein TMEM43/LUMA protein or SYNE1 and SYNE2 genes, encoding for nesprin 1 and nesprin 2, respectively, result in AD-EDMD. Autosomal recessive EDMD (AR-EDMD) is caused exclusively by mutations in *LMNA* gene[198,199]. At the same time, ≈ 45% of all EDMD patients do not carry mutations in one of the aforementioned genes which suggests that other causative genes are still undiscovered.

3.6.3 Discovery of emerin and link to X-EDMD

The earliest documentation of the distinguishing clinical features of Emery Dreifuss Muscular Dystrophy (EDMD) may go back to **1902** when they were first noted by Cestan and Lejonne of Salpêtrière[131] and later on by Schenk and Mathias of Breslau in **1920**[132]. However, in neither of the reports were the cardiac features of the disease mentioned. In **1961**, Dreifuss and Hogan reported the same features in a large Virginian family (8 affected males in 3 generations) and described the disease as a rare benign variant of Duchenne Muscular Dystrophy (DMD) but of later onset, slower course and non-disabling nature maintaining

***Humeroperoneal distribution**: In anatomy humeroperoneal means pertaining to the humerus and the fibula. In other words, it means the proximal muscles of the upper limbs (biceps and triceps) and the distal muscles of the lower limbs (anterior tibial and peroneal muscles).*
***Scapulo-humero-pelvo-peroneal distribution**: Scapulo- for the pectoral girdle musculature (shoulders muscles), and pelvo for the pelvic girdle muscles (knee and hip extensor muscles).*

everyday activities[133]. Thereafter in year **1966**, Emery extensively restudied the Virginian family and interpreted the disease as unusual type of benign X-linked muscular dystrophy. He delineated a uniform course of the disease in which the flexion contractures of the elbows and shortening of Achilles tendons were the earliest symptoms; in addition to slowly progressive muscle weakness and wasting of the humero-peroneal area; accompanied later by cardiac involvement which was the most life-threatening symptom. Although the described muscular dystrophy resembled Becker in the mode of inheritance, benign course, and muscle weakness distribution; other features had set it from Becker apart: the cardiac involvement, early childhood elbows contractures, Achilles tendon shortening, lack of pseudo-hypertrophy, and the unaffected distal muscles. Likewise, what differentiated it from DMD was the late onset (age 4-5) , lower degree of disability, and normal intellectual abilities[134]. Thereupon, it was put into evidence for the first time that the described disease was a distinct type of X-linked muscular dystrophy. In the following years others described families with syndromes resembling Emery's family: X-linked early-onset scapuloperoneal[135] or humeroperoneal[136] syndromes. It wasn't until **1979** that the described X-linked muscular dystrophy was termed Emery-Dreifuss disease by Rowland et al.[137]. Provided that timely insertion of the cardiac pacemaker is life-saving, Emery defined clearly the distinctive features of EDMD in **1989** so as to support early diagnosis of the disease. He assembled the triad of (1) early contractures of Achilles tendons, elbows and post-cervical muscles; (2) slowly progressive muscle weakness and wasting with humero-peroneal distribution in the beginning and scapula-humero-pelvo-

peroneal one later in the course of the disease; and (3) a cardiomyopathy presenting mostly as cardiac conduction defect and later heart block[138].

One of biggest surprises in the field of muscular dystrophies was unveiled in **1994** when the gene for X-EDMD, EMD/STA gene, was first identified. EMD/STA was mapped to the X chromosome (Xq28). The sequence suggested that the protein product, the emerin protein, is a transmembrane protein due to the presence of ≈ 20 amino acid hydrophobic helix near its C-terminus[54]. Before then, it was expected that the emerin would be a plasma membrane/cytoskeletal protein since the genes associated with DMD, Becker, and most cases of limb-girdle, and congenital muscular dystrophies all encode sarcolemmal proteins[139]. Discovering in **1996** that emerin was a nuclear envelope membrane[140,141] came with a surprise owing to the ambiguity of the link between the absence of a nuclear envelope protein and the associated triad of symptoms in X-EDMD. What further supported the presence of a nuclear periphery defect in EDMD was the discovery of the gene responsible for the autosomal dominant form of EDMD, LMNA gene, which encodes another nuclear envelope protein, lamin A/C [142] (Figure 9).

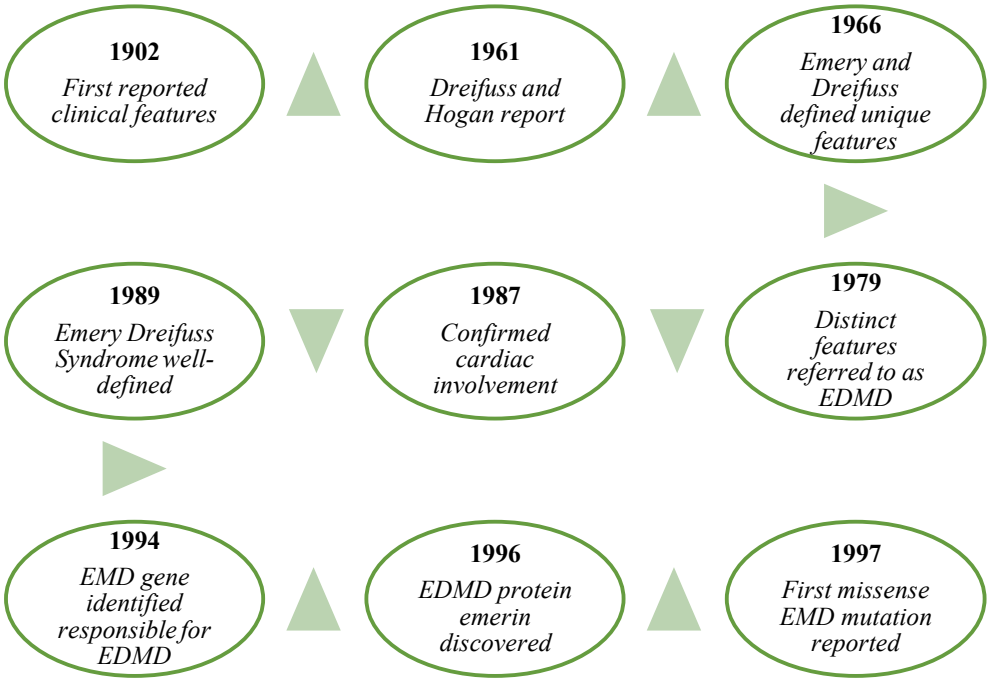

Figure 9 Tracing the discovery of EMD gene, emerin protein and EDMD

In the following years, EMD gene mutations present in EDMD patients were reported successively. According to UMD-EMD database there are 133 different EMD missense mutations reported in 448 patients (*last update 2013*). The majority (almost 93%) of EMD mutations are nonsense point mutations, small frameshifting deletions/insertions that introduce a stop codon, which result in complete loss of emerin. These mutations elicit the classical EDMD triad of symptoms. Conversely, there are, less common, emerin missense mutations (Table 3.a), which result in normal or reduced emerin level of normal localization or mislocalized to the cytoplasm (Table 3.b). The first EMD missense mutation resulting in reduction of emerin protein level was reported in 1997 which was the replacement of a glutamine residue at position 133 with histidine (Q133H)[143]. As shown in Table 3.b, some of the missense mutations (S54F[144], D72V[145], Q133H [143], P183T[146], P183H[144], R203H[147]) lead to non-functional emerin; resulting in classical X-EDMD despite the normal expression level and localization of emerin. The possible reason is the presence of these mutations in the nucleoplasmic domain of emerin, the hub of interactions with its binding partners. On the other hand, mutations (Δ235-240[148], and Δ236-241[146]), that result in reduced emerin expression, are mostly located near its transmembrane domain, which is a prerequisite for its correct nuclear localization.

Table 3.a Summary of EMD missense mutations (part 1)[149]

Mutation	Type of mutation	Number of patients	Number/gender		Origin	References
			Male	*Female*		
P22L	N/A*	2	2		N/A	Yaou et al., (2014) [150]
ΔK37	Inframe deletion	15	7	8	German, Russia, Poland	Karst et al., (2008) [151]
		11	6	5	Algeria	Ben Yaou et al.,

						(2007) [152]
T43I	N/A	1	N/A	N/A	N/A	*Ben Yaou, personal communication
S54F	Transition* (C → T)	1	1		Germany	Fairley et al., (1999) [144]
D72V	Transversion* (A → T)	1	1		Russia	Rudenskaia et al., (2006) [145]
Δ95-99	Inframe deletion	1	1		USA	Ellis et al., (1998)[124]
Q133H	Transversion (G → T)	1	1		Italy	Mora et al., (1997) [143]
P183T	Transversion (C → A)	7	5	2	UK	Yates et al., (1999) [146]
P183H	Transversion (C → A)	1	1		USA	Ellis et al., (1999) [144]
R203H	Transition (G → A)	1	1		Japan	Funakoshi et al., (1999) [147]
Δ235-240	Inframe deletion	4	1	3	UK	Manilal et al., (1998) [148]
Δ236-241	Inframe deletion	1	1		UK	Yates et al., (1999) [146]

*Transition: Interchange of two-ring purines (A⇔G) or one-ring pyrimidines (T⇔G)
*Transversion: Interchange between purines and pyrimidines (A or G⇔C or T)
*N/A: Not Available

Table 3.b Summary of EMD missense mutations (part 2)[149]

Mutation	Overall phenotype	Emerin protein level	Localization
P22L	ACD*	Reduced	Normal
ΔK37	ΔK37 + R298C/R298C* → X-EDMD + CMT2* ΔK37 → ACD ΔK37 + R298C/+ → CMT2	Reduced	Normal
T43I	ACD	N/A	N/A
S54F	X-EDMD	Normal	Normal
D72V	X-EDMD	Normal	Normal
Δ95-99	X-EDMD	Reduced	Mislocalized to cytoplasm
Q133H	X-EDMD	Slightly reduced	Normal
P183T	X-EDMD	Normal	N/A
	Asymptomatic		
P183H	X-EDMD	Normal	N/A
R203H	X-EDMD	Slightly reduced	N/A
Δ235-240	X-EDMD	Very reduced (<5%)	
	Asymptomatic	N/A	
Δ236-241	X-EDMD	Very reduced	Mislocalized

*ACD: Atrial Cardiac Disease
*R298C: *LMNA* mutation (transversion, C→T), associated with an autosomal recessive axonal type of CMT2
*CMT2: axonal Charcot-Marie-Tooth type 2

3.6.4 "Unique" EMD mutants present in patients with exclusive cardiac defect

This thesis focuses on three "unique" missense emerin mutations 1) all localize in the LEM-domain of emerin (P22L, ΔK37, and T43I) 2) their variants are present at low levels that can be detected in cells (P22L and ΔK37) 3) variants localize correctly at the inner nuclear envelope membrane (ΔK37 and P22L), and 4) present in patients with exclusively atrial cardiac defect (ACD) without any skeletal muscle involvement (P22L, ΔK37, and T43I). Patients bearing these mutations developed the cardiac phenotypes in late age stage (≈ age of 40) that required pacemaker implantation[149,152,153] ,R. Ben Yaou personal communication.

The ACD is characterized by bilateral atrial dilatation accompanied by atrial fibrillation, cardiac conduction defects and arrhythmias, which are the same cardiac defects present in classical X-EDMD[154]. Conversely, the cardiac defect in these mutations is distinct from the dilated cardiomyopathy (DCM), which is due to lamin A/C deficiency. DCM is primarily a ventricular defect that results in left ventricular enlargement accompanied by conduction defects or arrhythmias with no atrial involvement compared to ACD[155].

A total of 26 patients (13 females and 13 males) have been reported with the ΔK37 mutation from diverse geographic regions (Algeria, Germany, Poland and Russia)[152,156]. 18 of the 26 patients carried the ΔK37 mutation only, 5 carried both the ΔK37 and heterozygous *LMNA* R298C mutation and the remaining 3 carried the ΔK37 and homozygous *LMNA* R298C mutation. All patients carrying either ΔK37 or ΔK37 and heterozygous *LMNA* mutation (23 patients) developed ACD; whereas those who were homozygous for the *LMNA* mutation (3 patients) developed either X-EDMD and Charcot-Marie-Tooth type 2 (CMT2) or CMT2 only. The P22L and T43I mutations have been reported in 2 and 1 patients, *respectively*. Notably, the cardiac defect was more severe in P22L and T43I patients than ΔK37 ones[149,152,153] (R.Ben Yaou, personal communication).

3.6.5 Why is ΔK37 more frequent than any other EMD missense mutation?

Study of the exon distribution of mutations within EMD gene has identified exon 2 as a hot spot and an overall non-random mutations distribution in EMD gene when analyzing 130 EMD mutations for recurrent patterns[157]. Interestingly, exon 2 present an almost twofold non-random higher relative mutation frequency than expected. Such high frequency of mutations in exon 2 suggests either the prominent sensibility of exon 2 for harbouring mutations or the high tendency of mutations occurring in this exon for developing EDMD phenotype.

Additionally, there is an inherent genomic instability in exon 2 exemplified in the larger number of unequal crossing over and single nucleotide substitutions compared to other exons. Exon 2 has a striking high GC content rendering it the most GC-rich exon in EMD gene. It is proposed that these GC-rich regions will comprise hypermutable methylated CpG dinucleotides creating mutations hotspot at exon 2[157]. Taken together, these pieces of evidences may rationalize the unusually high frequency of ΔK37, which happens to be present in exon 2.

3.6.6 Clinical description and prognosis

Typically, the first symptoms of the disease are the joint contractures that begin in early childhood, generally during the first two decades, and predominate in the ankles, elbows, and post-cervical muscles. The latter is responsible for the limitation of neck flexion then the entire spine movement, which in severe contractures cases may lead to loss of ambulation. Early toe walking, rigid spine and inability to fully extend the elbows are key diagnostic clues[158].

Regarding the muscle weakness and wasting, they begin in a humero-peroneal pattern then later extend to the pelvic and scapular girdle muscles. The progression of muscle wasting is rather slow till age 30, after which it accelerates. However, loss of ambulation is rare in X-EDMD, compared to AD-EDMD[158]. Lastly, the cardiac defect usually occurs by the fourth decade and presents as presyncope and syncope, palpitations, poor exercise tolerance, brady-

or tachy-arrhythmias, dilated cardiomyopathy, and congestive heart failure[159]. It's important to realize that inter- and intrafamilial variability in age of onset, severity and progression of cardiac and muscular defects is very common[160].

Clinical terminology

Contracture: *The stiffening or shortening of connective tissues, muscles or skin leading to decreased range of motion and movement.*
Presyncope: *It is the feeling that someone almost fainted but without losing consciousness. It is accompanied by lightheadedness, blurry vision, and general weakness. The reason behind presyncope is usually cardiovascular where orthostatic hypotension is the common cause.*
Syncope: *It is fainting or complete loss of consciousness, and muscle strength of short duration and spontaneous recovery. Syncope reasons can be heart or blood vessel related, orthostatic hypotension or neutrally-mediated reflex.*
Palpitation: *Noticeable strong, rapid or irregular heartbeat due to exertion, agitation or illness.*
Bradyarrhythmia: *Describes slow heart rate (<60 beats per minute.) It comprises a number of rhythm disorders including atrioventricular conduction disturbances and sinus node, the heart's natural pacemaker where the electrical impulses begin, dysfunction.*
Tacharrythmia: *Defined as heart rate that exceeds normal rate (>100 beats per minute). It may be supraventricular, such as atrial flutter, atrial tachycardia, or atrial fibrillation, or ventricular, such as ventricular fibrillation or ventricular tachycardia.*
Dilated Cardiomyopathy: *Characterized by decreased function of the left ventricle associated by its dilation, is a condition in which the heart enlarges and becomes unable to pump blood effectively.*
Congestive heart failure: *It is a condition in which the heart fails to pump blood and oxygen around the body causing the blood and fluid to build into the lungs, feet, and legs.*

3.6.7 Management and treatment

At present, there are no etiological treatments for EDMD, thereby the available treatment is rather preventive/ or symptomatic. Management of EDMD comprises several strategies: *treatment of manifestations, prevention of primary manifestations, prevention of secondary manifestations, surveillance,* and *evaluation of relatives at risk. Treatment of manifestations* includes orthopedic surgery to release contractures and scoliosis; mobility aids (canes, walkers, wheelchairs, orthoses) to support ambulation; antiarrhythmic drugs, defibrillator, cardiac pacemaker to control cardiac symptoms as needed or heart transplantation

in case of heart failure; respiratory aids (mechanical ventilation, respiratory muscle training, assisted coughing techniques) as needed in progressive restrictive respiratory insufficiency in late stages. *Prevention of primary manifestations* embraces regular physical therapy and stretching to avoid contractures, and defibrillators implantation to prevent risk of sudden death. *Prevention of secondary manifestations,* such as thromboembolism of cardiac origin, can be achieved by using antithrombotic drugs. *Surveillance* for the cardiac (ECG, Holter monitor and echocardiography) and respiratory functions should be done at least annually. Lastly, *evaluation of relatives at risk* is highly recommended in particularly for female carriers of EMD mutations because they are usually asymptomatic, but they can develop later a cardiac disease[158]. Evaluations comprise molecular testing if pathogenic variants of EDMD causing mutations are known in the family or cardiac evaluation if they are unknown [158].

Clinical terminology

Scoliosis: *Abnormal sideways curvature of the spin that occurs most often during the growth spurt before puberty.*
Cane: *Is the simplest walking aid, which resembles a walking stick that is held in the hand and used as a crutch.*
Walker: *Is the most stable mobility aid, which consists of freestanding metal framework, placed in front of the user, with several points of contact on which the user grips during movement.*
Antiarrhythmic drugs: *Agents used in treatment of abnormal heart rates in order to restore the normal rhythm and conduction. There are different antiarrhythmic drug classes including sodium, potassium, and calcium channel blockers, and beta blockers.*
Defibrillator: *Is a device applied on patients in cardiac arrest to give a high energy electric shock to the heart via the chest wall.*
Antithrombotic drugs: *Agents that reduces the formation of blood clots (thrombi) by affecting the different blood clotting steps, such as: antiplatelet, anticoagulants and thrombolytic drugs.*
ECG: *It stands for electrocardiogram, which is used to record electrical activity of the heart muscle from different angles in order to identify and locate pathologies.*
Holter monitor: *Is a battery-operated portable cardiac monitoring device, it measures and records heart activity for 24-48 hours or weeks at a time.*
Echocardiography: *An echo test, also known as ultrasound of the heart, which is a sonogram of the heart, that is used to look at the heart's structure and function.*

3.6.8 Therapies under investigation

Although there is a unifying triad of clinical findings for the different subtypes of EDMD, these findings are eventually attained by traveling different paths depending on the mutated gene. Each EDMD associated gene encodes a protein that has various functions and interacts in a certain way with the NE to give rise to the disease phenotype. Unfortunately, little is yet known on how this occurs. At present, there are no clinical research protocols for EDMD, that had reached patient enrollment stage, available on ClinicalTrials.gov [161]. All current treatments are either symptomatic, preventive or to identify individuals at risk. However, they do not cure the disease. The way forward now is to understand the diversity in EDMD genes and mutations in order to develop novel treatments based on individual's mutation and response to treatment. In other words, EDMD future treatments should apply precision medicine rather than the "one size fits all" approach[162].

3.6.9 Animal models

There are two mouse models developed for EMD deficiency[163,164] , notwithstanding no vertebrate animal model for emerin deficiency recapitulates the clinical picture of X-EDMD in humans. For instance, there is absence of muscle weakness and wasting, joint abnormalities, and cardiac arrhythmias in these mice. Yet, mice older than 40 weeks of age display mild prolongation of atrioventricular conduction time, i.e delayed conduction time, and minor motor coordination problems and nuclear-associated vacoules[163]. After myotrauma, emerin-null mice also show disruption in Rb/MyoD pathway. In other words, they show some primary defects like the delayed muscle regeneration[164]. In contrast, AD-EDMD animal models expressing either *LMNA* knock-out mutation[67] or *LMNA* knock in mutation (*LMNA*$^{H222/H222P}$ [165] or N195K[166]) manifest cardiac and skeletal muscles dystrophic comparable to the conditions in patients. This is very intriguing since the clinical phenotype of AD-EDMD and X-EDMD is

very similar, yet not identical[154]. For example, joint contractures are a common early childhood symptom in both X-EDMD and AD-EDMD[154]. However, it is the first symptom to appear in X-EDMD, whereas muscle wasting precede it in AD-EDMD[154]. Also, muscle wasting results in most of AD-EDMD cases in loss of ambulation, which rarely happens in X-EDMD[154]. Finally, AD-EDMD patients are at higher risk for developing ventricular tachyarrhythmia and dilated cardiomyopathy compared with X-EDMD[154].

Collectively, the persevering question is: why do emerin-null mice exhibit a mild phenotype? It has been put forward that there may be biochemical redundancy by which cells compensate the loss of emerin since it is expressed in all tissues and not indispensable for the viability of cells. For example, LEM domain containing 2 and emerin are functionally redundant during myogenic differentiation of emerin-null mice[167]. In addition, one of the isoforms of LAP2 may be relevant in the "compensatory" mechanism, since *LAP2* gene is upregulated in EDMD patient muscle[116] and LAP2α, similar to emerin, is associated with cardiomyopathy[168]. As age advances, this compensatory mechanism could be inadequate in consistently stressed tissues. Hence, the individual shows symptoms of the disorder. It is very possible that these compensatory mechanisms are more effective in mice compared to humans. That's because mice life-span is shorter. Consequently, they do not show the symptoms of the disease.

Objectives and hypotheses

As mentioned earlier, the majority of EDMD-causing emerin mutations are nonsense mutations, which result in the complete loss of emerin on the protein level; and provoke the classical triad of symptoms in patients. Notwithstanding, this doctoral thesis is specifically concerned with three "unique" emerin missense mutations, which are all localized in its LEM-domain, the mutated emerin is detected in cells, and are manifested in patients with exclusive atrial cardiac defects without any skeletal muscle involvement. Hence, our primary research question is to determine what is peculiar about these mutations precluding the trigger of defects, which commonly couple EDMD.

The first objective of this thesis is to investigate for the first time the effects of three emerin LEM-domain missense mutations, namely: P22L, ΔK37, and T43I on:

a) emerin overall structure
b) emerin self-assembly capacity, which is essential for lamin A/C binding
c) interactions of emerin with its partners, BAF and lamin A/C

One of the intriguingly appealing features of these mutations is their location in emerin. Given the presence of the three mutations in the only folded region in emerin, the LEM-domain, we hypothesized that the mutations will impose alterations in the overall structure of emerin. That can in turn affect emerin localization, functions, and interaction with its binding partners.

Given that the LEM-domain is the binding site of the chromatin binding protein BAF, we further hypothesized that the mutations will disrupt this interaction. Such disruption could result in tissue-specific effects, which could explain the exclusive cardiac defect present in the mutations.

Zinn-Justin group has shown that the EDMD-causing emerin mutation, Δ95-99, impairs emerin self-assembly and binding to the Ig-fold domain of lamin A/C. Consequently, we wondered whether the mutations will impede binding to lamin A/C. The impairment of lamin A/C binding can support the structural hypothesis as an underlying cause for the symptoms present in patients.

Lastly, knowing that phosphorylation is considered the principal response of nuclei to mechanical stress, we questioned the phosphorylation capacity of ΔK37. Defects in phosphorylation can have multiple consequences on emerin interaction with binding partners and response to mechanical forces applied consistently on cardiomyocytes in the heart.

A second objective of this thesis is to characterize for the first time ΔK37 immortalized human fibroblasts, as a cellular model for one of the three mutations, with respect to:

a) expression of nuclear envelope and cytoskeletal proteins
b) mechanobiology (perinuclear actin organization and response to mechanical cues)

Since others have shown that the loss of nuclear envelope proteins, such as lamin A/C, result in disorganization of actin cytoskeleton and defects in mechanical responses, we hypothesized that ΔK37 fibroblasts may suffer from the same defects.

Chapter II: Manuscript

Characterization of emerin LEM-domain missense mutations present in patients with exclusive atrial cardiac defects

(Manuscript *In preparation)*

Abstract

Emerin is a LEM-domain protein anchored to the inner nuclear membrane with several functions due to its numerous binding partners. It is encoded by the *EMD* gene, which is responsible for more than 60% of X-linked Emery-Dreifuss Muscular Dystrophy (X-EDMD) cases. The majority of X-EDMD causing mutations are nonsense mutations resulting in complete absence of emerin on protein level and the classical triad of X-EDMD symptoms in the patients[1,2]. The aim of this work is to decipher the effects of three "unique" emerin LEM domain missense mutations (P22L, ΔK37, and T43I), present in patients with only isolated atrial cardiac defects, on their structure, self-assembly and interactions with their partners. To this end, the effect of the mutations on the global protein structure was analyzed by NMR using the emerin fragment (EmN: 1-187) expressing each of the three mutations. Solution-state NMR analysis of the three EmN mutants didn't show a change in the global structure of the P22L and T43I mutants. On the contrary, the deletion of residue K37 impaired the proper folding of the LEM domain; destabilizing it[3]. In addition, our results revealed an interaction between BAF and the three LEM mutants, regardless of the presence of the mutations at the known binding site. Conversely, ΔK37 demonstrated less affinity in binding to BAF. Moreover, observation of the samples by negative staining electron microscopy revealed that the three mutants maintained their capacity to self-assemble *in vitro* and form curvilinear filaments as wild-type. However, thioflavin T assays showed faster polymerization kinetics in the three mutants compared to EmN. Finally, two-dimensional ^{1}H-^{15}N HSQC spectra of the Ig-fold domain of Lamin A/C in presence of the self-assembled mutants validated the presence of interaction. In

conclusion, we illustrated that the LEM- domain missense mutations impair neither the self-assembly of the mutants nor their interaction with lamin A/C Ig-fold domain or BAF. Notably, the ΔK37 mutation destabilized the LEM domain and reduced its affinity to BAF. Taken together, our study ushers in subsequent investigations dismantling the correlation between the mutations and the pathology manifested in the patients.

Introduction

Nuclei in metazoan cells are surrounded by a nuclear envelope which is a highly organized double lipid membrane rich in proteins that separates the nucleus from the cytoplasm and encloses the nuclear genome[4]. The outer and inner nuclear envelope membranes are continuous with the endoplasmic reticulum (ER), separated by a luminal space called the perinuclear space (PNS) and fused at sites where nuclear pore complexes (NPC) are inserted.[5] The nuclear envelope comprises a variety of proteins that aren't normally enriched in the ER. Proteins at the nuclear envelope membrane can be categorized into four groups: nuclear pore complex (NPC), outer and inner nuclear membrane (ONM, INM) proteins and nuclear lamina[6]. A large number of human diseases are linked to nuclear envelope proteins underlining the critical role of this network for normal cell function[7].

The LEM (named for LAP2, Emerin and Man1) domain is a 40 amino acids residue that is well-conserved in prokaryotes and eukaryotes[8]. It's composed of a three-residue helical turn at its N-terminal and two large parallel alpha helices connected by a long loop[9] (Figure 1.b). There are eight human LEM domain proteins encoded by seven genes, namely: Lem1, Lem2, Lem 5, Man1, LAP2 (α, β, γ, δ, ε or ζ), Emerin, Ankle 1 (or Lem 3) and Ankle 2[10]. Several LEM-domain proteins bind to lamins[11]. The LEM domain adopts one main function, which is binding to the barrier to auto integration factor (BAF), a DNA binding protein associated to chromatin.

For these reasons, LEM-domain proteins influence both nuclear structure and genome organization[12].

Emerin is a 34 kDa LEM-domain protein composed of 254 AA residues. It has a transmembrane domain (23 AA) located at the inner nuclear envelope membrane and a large nucleoplasmic domain through which it interacts with other nuclear envelope proteins[13] (Figure 1.a).

In the cells, emerin has several functions due to its various binding partners. Emerin regulates gene transcription by binding to several transcription regulators and RNA splicing factors such as: HDAC3, GCL, Btf and YT521B. Moreover, it binds to several signaling and structural components such as: β-catenin, Lmo7, Man1, Lamins, BAF, actin, tubulin and nuclear myosin 1C; hence it governs the nuclear architecture. Importantly, it takes part in the response to mechanical stress by binding to SUN1, SUN2, lamins and nesprin. Being associated with the linker of nucleoskeleton and cytoskeleton (LINC) complex, it contributes to the mechanical link between the nucleo and cytoskeleton[14]. Furthermore, emerin was observed as tyrosine phosphorylated in response to force applied to the nucleus and these phosphorylation events were critical for mediating the nuclear mechanical response to tension[15]. Finally, force-driven enrichment of emerin at the outer nuclear membrane of epidermal stem cells was reported and it induced reorganization of the heterochromatin anchoring to the nuclear lamina[16].

Emerin is able, as well, to self-assemble *in vitro* and in cells. Although several studies have demonstrated that emerin can exhibit different self-assembly configurations[17,18], the molecular details of emerin self-assembly and its biological significance haven't been adequately untangled yet.

The gene encoding for emerin was first discovered in 1994 when the mutations in this gene were linked to X-linked Emery-Dreifuss Muscular Dystrophy (X-EDMD)[19]. The prevalence of X-EDMD is 1:100,000 and EDMD is considered the third most common muscular dystrophy after Duchenne Muscular Dystrophy (DMD) and Becker's muscular dystrophy[20]. Although emerin is expressed in almost all tissues, EDMD affects skeletal and cardiac muscles; resulting in early contractures of the elbows, neck and Achilles tendons, slowly progressive skeletal muscle weakness and cardiac conduction defects that can result in lethal cardiac arrest unless a pacemaker is inserted[21].The exact mechanism by which mutations in a single gene, that is almost ubiquitously expressed, cause the tissue-specific clinical features of EDMD; as well as the relationship between changes in a nuclear envelope protein and the observed clinical symptoms in EDMD, remain elusive. Yet, two proposed mechanisms that aren't mutually exclusive have been proposed[22]. According to the "structural hypothesis", loss of emerin from the nuclear envelope could lead to nuclear structural abnormalities prominently in mechanically stressed tissues such as the heart and skeletal muscles[23]. On the other hand, the "gene regulation hypothesis" suggests that the binding of emerin to several transcription and splicing factors could result in tissue-specific effects upon its loss[24]. There is a profound belief that the heart and muscle cells are particularly sensitive to mechanical stress and that emerin, as a member of the nucleoskeleton network, may play role in protecting these cells from mechanical stress.

The majority of reported X-EDMD causing mutations are nonsense point mutations: small frameshifting deletions/insertions that introduce a stop codon; resulting in complete absence of emerin on the protein level and the classical triad of symptoms in the patients[1,25]. Interestingly, there are few reported emerin missense mutations that result in lower (Δ235-240, Δ236-241, Δ95-99, ΔK37) or normal expression of emerin that is correctly localized at the nuclear envelope membrane or mislocalized to the cytoplasm (Δ235-240, Δ236-241, Δ95-99) resulting

in classical X-EDMD (P183H/T, S54P, D72V, Q133H, R203H, Δ235-240, Δ236-241, Δ95-99) or isolated Atrial Cardiac Defect (P22L, T43I, ΔK37)[1,26–28,29] ,R. Ben Yaou, personal communication. The isolated atrial cardiac disease (ACD) is characterized by bilateral atrial dilatation accompanied by atrial fibrillation, cardiac conduction defects and arrhythmias without obvious skeletal muscle involvement.

The present paper investigates for the first time the effects of three emerin LEM domain missense mutations (P22L, ΔK37 and T43I; Figure 1.b,c) existing in patients with ACD on their structure, self-assembly and interactions with their main binding partners. Thus, our study sheds new lights on how these mutations contribute to the associated pathology.

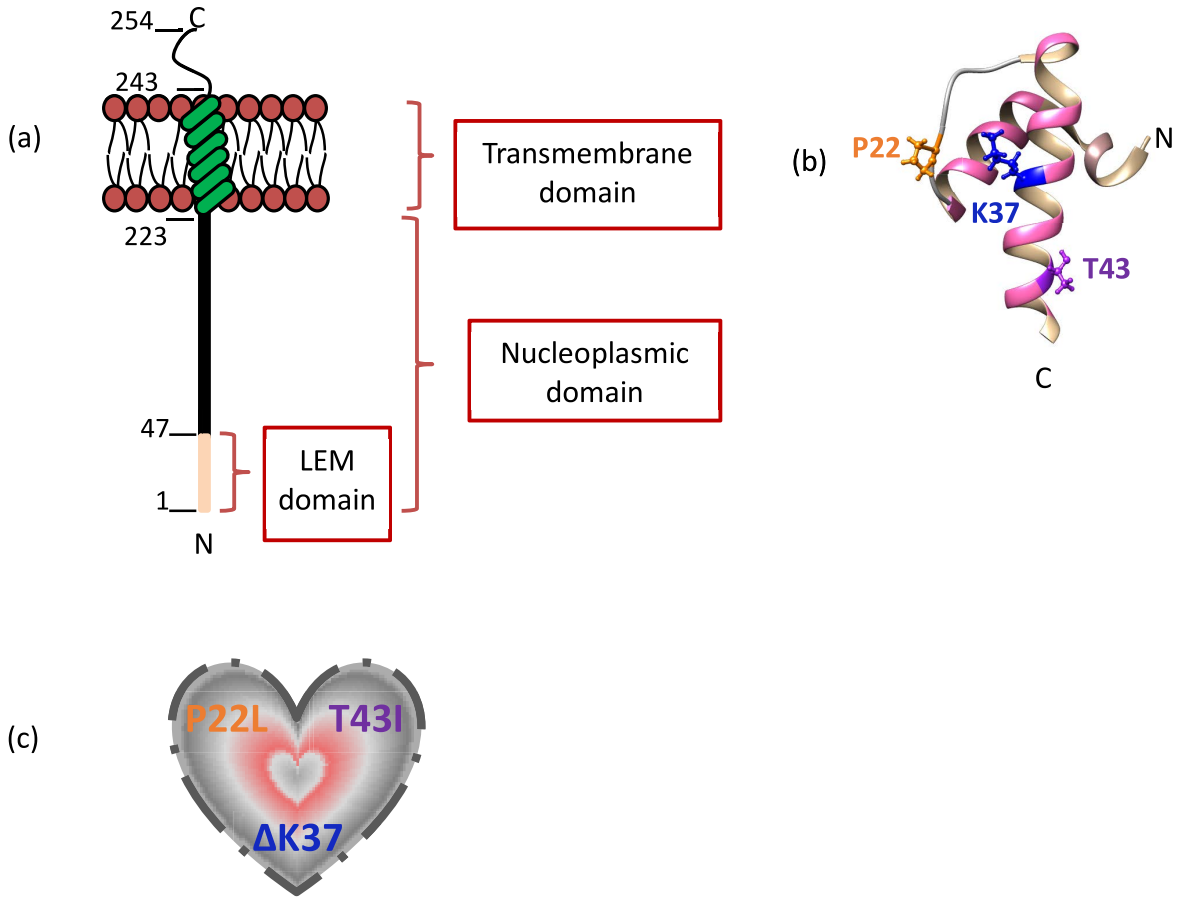

Figure 1. Emerin LEM domain is mutated in patients with Atrial Cardiac Disease (ACD). (a) Emerin is composed of 254 AA residues; including N-terminal

nucleoplasmic domain (residues 1-222), transmembrane domain (residues 223-243) and C-terminal luminal domain (244-254). (b) Ribbon diagram of emerin LEM domain with 3-10 helix in rosy brown, $\alpha 1$ and $\alpha 2$ helices in deep pink and $\beta 1$ strand in light grey. Ball and stick representation of proline 22 in orange, lysine 37 in blue and threonine 43 in purple. (c) P22L, K37, and T43I missense mutations are present in patients with isolated atrial cardiac disease (ACD).

Results

P22L and T43I mutants have the same overall structure as EmN. To assess the effect of the presence of the mutations on the overall structure of the mutants, we recorded ^{1}H-^{15}N HSQC spectra of EmN, P22L and T43I at concentrations of 150 µM at 30°C (Figure 2). The chemical shifts of the amino acids in mutants were similar to those in wild-type except for the residues close to the mutations positions. In the P22L spectrum, we did not observe large changes in the chemical shifts of amino acids compared to EmN. We only identified small shifts for peaks corresponding to residues H23, G24, T43, R47, as well as A116 and R118 that should be confirmed. E42, T43, Q44 peaks were largely shifted in the T43I spectrum, whereas E35, E40, R46, R47 were slightly shifted. We concluded that the presence of P22L and T43I mutations didn't affect the overall structure of EmN.

(a)

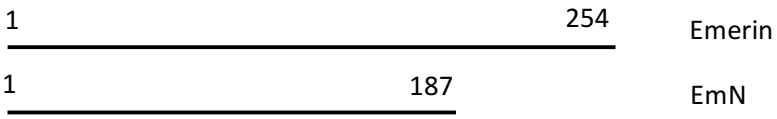

(b) MDNYADL[7]SDTELTTLLRRYNIPH[23]G[24]PVVGSTRRLYEKKIFEYET[43]
QRRR[47]LSPPSSSAASSYSFSDLNSTRGDADMYDLPKKEDALLYQSKGYNDDYYEES
YFTTRTYGEPESAGPSRA[116]VR[118]

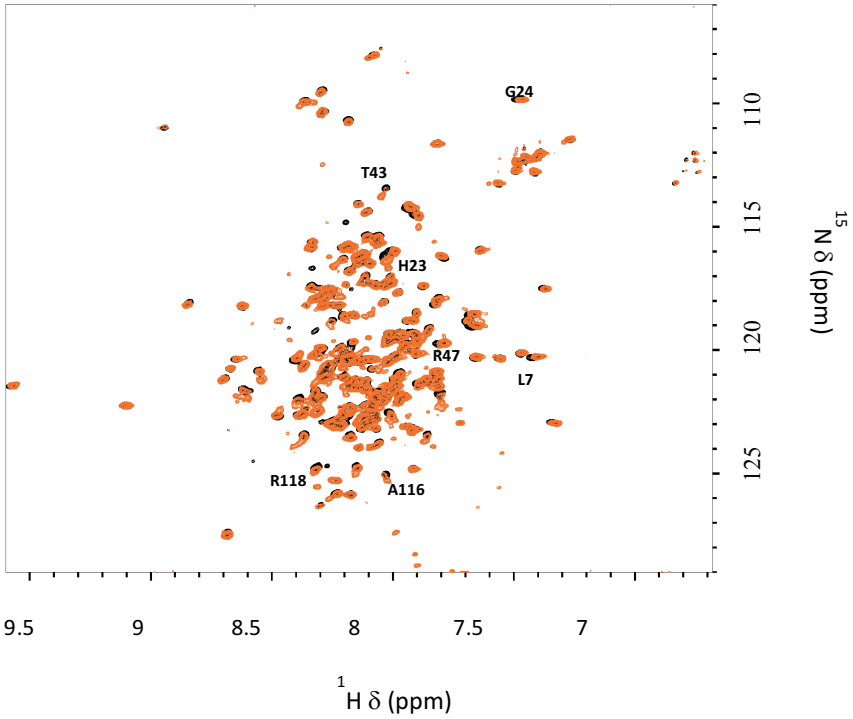

(c) MDNYADLSDTELTTLLRRYNIPHGPVVGSTRRLYE[35]KKIFE[40]YE[42]T[43]Q[44]RR[46]R[47]L
SPPSSS

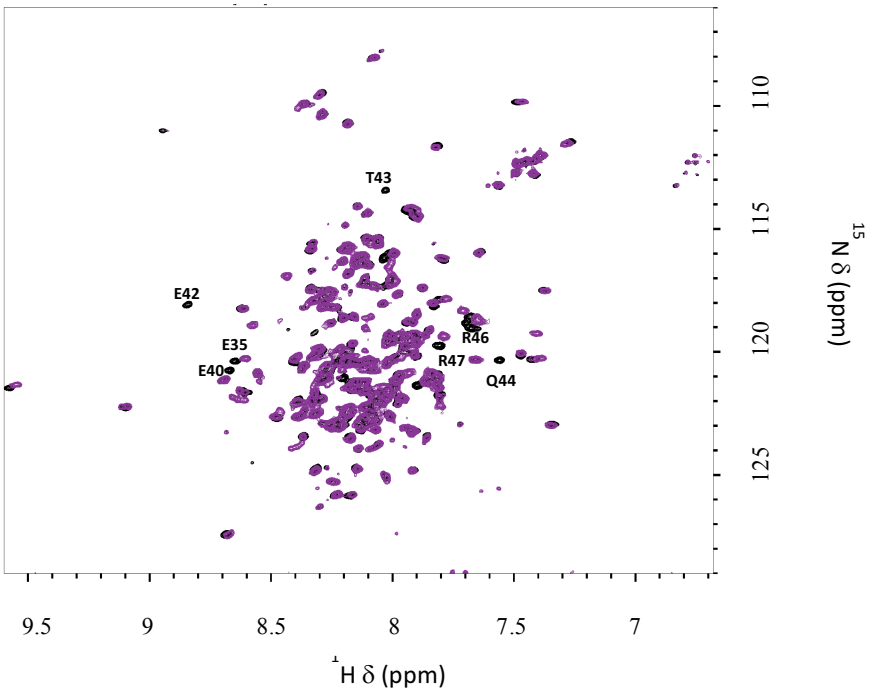

Figure 2. P22L and T43I EmN mutants have the same overall structure as EmN. (a) Representation of full length emerin (residues 1-254), EmN fragment (residues 1-187) (b) LEM-domain sequence (residues 1-45) with the residues colored in purple when corresponding to peaks shifted in the mutant. The shifts are annotated on the superimposition of the ^{1}H - ^{15}N HSQC spectra of EmN (in black) and P22L (in orange). (c) Emerin sequence (residues 1-118) with the residues colored in orange when corresponding to peaks shifted in the mutant. The shifts are annotated on the superimposition of the ^{1}H - ^{15}N HSQC spectra of EmN (in black) and T43I (in purple). All spectra were recorded at 30°C, 750 MHz and 150 μM.

***Δ*K37 mutant is mostly unfolded in solution.** In our previous work we demonstrated that ΔK37 NMR 2D ^{1}H- ^{15}N HSQC spectrum lacked peaks representing the signal of the folded LEM domain residues at 30°C[30] (Supplementary Figure 1). Conversely, we didn't detect the signal of the unfolded ones on the same spectrum at 30°C[30] (Supplementary Figure 1). We also observed that the ^{1}H NMR spectrum of ΔK37 did not show major changes when recorded from 30°C to 10°C, suggesting that the peptide is not properly folded on this temperature range (Supplementary Figure 2). To further characterize the folding state of ΔK37, we carried out a fluorescence-based thermal shift assay (FBTSA) and characterized its thermal stability compared to EmN. Denaturation profiles usually display augmentation of fluorescence as a function of increased temperature, with a single denaturation transition observed at the melting temperature of the peptide. In the case of EmN, we observed a slight increase of fluorescence as a function of the temperature, and plotting the negative of the derivative of the fluorescence as a function of the temperature clearly showed that the LEM domain unfolds with a melting temperature of about 47°C (Figure 3). In the case of ΔK37, no single denaturation transition was observed (Figure 3). ΔK37 showed no cooperative unfolding event, revealing that it is mostly unstructured.

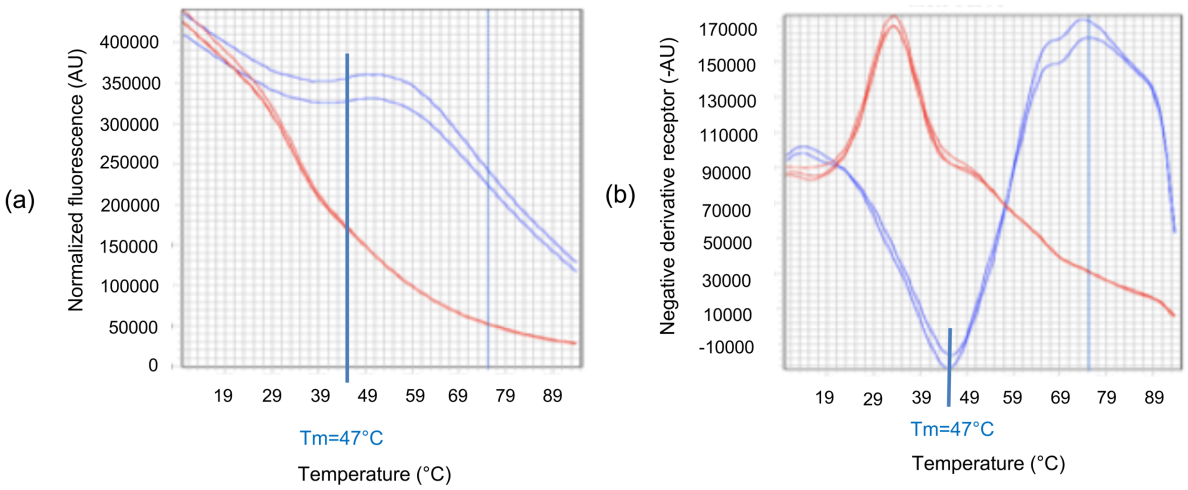

Figure 3. ΔK37 mutant lacks the denaturation signal present in EmN. (a) Comparing the fluorescence melt curve plots of EmN (261uM) in blue and ΔK37 (300uM) in red under same experimental conditions, we manifested the total absence of the weak denaturation signal observed in the EmN profile at 47°C. (b) Negative derivative curve plot of the denaturation profiles confirms the same finding.

No defect detected in the self-assembly capacity of EmN mutants. We investigated the effect of the LEM domain missense mutations P22L and T43I on EmN self-assembly. Because the LEM domain is essential for EmN self-assembly[30], an impact of the mutations is expected. Moreover, we previously showed that mutant ΔK37 maintains the capacity to self-assemble (Supplementary Figure 3)[30]. Observation by negative staining electron microscopy of the P22L and T43I samples after incubation at 65°C during 1 h showed that the two mutants maintained their capacity to self-assemble *in vitro* and form curvilinear filaments of approximately 10 nm diameter as the wild-type (Figure 4A, B).

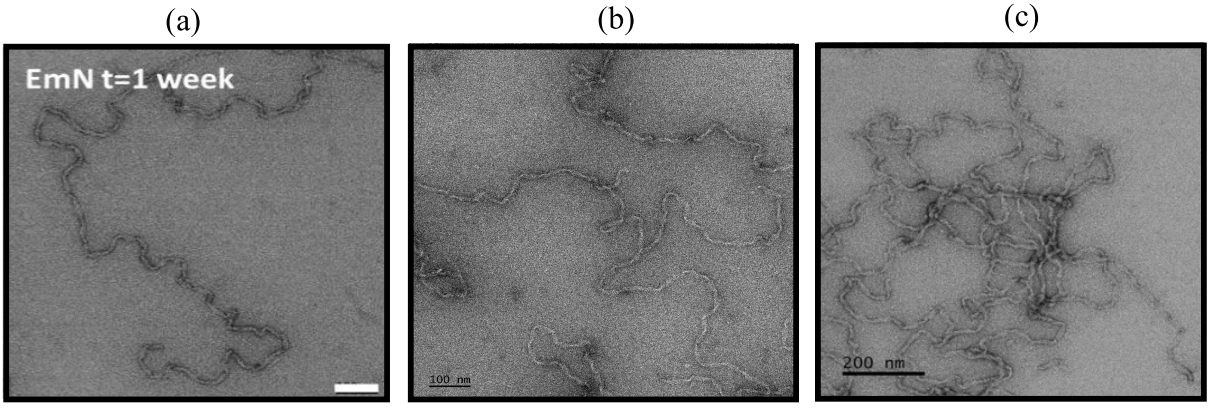

Figure 4. No defect detected in the self-assembly capacity of EmN mutants. Self-assembled (a) EmN (b) P22L (c) T43I (500 μM) heated for 1 hr at 65°C then incubated for one week at 20°C were analyzed using negative stain imaging. The 3 mutants were capable to self-assemble and form filaments similar to EmN ones. We concluded that there is no defect in the self-assembly capacity of the three mutants. Scale bar, 100 nm.

EmN mutants self-assemble faster than EmN. We have demonstrated that ΔK37 mutation favors self-assembly[30] (Supplementary Figure 4). In order to explore the effect of the mutations on the kinetics of self-assembly, a solution of each EmN mutant (20 μM) containing ThT (2.5 μM) was incubated at 37°C for 4 hours and the change in ThT fluorescence emission was monitored each hour (Figure 5). As observed for ΔK37[30] (supplementary Figure 4), the ThT fluorescence of the two mutants was increasing faster than the wild-type, which is indicative of the mutants' faster polymerization.

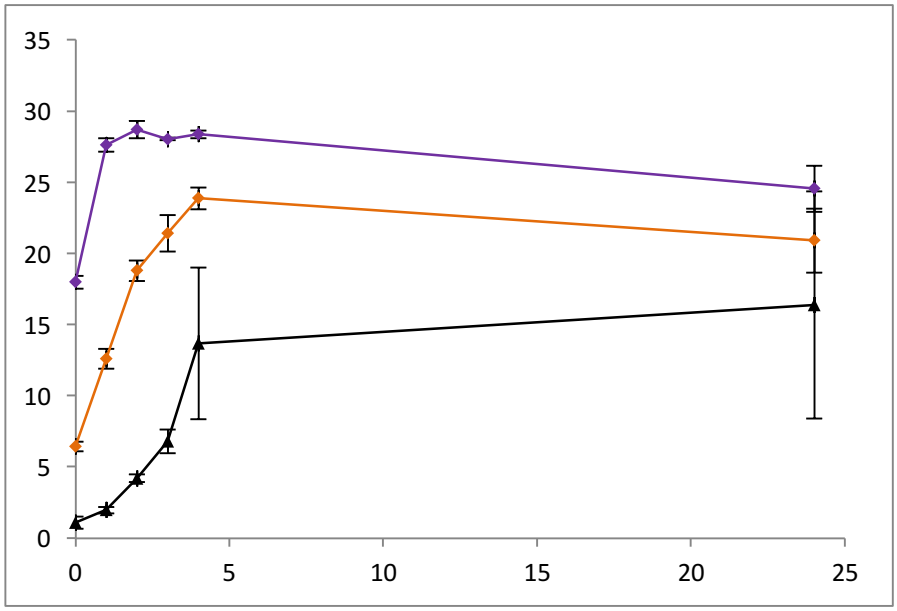

Figure 5. EmN mutants self-assemble faster than EmN. Thioflavine T (ThT) fluorescence was measured as a function of the incubation time at 37°C for EmN, P22L, and T43I, *shown in black, orange, and purple,* respectively (all proteins were at 600 µM final concentration). The fluorescence signal was higher for the two mutants than for the EmN. This indicates the faster polymerization kinetics of their self-assembled state compared to EmN.

The three EmN mutants are able to interact with BAF *in vitro*. As the monomeric LEM domain is responsible for BAF binding, we hypothetized that mutations could impair the interaction of EmN with BAF. To test whether the three LEM domain mutants were able to interact with BAF, size-exclusion chromatography (150 µM proteins on Superdex 75 10/300 GL column) was carried out using BAF, EmN, ΔK37, P22L, and T43I separately to obtain the reference chromatograms of each protein then in presence of BAF in order to obtain the binary complexes. The three EmN mutants co-eluted with BAF revealing an interaction between BAF and the mutants (Figure 6). ΔK37-BAF binary complex eluted (9.5 ml) significantly after EmN-BAF (9 ml) indicating lower affinity of ΔK37 to BAF. P22L-BAF and T43I-BAF eluted slightly after EmN-BAF, suggesting that P22L and T43I might also exhibit a decreased affinity to BAF.

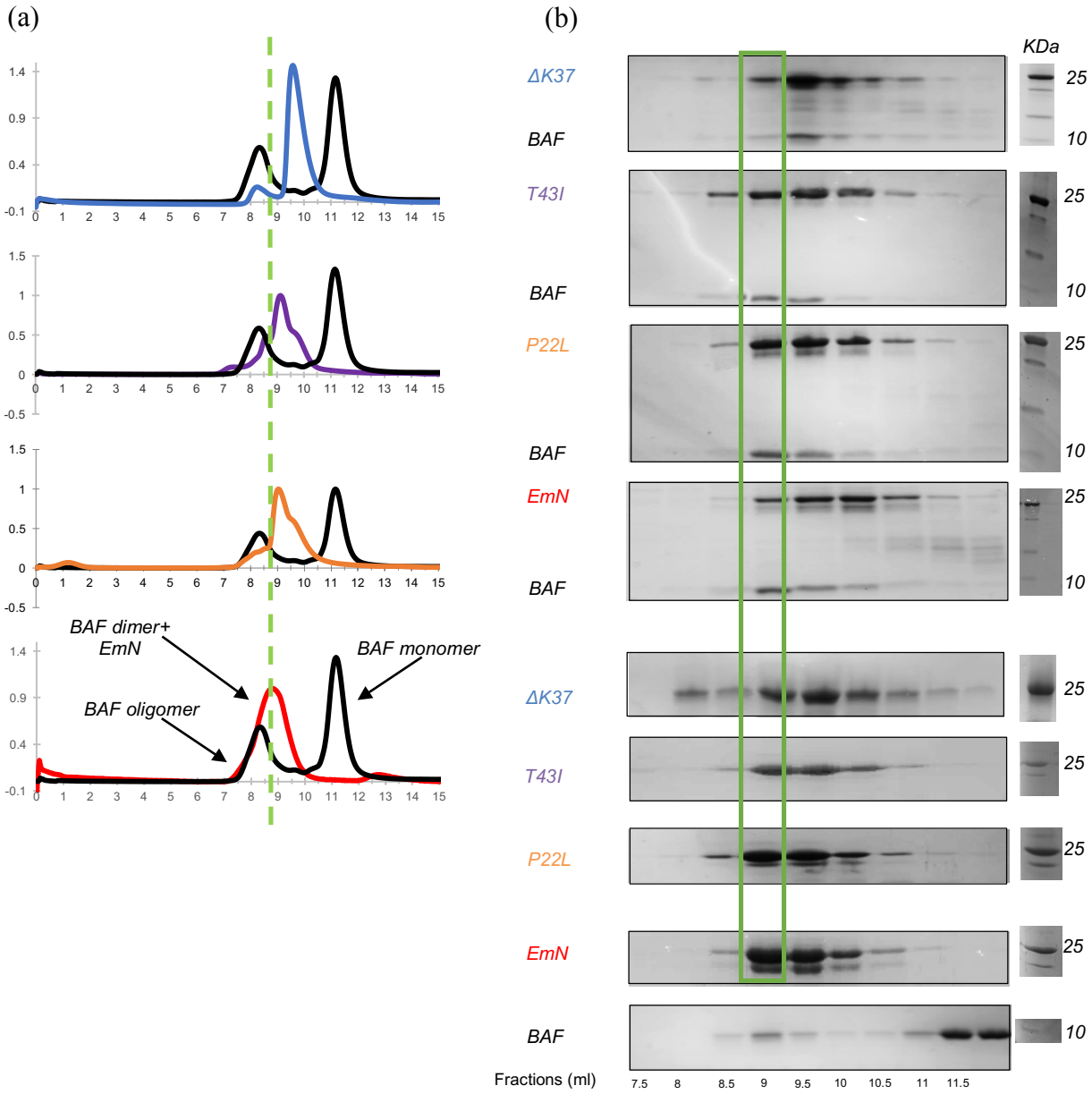

Figure 6. The three EmN mutants are able to interact with BAF *in vitro*. Size-Exclusion Chromatography was performed on the three EmN mutants and the wild-type in absence and presence of BAF in order to obtain reference and binary complexes chromatograms, respectively. In all experiments, proteins were injected at same final concentration (EmN and its mutants were used at 100 µM and BAF at 200 µM), using same buffer and same column (Superdex 75 10/300 GL). (a) The elution of BAF alone is shown in *black*, EmN-BAF in *red*, P22L-BAF in *orange*, T43I-BAF in *purple,* and ΔK37-BAF in *blue*. Chromatograms representing the elution fractions of the binary complexes are shown, from bottom: EmN-BAF, P22l-BAF, T43I-BAF and ΔK37-BAF. The three mutants co-eluted with BAF similar to EmN, however ΔK37-BAF is the only complex that eluted significantly after (9.5ml) EmN-BAF (9 ml). (b) Gels corresponding to references and binary complexes chromatograms are represented, from bottom: BAF, EmN, P22L, T43I and ΔK37 references followed by

EmN-BAF, P22l-BAF, T43I-BAF and ΔK37-BAF binary complexes. The wild-type binary complex is boxed in green rectangle.

Monomeric T43I binds to BAF and lamin A/C Igfold, forming the same 3D structure as EmN. In order to further characterize the binding of mutants to BAF, we solved the X-ray crystallography structure of T43I mutant bound to BAF at 2.3 A° (Figure 7). Comparing the 3D structure of T43I mutant bound to BAF (Figure 7) to that of EmN bound to BAF (Samson et al., under review), highlights that T43I mutation did not affect the structure of EmN. Figure 7 shows that the structure is superimposable to that of EmN-BAF.

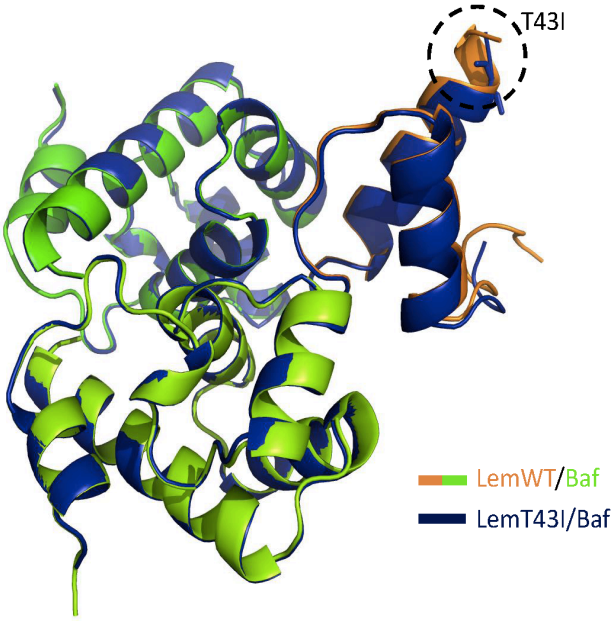

Figure 7. The 3D structure of the T43I-BAF complex resolved by X- ray crystallography using hanging drop vapor diffusion method (conditions: 18% PEG 3350, 100 mM Tris Bis pH 5.5, 0.1 M NH_4SO_4). Superimposing the 3D structure of the LEM domain of emerin wild-type bound to BAF (Samson et al., under review) on that of T43I showed no differences explaining the ability of the mutant to still bind to BAF.

Self-assembled EmN mutants can interact with the Ig-fold domain of lamin A/C. To investigate the ability of the three mutants filaments to interact with the lamin A/C Ig-fold domain, we recorded ^{1}H-^{15}N HSQC correlation spectra of the Ig-fold domain (150 uM) in

presence of the filaments (150 uM), after confirming their presence by EM (Figure 8). The spectra of the Ig-fold domain in presence of the mutants filaments confirmed the presence of interaction as we can clearly see only the peaks of the residues in the intrinsically disordered region of lamin A/C not involved in the interaction (Figure 8).

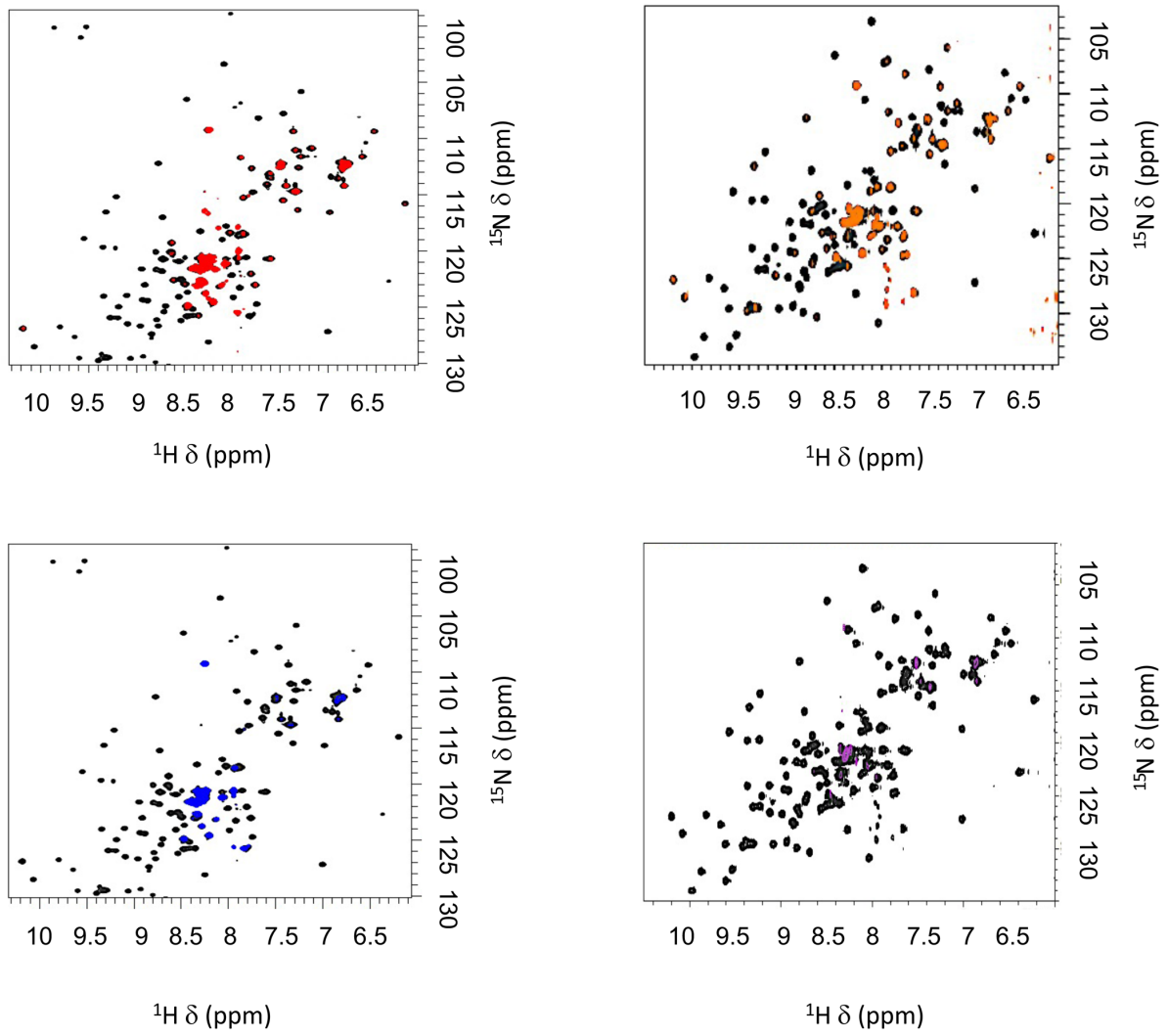

Figure 8. Self-assembled EmN mutants can interact with Ig-fold domain of lamin A/C. Superimposition of the solution state NMR ^{1}H-^{15}N HSQC spectra of the Ig-fold domain of lamin A/C only in *black* or in presence of EmN, P22L, *Δ*K37, and T43I filaments in *red, orange, blue, and purple,* respectively. The spectra were recorded at pH 8, 30°C, 750 MHz, 150 µM of proteins and filaments. The spectra observed after the addition of mutants filaments confirms the presence of interaction between the proteins.

The Ig-fold domain of lamin A/C has no effect on the stability of EmN mutants filaments. Changes in mutants filaments stability were analyzed by recording 12 consecutive 1D ^{1}H spectra each for 1 hour in the absence (as control) and presence of Ig-fold domain (Supplementary Figure 5). The analysis of mutants filaments spectra after being in contact with the Ig-fold domain for 12 hours didn't show changes in the stability of the filaments (Supplementary Figure 5) and consequently their interaction with the Ig-fold domain (HSQC spectra recorded for the filaments and Ig-fold domain interactions after 12 hours not shown). Hence the lamin A/C Ig-fold domain doesn't impact the stability of the mutants' filaments.

Discussion

After emerin-emerin associations were reported *in vitro* and in cells, it has been suggested that emerin can have multiple configurations forming intermolecular emerin network anchoring at the nuclear envelope[17]. These associations influence emerin retention at inner nuclear envelope membrane[17] and lamin A/C binding (Samson et al., under review). Berk et al., deduced that cells could inhibit these emerin-emerin associations by post translational modifications in order to target native emerin to new locations[14]. We confirmed that that the three mutants are able to self-assembly as wild-type, yet with faster polymerization kinetics. Further, our analysis showed that the mutations did not affect the disassembly of these filaments. Both BAF and LEM domain are highly conserved cellular proteins in metazoan kingdom[31]. BAF is a DNA-binding protein that interacts with LEM-domain proteins[32] where a BAF dimer bridges DNA and binds to LEM- domain proteins[31]. A touch and go model was proposed explaining such interaction in which BAF, contrary to emerin, is highly mobile at the nuclear envelope enabling BAF to bind emerin transiently but frequently during interphase[31]. Phosphorylation of LEM proteins disrupts their interaction with BAF and consequently suppresses the chromosome - nuclear envelope link mediated by BAF[33]. Opposite to previous studies that linked BAF's important function in nuclear assembly to its

ability to recruit LEM-domain proteins[31,34], it has been shown lately that such BAF-LEM interaction is not required for nuclei assembly in human cells[35]. The interaction between emerin and a variety of transcriptional regulators such as BAF governs one of the two suggested hypotheses for the disease mechanism in X-EDMD, the "gene hypothesis", in which defects in emerin expression could lead to tissue-specific response. We investigated whether the LEM domain mutations impaired their interaction with BAF. Contrary to expectations, size-exclusion chromatography showed that the P22L and T43I mutants are still able to bind to BAF. In the same line, the 3D crystal structure of the LEM domain of the T43I mutant bound to BAF was similar to that of the wild-type; substantiating the presence of interaction. On the other hand, the instability of the ΔK37 LEM domain generated weaker affinity to BAF. Unfortunately, it was not possible to quantify the reduced affinity using different biophysical tools (Isothermal Titration Calorimetry or Surface Plasmon Resonance) due to technical limitations. Taken together, the LEM domain mutations studied don't impair the interaction of the mutants with BAF. The structural significance of emerin is due to its ability to bind several structural proteins, such as lamin A/C, lamin B, nuclear actin and nesprin-1α/2, in addition to promoting *in vitro* actin polymerization[12,36,37]. Hence, the loss of emerin from the nuclear envelope could interfere with the normal functions of these proteins and justify the nuclear structural abnormalities. Furthermore, isolated nuclei from emerin deficient cells displayed increased nuclear rigidity and failed to adapt to nuclear mechanical forces[15]. These data collectively support the "structural hypothesis" as a mechanism for X-EDMD. In order to challenge the involvement of the "structural hypothesis" in the pathogenesis of the isolated atrial cardiac defects caused by our mutants we studied the interaction between the self-assembled state of the mutants and lamin A/C Ig-fold domain. Our two-dimensional ^{1}H-^{15}N HSQC spectra of the Ig-fold domain in presence of the three mutants filaments confirmed the presence of interaction. That didn't come as a surprise

because the three mutations are not located in the interacting protein region (residues 70-170 in emerin), and they are correctly localized at the nuclear envelope which rules out the disruption of the direct interaction between the emerin mutants and lamin A/C. However, whether such interaction is able to provoke the normal biological events cascade as the wild-type remains an unanswered question.

Where is the defect?

Cardiac differentiation and regeneration defect?

Studies have recently explained how loss of emerin at nuclear periphery could impair differentiation and regeneration. Concerning differentiation, emerin null myogenic progenitors failed to respond to differentiation cues by reorganizing their genomes and expressing important differentiation genes such as: MyoD, Myf5, Pax7; resulting in delayed differentiation[38,39]. Particularly, there are accumulating evidences supporting emerin role in maintaining the repressive chromatin environment established by the nuclear lamina[38]. In line with this, X-EDMD patients' primary fibroblasts have less heterochromatin at the nuclear periphery and embrace a more relaxed chromatin architecture[40–42]. Indeed, chromatin remodelling may explain the large number of transcripts that are differentially expressed in emerin null muscle progenitors[38]. With respect to regeneration, cell cycle exit is indispensable for the proliferating myogenic progenitors to commit to differentiation. However, emerin null myogenic progenitors failed to exit cell cycle thus, impairing myogenic differentiation. Besides, the JAK-STAT pathway, which is important for the satellite cell expansion, is enriched in emerin null myogenic progenitors. As a result of its excessive activation, the satellite cell niche might be depleted by time. In fact, this could link the slow onset of skeletal muscle wasting in EDMD with the cumulative loss of satellite cell niche and thereby loss of skeletal muscle regeneration capacity[38]. Hence, there could a cardiac differentiation or regeneration defect in our mutations of interest.

Conclusion

Using different biochemical approaches, we investigated three "unique" emerin LEM-domain missense mutations present in patients with exclusive isolated atrial cardiac disease (ACD). In this paper, we explored the effect of the mutations on emerin's structure, self-assembly and interactions with structural partners (lamin A/C) and transcription regulators (BAF). The results of this study corroborate that the three mutants are able to self-assemble *in vitro* and bind to BAF and lamin A/C. The only striking difference is the instability of the LEM domain of ΔK37 which provoked lower affinity to BAF. Further, we demonstrated that the three mutants polymerize faster than EmN wild-type. We are currently in the process of investigating possible defects in emerin interactions with other partners, particularly cardiac specific ones using mass spectrometry. Further work will concentrate as well on defects in Wnt/β-catenin pathway in ΔK37 immortalized patients cells. Our research could eventually help in understanding emerin functions in the heart and its role in ACD.

Materials and Methods

Protein expression and purification

Optimized emerin fragment **EmN** (region 1-187) and **BAF_{CtoA}** were cloned into pETM-13 expression vector by Genscript as a fusion protein with His_8-tag at its N-terminus and expressed in Escherichia coli BL21(DE3) cells. **ΔK37, P22L and T43I** expression vectors were obtained by site-directed mutagenesis (Quikchange kit, Agilent) of **EmN** expression vector. **lamin A/C Ig-fold domain** (residues 411-566) previously cloned in pGEX-4T vector (offered by Prof Howard J. Worman, Department of Medicine, College of Physicians & Surgeons, Columbia University, New York, USA) was expressed as GST-tagged fusion protein. Cultures were grown in LB broth medium for all experiments, only labelled cultures for NMR experiments were grown in M9 minimal medium using $^{15}NH_4Cl$ as the sole source

of nitrogen (1X M9 salts (10x: 60 g Na_2HPO4, 30g KH_2PO4, 5 g NaCl), 1X Trace elements (500X: 13.4 mM EDTA, 3.1 mM $FeCl_3$-$6H_2O$, 0.62 mM $ZnCl_2$, 76 µM $CuCl_2$-$2H_2O$, 42 µM $CoCl_2$-$2H_2O$, 162 µM H_3BO_3, 8.1 µM $MnCl_2$-4H2O), 1 mM Thiamine, 1 mM Biotin, 300 mM $CaCl_2$, 1M $MgSO_4$, 0.05% $^{15}NH_4Cl$, 0.2% glucose). Cells grown at 37°C till OD_{600} of 0.8 and induced with 0.5 mM isopropyl β-D-1-thiogalactopyranoside (IPTG) overnight at 20°C. Cell pellets were suspended in 20 ml lysis buffer (50 mM Tris-HCl pH 8, 300 mM NaCl, 5% glycerol, 1% Triton TX-100 and 10 mM PMSF) per liter of culture and lysed by sonication (power, 70%; time, 4 min; pulse, 1 s; temp, 10°C in case of Ig-fold domain of lamin A/C and 20°C in case of BAF, EmN and its' mutants). Ig-fold domain of lamin A/C was found mostly in the soluble fraction that was isolated by centrifugation. BAF, EmN and its' mutants form inclusion bodies that were recovered from cell pellets by solubilization using C8 buffer (50 mM Tris-HCl pH8, 150 mM NaCl, 20 mM Imidazole, 8 M urea) for at least one hour at room temperature then centrifugation to get rid of cellular components and membranes. Supernatants were purified by affinity chromatography resins (Glutathione Sepharose resin in case of Lamin A/C Ig-fold domain; NiNTA resin in case of BAF, EmN and its mutants) and the inclusion-body proteins were then refolded by dialysis overnight (EmN and its mutants, 50 mM Tris-HCl pH 8, 30 mM NaCl; BAF, 50 mM Tris-HCl pH 8, 150 mM NaCl) then two times one hour the next day. Purified protein peptides were separated from their tags by either thrombin cleavage in case of Ig-fold domain of lamin A/C or Tobacco Etch Virus **(**TEV) cleavage in case of BAF, EmN and its' mutants.

Characterization of protein self-assembly by electron microscopy (EM)

To obtain the self-assembled state of EmN and its mutants, purified proteins were first dialyzed (Buffer E: 20 mM Tris-HCl pH8 and 30 mM NaCl) using dry Spectra/Por dialysis membrane (6-8 kDa) then concentrated (500 µM final concentration, 5 mM DTT), heated for 1 hour at 65°C and incubated for one week at 20°C. Sample suspensions were applied to

glow discharge carbon-coated grids, stained by 2% w/v aqueous uranyl acetate, visualized at 100 kV with a Tecnai Spirit transmission electron microscope (FEI, New York), captured by K2 4k x 4k camera (Gatan, CA) at 4,400 or 15,000 magnification.

Self-assembly kinetics followed by Thioflavin T (ThT) fluorescence

Purified EmN and its mutants were dialyzed (Buffer E), concentrated (final concentration 300 μM, 5 mM DTT) and heated at 37°C. Their oligomerization was monitored over time (each hour for 4 hours) by measuring changes of fluorescence intensity of ThT at 20°C. Fluorescence intensity of aliquots of protein solutions (20 μM protein and 2.5 μM ThT in 20 mM Tris pH 8, 30 mM NaCl, 5 mM DTT) in 60 μl cuvette was measured at 480 nm after excitation at 440 nm using a JASCO fluorimeter equipped with an ADP-303T Peltier temperature controller (JASCO Inc., Easton, MD)

Size-Exclusion Chromatography (SEC)

Interactions between EmN and its mutants with BAF (EmN and its mutants were used at 100 μM and BAF at 200 μM final concentration in 500 μl) were identified by size-exclusion chromatography on a Superdex 75 10/300 GL column (GE Healthcare) pre-equilibrated in running buffer (20 mM Tris-HCL pH 8, 30 mM NaCl, 2 mM DTT) and run at the flow rate of 0.5ml/min at 4°C.

Fluorescence-based thermal shift assay (FBTSA)

EmN and ΔK37 were purified and concentrated (261 μM and 300 μM, respectively) in buffer (20 mM TrisHCl pH-8, 30 mM NaCl, 1mM EDTA, 1 mM PMSF, 5 mM β-mercaptoethanol, 5 mM DTT, 1X complete EDTA-free Protease Inhibitor (Roche)). The thermal stability of EmN and ΔK37 was studied using a QuantStudio 12K Flex instrument (LifeTechnologies). 10 μg of each tested protein was mixed with SYPRO Orange dye (800-fold dilution from 5000-fold stock solution, Invitrogen) in 20 mM TrisHCL pH 8, 30 mM

NaCl, 1 mM EDTA, 1 mM PMSF, 5 mM β-mercaptoethanol. Reactions were performed in duplicate in 96-well plate at a final volume of 20 µl and each experiment was carried out at least twice. Samples were subjected to denaturation kinetic from 10 to 95°C at a rate of 3°C/min and. Fluorescence of Sypro Orange dye was monitored in real time and recorded. The denaturation temperature was calculated for EmN using the Protein Thermal Shift software v1.3 (LifeTechnologies) as the maximum of the derivative of the obtained fluorescence curves.

Nuclear Magnetic Resonance (NMR) spectroscopy

NMR samples were prepared in buffer containing 20 mM Tris pH 8, 30 mM NaCl, 5 mM DTT and 5% D_2O. One and two-dimensional ^{1}H-^{15}N correlation spectra were recorded at 30°C on Bruker 700 or 750 MHz spectrometers. All NMR data were processed using Topspin 3.1 (Bruker).

X-ray crystallography

The ternary complex (T43I/BAF/Ig-fold domain of lamin A/C) purified by size-exclusion chromatography (aforementioned conditions) was concentrated (5 mg/ml) and incubated for a week at 4°C to ensure the proteolysis of T43I in order to eventually have only the LEM domain of T43I bound to BAF and lamin A/C Ig-fold domain in the complex. Hanging drop vapor diffusion was set up at 4°C with a drop (1 µl complex solution, 1 µl reservoir solution) suspended from a glass coverslip over the reservoir solution (500 µl; 18% PEG 3350, 100 mM Tris Bis pH 5.5, 0.1 M NH_4SO_4). The 3D structure of the ternary complex was determined by molecular replacement method (MolRep, CCP4i2). Coordinate files of BAF dimer bound to DNA (PDB entry 2BZF), lamin A/C globular domain (PDB entry 1IFR) and emerin LEM domain (PDB entry 2ODC) were used to construct the structural model. The resulting model was rebuilt by PHENIX, manual correction was performed using Coot

according to $|F_o| - |F_c|$ and $2|F_o| - |F_c|$ maps, and further refinement was carried out by phenix.refine. All structure figures were generated with PyMOL (Schrödinger, LLC).

Supplementary data

(a) MDNYADL[7]SD[9]TE[11]L[12]TTL[15]LR[17]RYN[20]IPHG[24]PV[26]V[27]G[28]ST[30]RR[32]L[33]Y[34]E[35]K[36]KIFE[40]YE[42]T[43]Q[44]R[45]R[46]RLSPPSSS

(b)

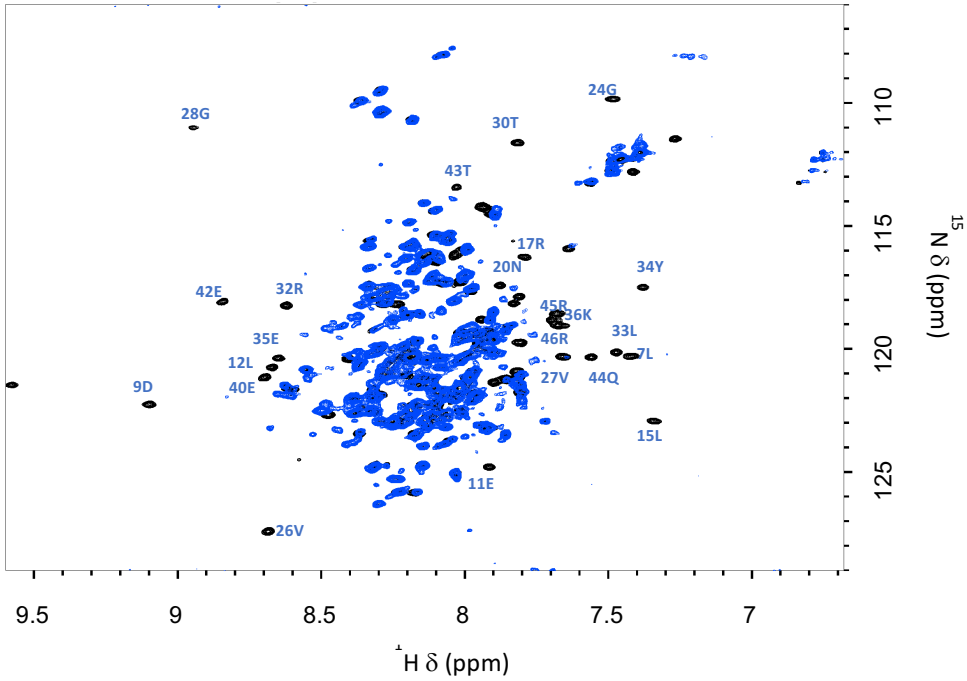

Supplementary Figure 1. (a) LEM-domain residues with the missing residues from ΔK37 spectrum colored in blue. (b)Superimposition of ^{1}H - ^{15}N correlation spectra of EmN (in black), ΔK37 (in blue) recorded at 30°C, 750 MHz and 150 µM showing the absence of the peaks representing the majority of the folded LEM domain.

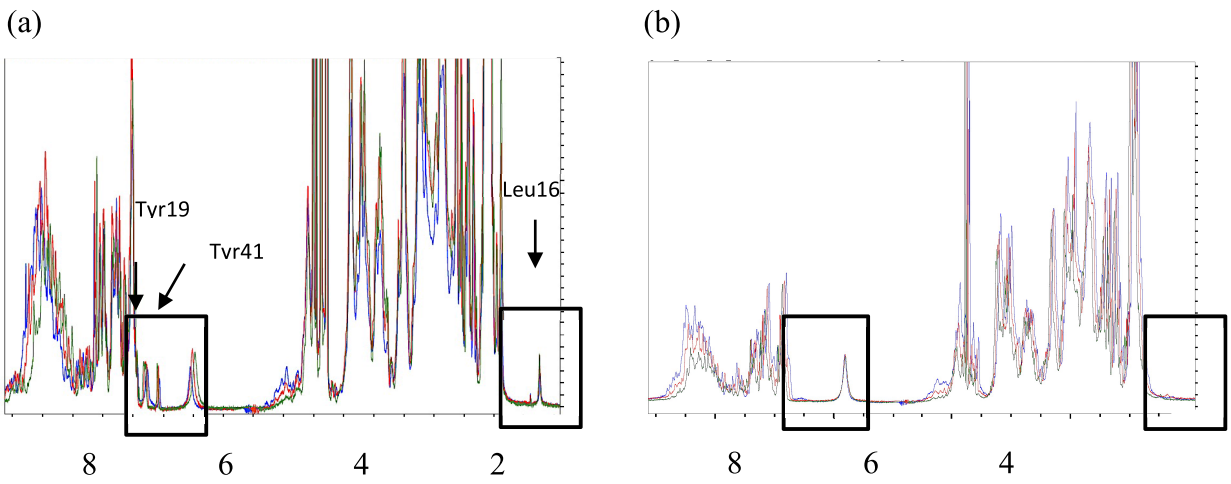

Supplementary Figure 2. Even at low temperature, ΔK37 mutant lacks the folded domain signal present in EmN. ^{1}H chemical distribution detected by ^{1}H NMR spectroscopy was used to probe ΔK37 structural stability at different temperatures compared to wild-type. Superimposition of the solution-state NMR 1D spectra of (a) EmN (b) ΔK37 recorded at pH 8, 750 MHz and varying temperatures (10°C, 20°C, 30°C *shown in blue, green and red*, respectively). The signals of the side-chain protons of Leu16, Tyr19, and Tyr41 which are embedded in the hydrophobic domain of LEM domain probing the folding of the LEM domain are surrounded by a rectangle in each spectrum. The aforementioned signals are only missing in ΔK37, at all tested temperatures; signifying the unfolding of ΔK37 LEM domain even at low temperature (10°C).

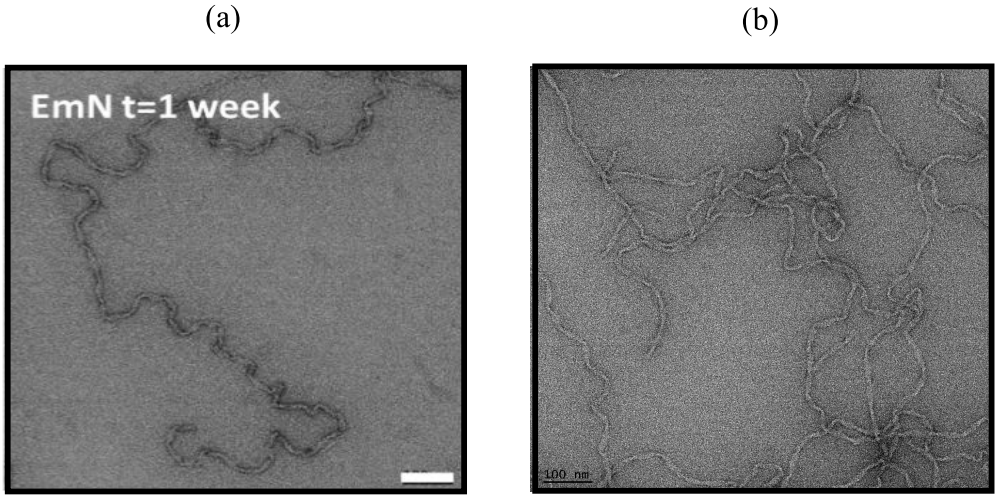

Supplementary Figure 3. No defect detected in the self-assembly capacity of ΔK37. (a) EmN (b) ΔK37 (500 µM) heated for 1 hr at 65°C then incubated for one week at 20°C were analyzed using negative stain imaging. The mutant was capable to self-assemble and form filaments similar to EmN ones. Scale bar, 100 nm in a and 200 nm in b.

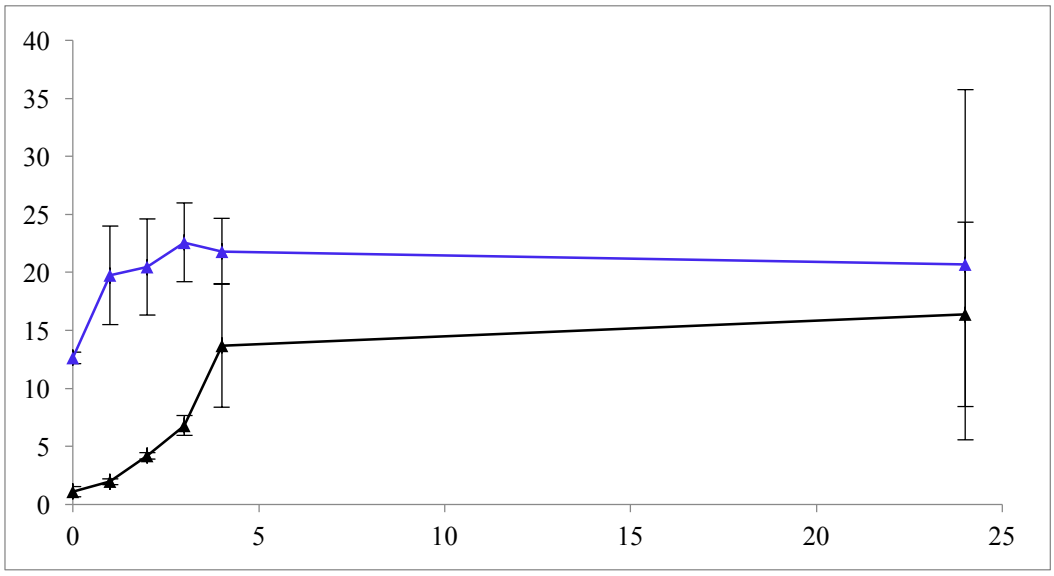

Supplementary Figure 4. ΔK37 self-assemble faster than EmN. Thioflavine T (ThT) fluorescence was measured as a function of the incubation time at 37°C for EmN, and *Δ*K37, *shown in black, and purple,* respectively (all proteins were at 600 µM final concentration). The fluorescence signal was higher for the mutant than for the EmN. This indicates the faster polymerization kinetics of their self-assembled state compared to EmN.

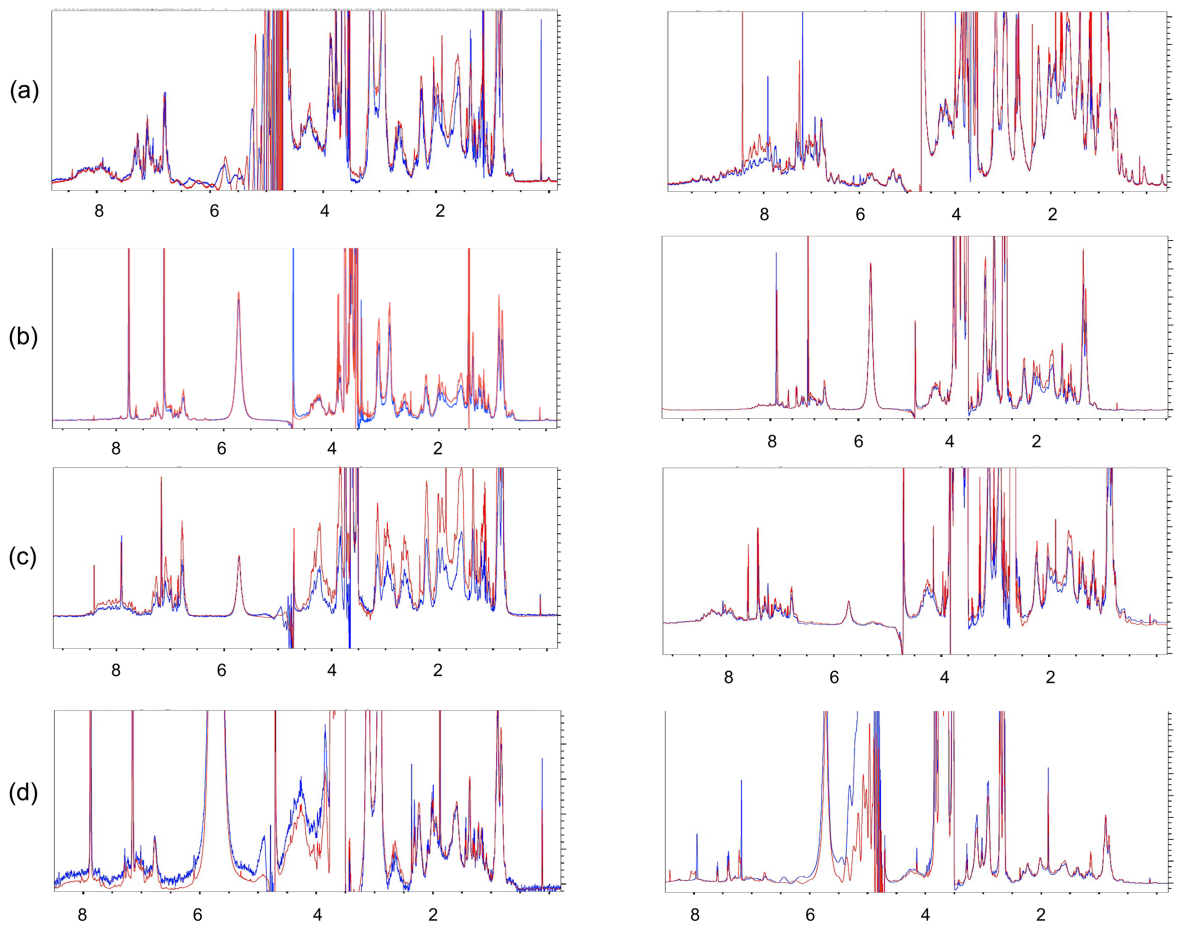

Supplementary Figure 5. The Ig-fold domain of lamin A/C has no effect on the stability of EmN mutants filaments. The figure displays overlay of solution-state NMR 1D spectra recorded after 1 and 12 hours shown in *red* and *blue*, respectively, at 30°C, 750 MHz, for the filaments of a) EmN (b) P22L (c) ΔK37 (d) T43I (150 µM) in absence (*left-side spectra)* and presence of ^{15}N Ig-fold domain (150 µM) (r*ight-side spectra*).

References

1. UMD-EMD. Available at: http://www.umd.be/EMD/.
2. Manilal, S. *et al.* Mutations in Emery – Dreifuss muscular dystrophy and their effects on emerin protein expression. **7,** 855–864 (1998).
3. Samson, C. *et al.* Emerin self-assembly mechanism: role of the LEM domain. *FEBS J.*

284, 338–352 (2017).

4. GL, K. The relative permeability of the surface and interior portions of the cytoplasm of animal and plant cells. *Biol Bull* **25,** 1–7 (1913).
5. Watson, M. L. The nuclear envelope; its structure and relation to cytoplasmic membranes. *J. Biophys. Biochem. Cytol.* **1,** 257–70 (1955).
6. Hetzer, M. W. The nuclear envelope. *Cold Spring Harb. Perspect. Biol.* **2,** 1–16 (2010).
7. Muchir A, W. H. The nuclear envelope and human disease. *Physiology* **19,** 309–314 (2004).
8. Wilson, K. L. & Dawson, S. C. Evolution: functional evolution of nuclear structure. *J. Cell Biol.* **195,** 171–81 (2011).
9. Cai, M. *et al.* Solution structure of the constant region of nuclear envelope protein LAP2 reveals two LEM-domain structures: One binds BAF and the other binds DNA. *EMBO J.* **20,** 4399–4407 (2001).
10. Lee K., K. . W. All in the family: evidence for four new LEM-domain proteins Lem2 (NET-25), Lem3, Lem4 and Lem5 in the human genome. *Oxford, UK BIOS Sci. Publ. LTD* (2004).
11. Margalit, A., Brachner, A., Gotzmann, J., Foisner, R. & Gruenbaum, Y. Barrier-to-autointegration factor - a BAFfling little protein. *Trends Cell Biol.* **17,** 202–208 (2007).
12. Bengtsson, L. & Wilson, K. L. Multiple and surprising new functions for emerin, a nuclear membrane protein. *Curr. Opin. Cell Biol.* **16,** 73–79 (2004).
13. Cartegni, L. Heart-specific localization of emerin: new insights into Emery-Dreifuss muscular dystrophy. *Hum. Mol. Genet.* **6,** 2257–2264 (1997).
14. Berk Tifft, K. E. and Wilson, K. L, J. M. The nuclear envelope LEMdomain protein emerin. *Nucleus* **4,** 298–314 (2013).
15. Christophe Guilluy Laurianne Van Landeghem, Lisa Sharek, L. D. O. & Richard Superfine and Keith Burridge, R. G.-M. Isolated nuclei adapt to force and reveal a mechanotransduction pathway within the nucleus. *Nat Cell Biol* **16,** 376–381 (2014).
16. Le, H. Q. *et al.* Mechanical regulation of transcription controls Polycomb-mediated gene silencing during lineage commitment. *Nat. Cell Biol.* **18,** 864–875 (2016).
17. Jason M. Berk, Dan N. Simon, Clifton R. Jenkins-Houk, Jason W. Westerbeck, Line M. Grønning-Wang, Cathrine R. Carlson, and K. L. W. The molecular basis of emerin–emerin and emerin–BAF interactions. *J. Cell Sci.* **127,** 3956–3969 (2014).

18. Sakata, K. *et al.* High incidence of sudden cardiac death with conduction disturbances and atrial cardiomyopathy caused by a nonsense mutation in the STA gene. *Circulation* **111,** 3352–3358 (2005).
19. Bione, S. *et al.* Identification of a novel X-linked gene responsible for Emery-Dreifuss muscular dystrophy. *Nat. Genet.* **8,** 323–7 (1994).
20. Quijano-roy, S. Other Nuclear Envelopathies . (2013).
21. Gisèle Bonne, France Leturcq, and R. B. Y. Emery-Dreifuss Muscular Dystrophy. *GeneReviews* (2015).
22. Lammerding, J. *et al.* Abnormal nuclear shape and impaired mechanotransduction in emerin-deficient cells. *J. Cell Biol.* **170,** 781–791 (2005).
23. Vaughan M. Alvarez-Reyes, J.M. Bridger, J.L. Broers, F.C. Ramaekers, M. Wehnert, G.E. Morris, W.G.F. Whitfield, and C.J. Hutchison, A. Both emerin and lamin C depend on lamin A for localization at the nuclear envelope. *J. Cell Sci.* **114,** 2577–2590 (2001).
24. Cohen, M., Gruenbaum, Y., Lee, K. K. & Wilson, K. L. Transcriptional repression, apoptosis, human disease and the functional evolution of the nuclear lamina. *Trends Biochem. Sci.* **26,** 41–47 (2001).
25. Manilal, S. *et al.* Mutations in Emery – Dreifuss muscular dystrophy and their effects on emerin protein expression. **7,** 855–864 (1998).
26. Yaou, R. Ben *et al.* Multitissular involvement in a family with LMNA and EMD mutations: Role of digenic mechanism? *Neurology* **68,** 1883–1894 (2007).
27. Ben Yaou, R. *et al.* G.P.142. *Neuromuscul. Disord.* **24,** 843–844 (2014).
28. Fairley, E. a, Kendrick-Jones, J. & Ellis, J. a. The Emery-Dreifuss muscular dystrophy phenotype arises from aberrant targeting and binding of emerin at the inner nuclear membrane. *J. Cell Sci.* **112 (Pt 1,** 2571–2582 (1999).
29. KARST, M. L., HERRON, K. J. & OLSON, T. M. X-Linked Nonsyndromic Sinus Node Dysfunction and Atrial Fibrillation Caused by Emerin Mutation. *J. Cardiovasc. Electrophysiol.* **19,** 510–515 (2008).
30. Samson, C. *et al.* Emerin self-assembly mechanism: role of the LEM domain. *FEBS J.* **284,** 338–352 (2017).
31. Cai, M. *et al.* Solution NMR structure of the barrier-to-autointegration factor-emerin complex. *J. Biol. Chem.* **282,** 14525–14535 (2007).
32. Shimi T Segura-Totten M, Wilson KL, Haraguchi T, Hiraoka Y, K. T. Dynamic interaction between BAF and emerin revealed by FRAP, FLIP, and FRET analyses in

living HeLa cells. *J Struct Biol* **147,** 31–41 (2004).

33. Hirano, Y., Segawa, M., Ouchi, F.S., Yamakawa, Y., Furukawa, K., T. & K., and Horigome, T. Dissociation of emerin from barrier-to-autointegration factor is regulated through mitotic phosphorylation of emerin in a xenopus egg cell-free system. *J. Biol. Chem* **280,** 39925–39933 (2005).
34. Lee Et Al 2001.Pdf. doi:10.1007/s002210100725
35. Samwer, M. *et al.* DNA Cross-Bridging Shapes a Single Nucleus from a Set of Mitotic Chromosomes. *Cell* **170,** 956–972.e23 (2017).
36. Holaska Kowalski, A. K., and Wilson, K. L, J. M. Emerin caps the pointed end of actin filaments: evidence for an actin cortical network at the nuclear inner membrane. *PLoS Biol.* **2,** (2004).
37. Zhang Q, Ragnauth CD, Skepper JN, Worth NF, Warren DT, Roberts RG, Weissberg PL, Ellis JA, S. C. .Nesprin-2 is a multi-isomeric protein that binds lamin and emerin at the nuclear envelope and forms a subcellular network in skeletal muscle. *J Cell Sci* **118,** 673–687 (2005).
38. Iyer, A., Koch, A. J. & Holaska, J. M. Expression Profiling of Differentiating Emerin-Null Myogenic Progenitor Identifies Molecular Pathways Implicated in Their Impaired Differentiation. *Cells* **6,** 38 (2017).
39. Demmerle, J., Koch, A. J. & Holaska, J. M. Emerin and histone deacetylase 3 (HDAC3) cooperatively regulate expression and nuclear positions of MyoD, Myf5, and Pax7 genes during myogenesis. *Chromosom. Res.* **21,** 765–779 (2013).
40. Meaburn, K. J. *et al.* Primary laminopathy fibroblasts display altered genome organization and apoptosis. *Aging Cell* **6,** 139–153 (2007).
41. Mewborn, S. K. *et al.* Altered chromosomal positioning, Compaction, and gene expression with a lamin A/C gene mutation. *PLoS One* **5,** (2010).
42. Ognibene, A. *et al.* Nuclear changes in a case of X-linked Emery-Dreifuss muscular dystrophy. *Muscle and Nerve* **22,** 864–869 (1999).

Chapter III: Additional data

Additional results

1 Characterization of KO myoblasts and ΔK37 fibroblasts versus their respective wild-types

1.1 Genotyping

Cellular analyses were performed using *EDMD* male patient immortalized myoblasts with mutated *EMD* gene leading to the *complete absence of emerin* (referred to as KO); and immortalized mutant *emerin fibroblasts* (referred to as ΔK37) obtained from a *female* with *ACD*. Immortalized wild type myoblasts and fibroblasts without any muscle disorder were used as controls. Table 4 summarizes the two patients clinical, genetic features, and overall phenotype. Immortalization of the four cell lines was carried out in the platform for immortalization of human cells in the Institute of Myology, Paris, France according to their published protocol[169]. The genotyping results confirmed that in the myoblasts there is a null mutation that introduces a stop codon in exon 6 of *EMD* gene, whereas in the fibroblasts, there is an in-frame deletion in exon 2 resulting in single amino acid loss at the protein level (lysine 37). There is X-inactivation bias in the female ΔK37 fibroblasts (2% in active allele: 98% in inactive allele); and the active allele is the mutant one[152].

Table 4. Clinical and genetic summary of KO and ΔK37 patients

Cell line	KO	ΔK37
Patient Sex	Male	Female, X-inactivation (2%:98%)
Patient age at onset of disease	4 years old	45 years old
cDNA nomenclature	c.651-655dup	c.110-112delAGA
Protein nomenclature	p.Gln219TrpfsX20	p.Lys37del
Exon	6	2
Codon	219	37
Mutation type	Frameshift	In frame deletion
Mutation event	Stop at 238	In frame deletion
Mutation status	Hemizygous	Heterozygous
Control cells	Myoblasts of 25 years old healthy male	Fibroblasts of 19 years old healthy female
Phenotype	Emery Dreifuss Muscular Dystrophy (EDMD)	Atrial Cardiac Disease (ACD)
Clinical implications	Dystrophic features with inflammation and necrosis (last update age 13)	• Sinusal pauses (>2.5s) • Pacemaker at age 45 • No dystrophic features

1.2 Nuclear envelope proteins expression and localization: Emerin, lamin A/C, SUN2

The expression and localization of emerin in the two cell lines were verified by immunoblotting and immunohistochemistry. Indeed, there was complete absence of emerin at the protein level in the KO myoblasts, whereas the expression of emerin was reduced in ΔK37 fibroblasts (Figure 10).

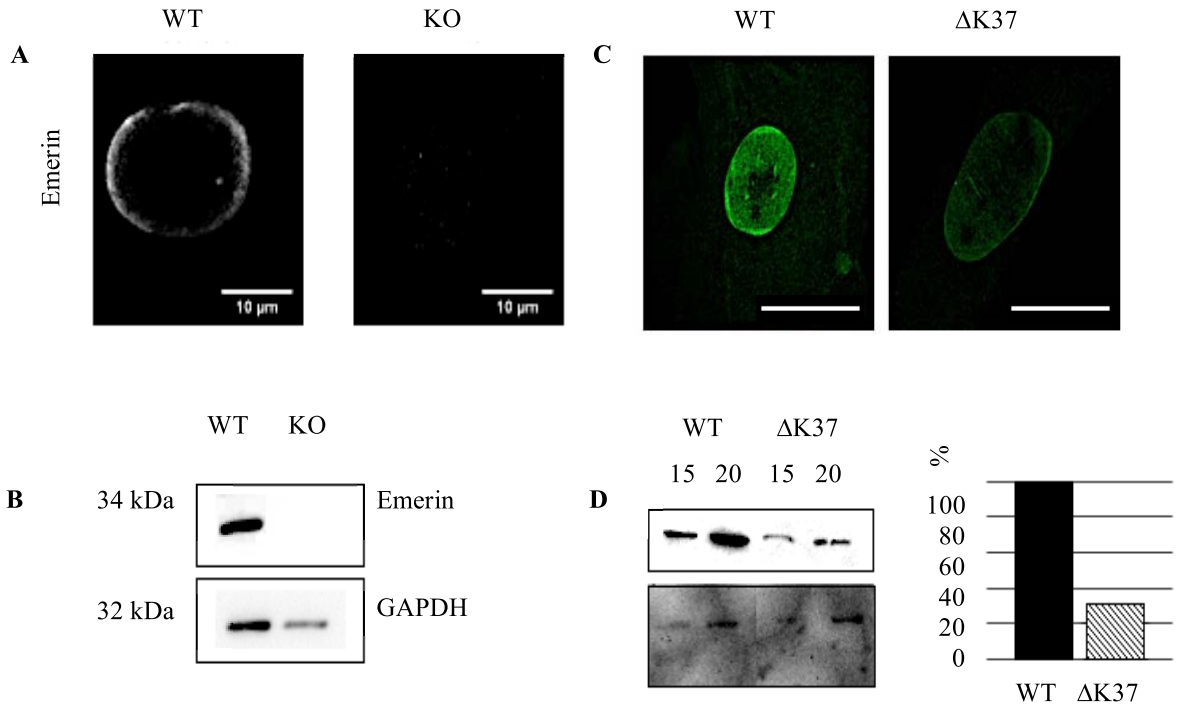

Figure 10. Absence of emerin in KO myoblasts and reduced expression in ΔK37 fibroblasts. (A) Representative immunofluorescence confocal microscopy images of nuclear envelope emerin staining of wild-type and KO myoblasts. Scale bar, 10µm. (B) Immunoblot illustrating the absence of emerin in KO myoblasts; N=3 (C) Representative immunofluorescence confocal microscopy images of nuclear envelope emerin staining of control and ΔK37 fibroblasts. Scale bar, 30 µm. (D) Immunoblot showing the reduction in the emerin expression in ΔK37 fibroblasts. Graph of the quantification of the reduction in emerin expression in ΔK37 compared to wild-type fibroblasts (almost 70% less); N=2.

Emerin interaction with A type lamins and members of LINC complex is crucial for relaying mechanical signals across the nuclear envelope membrane. Hence, we raised the question as to whether the emerin mutations could induce changes in the localization or expression of members of LINC complex.

As a result, we studied the expression of nuclear envelope proteins, namely lamin A/C and SUN 2, in the KO myoblasts and ΔK37 fibroblasts. No differences in lamin A/C localization (Figure 11.A**)** or expression (Figure 11.B**)** were detected in the KO myoblasts and ΔK37 fibroblasts (Figure 11.C**)** compared to their respective wild-types.

In addition, we detected a possible inverse relationship between matrix stiffness and lamin A/C phosphorylation in our KO myoblasts (Figure 11.D**)**. We observed less phosphorylation of serine 22 in lamin A in the KO myoblasts on hard substrate compared to soft substrate, indicative of the solubilization of lamin A on hard substrate. This corroborates what was put forward by Buxboim (2013)[170]. Yet, this needs to be confirmed.

Further, we studied the localization of SUN2 in the two mutations. Although it's difficult to conclude from one experiment, it seems that there is a defect in SUN2 inner nuclear envelope membrane localization in the two mutants compared to their wild-types (Figure 11.E, F). However, this result needs to be further confirmed.

1.3 Focal adhesions and microtubules: Vinculin, β-tubulin

Subsequently, we questioned if there was a defect in focal adhesions in KO myoblasts. We therefore analyzed the organization and expression of vinculin on hard and soft substrates (Figure 11.G, H). No difference was detected in the expression of vinculin in KO myoblasts on hard or soft substrates.

Finally, we wondered whether the mutations induced defects in microtubule cytoskeleton. Accordingly, we stained the KO myoblasts and ΔK37 fibroblasts for β-tubulin (Figure 11.I). We didn't observe differences in β-tubulin organization in the two mutants, which is consistent with what was reported for X-EDMD patients' cells (null for emerin)[87]. However, no centrosome staining was done.

Taken all together, obtained data revealed the absence of emerin in the KO myoblasts and its reduction in the ΔK37 fibroblasts. In addition, there were no changes in lamin A/C localization or expression in the two mutants; and no defects in β-tubulin and vinculin.

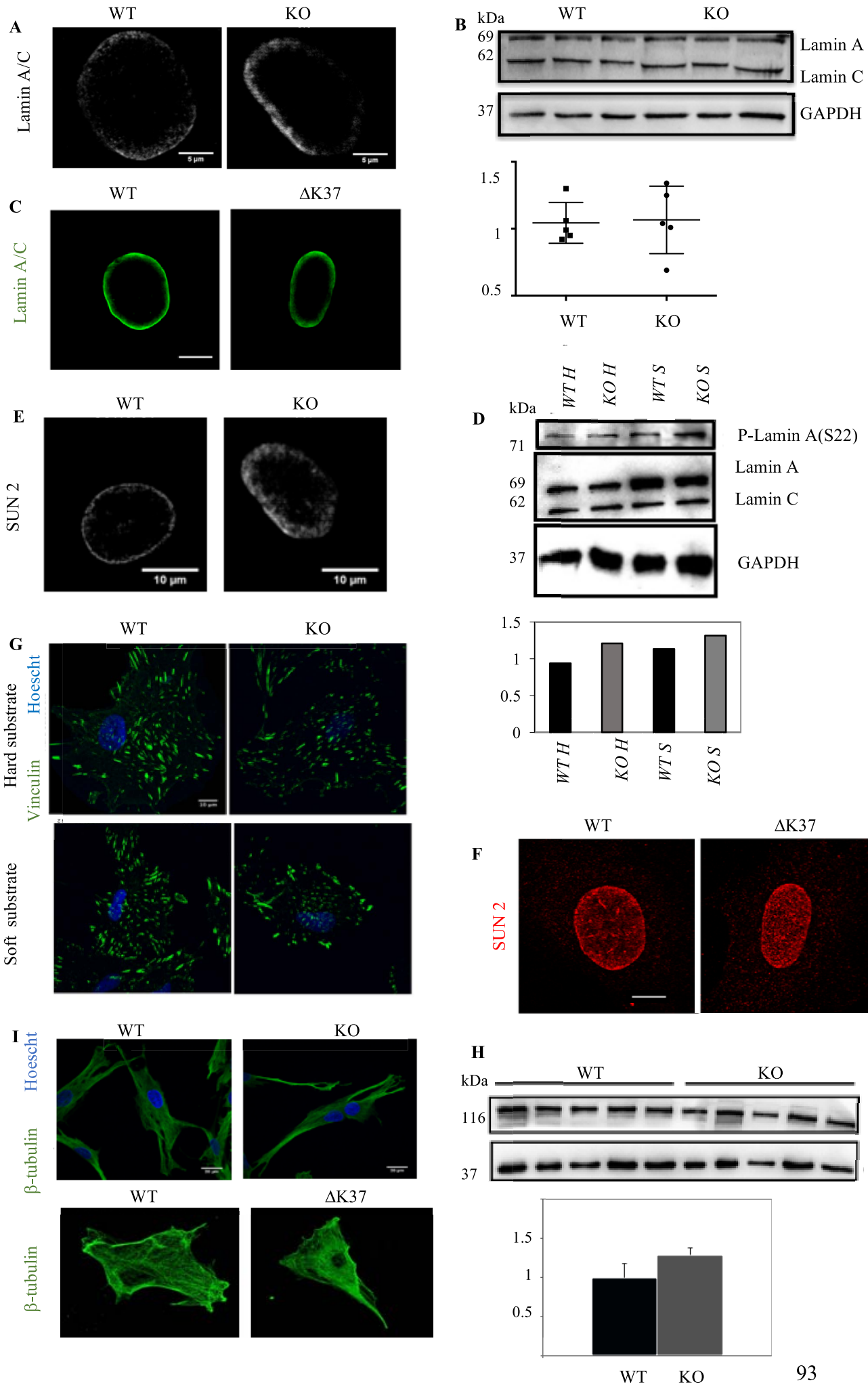
A
WT
KO
Lamin A/C
B
kDa
WT
KO
69
62
Lamin A
Lamin C
37
GAPDH
1.5
1
0.5
WT
KO
C
WT
ΔK37
Lamin A/C
D
kDa
WT H
KO H
WT S
KO S
71
P-Lamin A(S22)
69
62
Lamin A
Lamin C
37
GAPDH
1.5
1
0.5
0
WT H
KO H
WT S
KO S
E
WT
KO
SUN 2
10 μm
10 μm
F
WT
ΔK37
SUN 2
G
WT
KO
Hard substrate
Hoescht
Vinculin
Soft substrate
H
kDa
WT
KO
116
Vinculi
37
GAPDH
1.5
1
0.5
WT
KO
I
WT
KO
Hoescht
β-tubulin
WT
ΔK37
β-tubulin

Figure 11. Characterization of KO myoblasts and ΔK37 fibroblasts. (A) Representative confocal microscopy images of wild-type and KO myoblasts stained for lamin A/C. Scale bar, 5 μm. (B) Immunoblot showing no difference in the expression of lamin A/C in KO myoblasts on hard substrate in 2D culture. Graph of the quantification of normalized lamin A/C expression in KO compared to wild-type myoblasts; N=5, P-value = ns. (C) Representative confocal microscopy images of wild-type and ΔK37 fibroblasts stained for lamin A/C. Scale bar, 30 μm**.** (D) Immunoblot showing phosphorylated (Ser22) lamin A and total lamin A/C expressions in wild-type and KO myoblasts on hard and soft (20 kPa) substrates. Graph of the quantification of phosphorylated Ser22 lamin A expression in KO compared to wild-type myoblasts on hard and soft (20 kPa); N=1. (E) Representative confocal microscopy images of wild-type and KO myoblasts stained for SUN2. Scale bar, 30 μm. (F) Representative confocal microscopy images of wild-type and ΔK37 fibroblasts stained for SUN2. Scale bar, 5 μm (G) Representative confocal microscopy images of wild-type and KO myoblasts plated on hard (upper panel) and soft (20 kPa) substrates (lower panel) stained for vinculin. Scale bar, 10 μm. (H) Immunoblot showing no difference in the expression of vinculin in KO myoblasts on hard substrate in 2D culture. Graph of the quantification of vinculin expression in KO compared to wild-type myoblasts; N=3, P-value = ns. (I) Representative confocal microscopy images of wild-type and KO myoblasts (upper panel); wild-type and ΔK37 fibroblasts (lower panel) stained for β-tubulin. Scale bar, 10 μm.

2 Effect of KO and ΔK37 mutations on mechanobiology

In an attempt to determine whether there is a defect in mechanical responses in KO and ΔK37 first, we analyzed the responses of the two mutations to changes in substrate stiffness. Second, we analyzed changes in the perinuclear actin network on hard substrate. lastly, we investigated the export of nuclear emerin upon mechanical stretch in ΔK37. In light of the obtained data for the two mutations in our experimental setting (cell type and approaches adopted), we didn't detect a mechanosensing defect.

2.1 Mutations response to changes in substrate stiffness in two-dimensional culture

In vivo cells attach to much softer surfaces (0.05 – 20 kPa), than the classic culture plates (2-4 GPa) on which most studies are done *in vitro*[171]. To exemplify, fibroblasts, smooth muscle and skeletal muscle tissue stiffness is only around 3-5 and 12 kPa, respectively[171]. Cell morphology and functions strongly depend on substrate stiffness when chemical signals are constant[171]. For instance, cells generate more force and exhibit more surface area on a stiff

matrix compared to similar cells interacting with a softer matrix[171]. We wondered whether the KO and ΔK37 cells were capable to sense changes in substrate stiffness and respond by accommodating their spreading area reciprocally.

To this end, cells expressing KO and ΔK37 were plated on soft bio-compatible substrate of 20 and 8 kPa modulus, respectively. Obtained data show that KO myoblasts were able to adapt their spreading area to the rigidity of their substrates (mean spreading area = 2030 ± 736 μm^2 for KO on hard substrate and 980 ± 760 μm^2 on soft one, ****P<0.0001, Figure 12.A). Similarly, ΔK37 fibroblasts were able to respond to changes in substrate rigidity (5600 ± 424 μm^2 for ΔK37 on hard substrate and 3234 ± 228 μm^2 on soft one, P<0.05. In addition, we didn't observe differences in nuclear roundness in the KO myoblasts on hard substrate (mean contour ratio= 0.82 ± 0.003 μm^2 for KO on hard surface and 0.83 ± 0.006 μm^2 on soft one, Figure 12.C). Conversely, previous findings[82] reported that emerin KO fibroblasts displayed significant decrease in nuclear roundness (mean contour ratio= 0.89 and 0.86 for wild-type and KO, respectively), and that it was a milder phenotype compared to A-type lamin-deficient cells.

We are aware that our experiment may have one limitation which is the unexpected behavior of wild-type myoblasts. This is evident because 1) their mean spreading area on soft substrate was higher than on hard one 2) the contour ratio of our KO myoblasts (0.82) is close to that of Lammerding group (0.86), whereas our wild-type (0.82) is strikingly far from the 0.9 value of ideally round nuclei compared to Lammerding's group wild-type cells (0.89). It is plausible that it was due to cell culture problems. Consequently, we limited our analysis to comparing KO myoblasts responses on hard to that on soft in order to determine if they were able to sense changes in substrate stiffness, regardless of the wild-type behavior under these conditions.

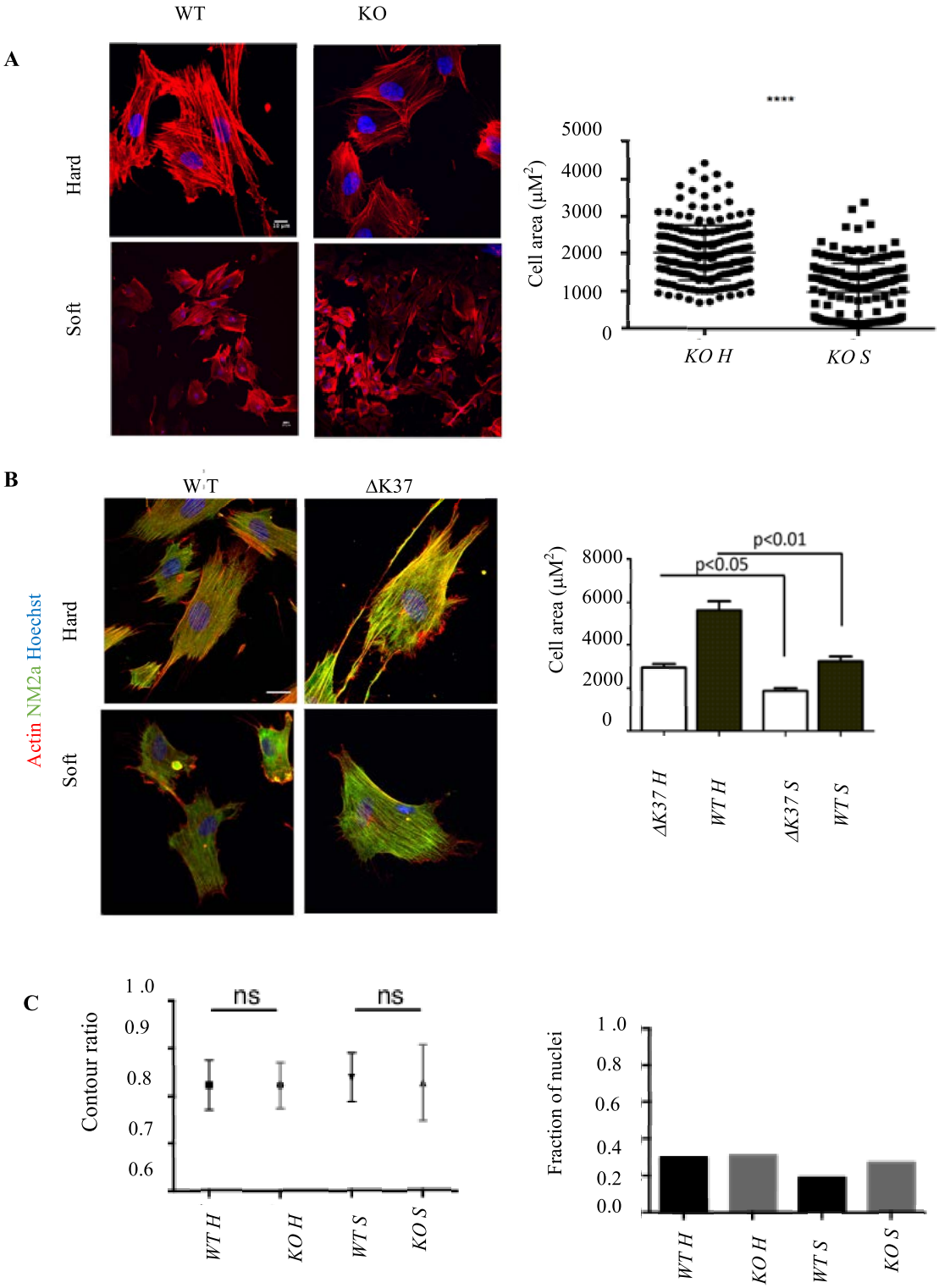
A
WT
KO
Hard
Soft
****
5000
4000
3000
2000
1000
0
Cell area (μM²)
KO H
KO S
B
W T
ΔK37
Actin NM2a Hoechst
Hard
Soft
p<0.01
p<0.05
8000
6000
4000
2000
0
Cell area (μM²)
ΔK37 H
WT H
ΔK37 S
WT S
C
1 .0
0.9
0.8
0.7
0.6
Contour ratio
ns
ns
WT H
KO H
WT S
KO S
1 .0
0.8
0.6
0.4
0.2
0.0
Fraction of nuclei
WT H
KO H
WT S
KO S

Figure 12. KO and ΔK37 are able to respond to changes in substrate stiffness in 2D cell culture (A) Representative confocal microscopy images of wild-type and KO myoblasts plated on hard and soft (**20 kPa)** substrates stained for F-actin (phalloidin, red) and nuclei (Hoescht, blue). Scale bar,10 μm on hard substrate and 20 μm on soft one. Graphs showing quantification of KO cells spreading area, values are mean ± standard deviation (mean spreading area = 2030 ± 736 μm^2 for KO on hard substrate and 980 ± 760 μm^2 on soft one, ****P<0.0001; n >150 cells for each group from three independent experiments). (B) Representative confocal microscopy images of WT and ΔK37 fibroblasts plated on hard and soft (**8 kPa**) substrates stained for F-actin (Phalloidin, red), non-muscle myosin IIa (NM2a, green) and nuclei (Hoescht, blue). Scale bar, 10 μm. Graph showing quantification of ΔK37 fibroblasts spreading area, values are mean ± standard deviation. (mean spreading area= 2943 ± 171 μm^2 for wild-type on hard substrate, 1862 ± 127 μm^2 on soft one, P<0.01; 5600 ± 424 μm^2 for ΔK37 on hard substrate and 3234 ± 228 μm^2 on soft one, P<0.05; n >82 cells for each group in one experiment). (C) Contour ratio (4π area/perimeter^2) as a measurement of nuclear circularity or roundness was calculated for KO on hard and soft substrates, values are mean ± standard deviation. (mean contour ratio= 0.82 ± 0.003 for wild-type on hard substrate, 0.84 ±. 0.003 on soft one; mean contour ratio= 0.82 ± 0.003 μm^2 for KO on hard surface and 0.83 ± 0.006 μm^2 on soft one; n > 170 cells for each group from three independent experiments). Given that ideally round nuclei have contour ratio between 0.8-1, we presented the fractions of nuclei with contour ratio < 0.8 in a graph (0.3 and 0.19 for wild-type on hard and soft substrates respectively; 0.31 and 0.27 for KO hard and soft substrates respectively). ns, not significant.

2.2 Actin cytoskeleton and perinuclear actin organization in mutants

Perinuclear actin is composed of thick parallel highly contractile actomyosin filament bundles located at the apical plane of the cell and attached to the nucleus through the LINC complex. On the other hand, basal actin is composed of basal stress fibers, transverse arcs and dorsal fibers positioned at the basal plane of the cell[172]. As illustrated in the Figure 13, NIH3T3 cells transfected with emerin siRNAs exhibited a defect in the perinuclear actin cap compared to wild-type ones[173]. Given that perinuclear actin dominates mechanosensing responses to changes in matrix stiffness[174], we analyzed the perinuclear actin network in KO and ΔK37 on hard surface.

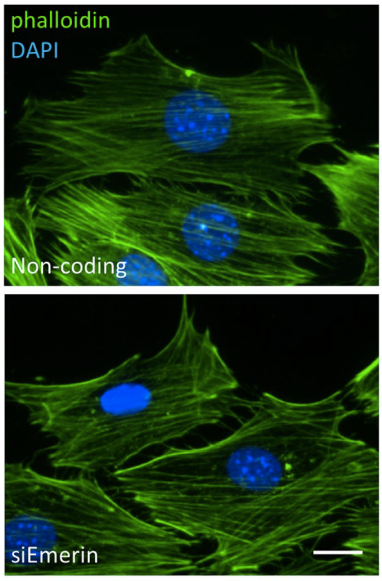

Figure 13. Perinuclear actin defects in emerin-null cells. Immunoflurescence images of F-actin in green and nuclei in blue in NIH3T3 cells transfected with either non-coding or emerin siRNAs.

On the contrary, there was no observed defect in the perinuclear actin network in the KO myoblasts and ΔK37 fibroblasts (Figure 14).

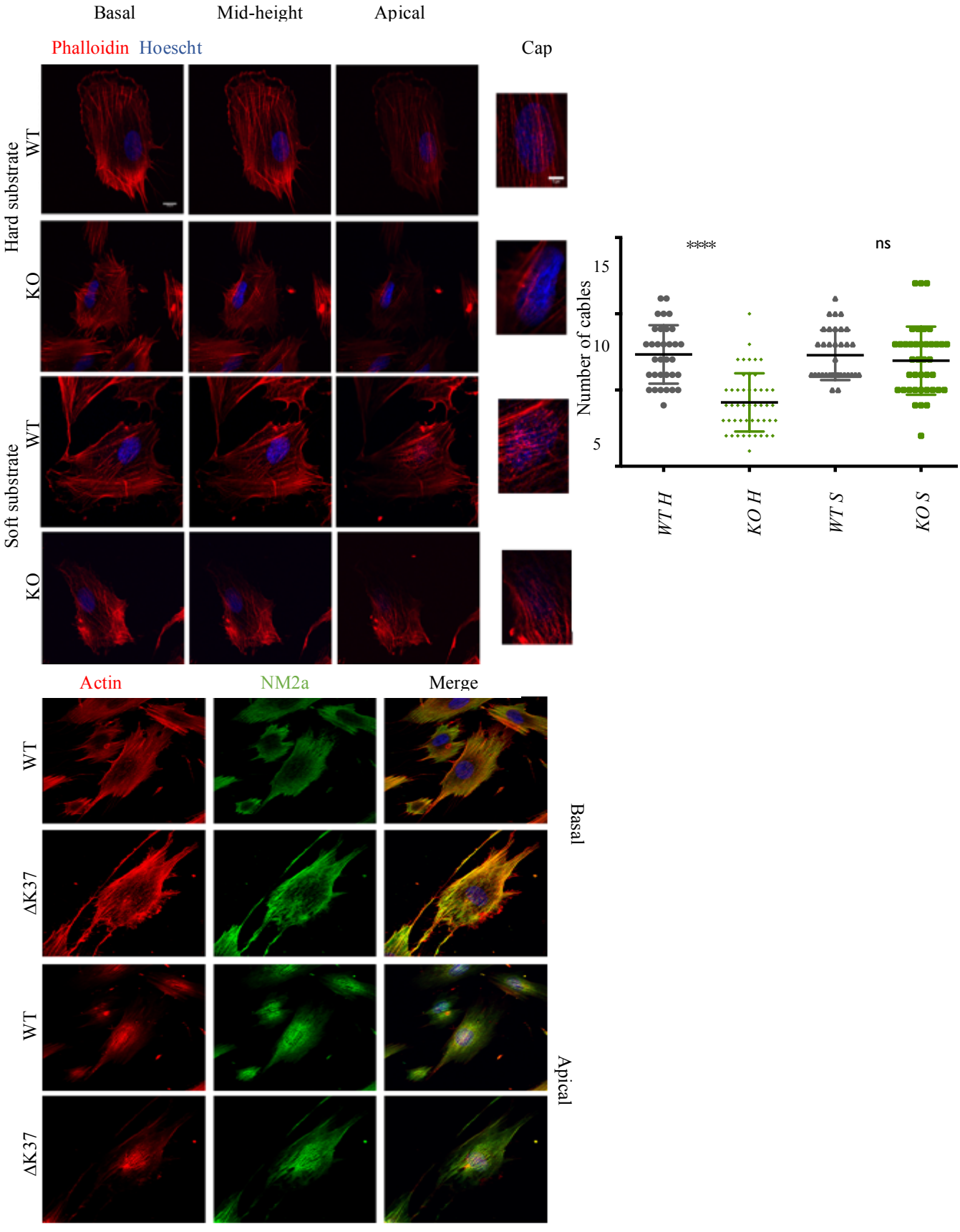
Basal
Mid-height
Apical
Phalloidin Hoescht
Cap
Hard substrate
WT
KO
Soft substrate
WT
KO
Number of cables
15
10
5
****
ns
WT H
KO H
WT S
KO S
Actin
NM2a
Merge
WT
ΔK37
WT
ΔK37
Basal
Apical

Figure 14. Perinuclear actin network analysis in KO and ΔK37. (A) Representative confocal microscopy images of wild-type and KO myoblasts plated on hard and soft (**20 kPa)** substrates stained for F-actin (phalloidin, red) and nuclei (Hoescht, blue). Sections showing the actin filament network at apical surface, mid-height and basal surface as well as the perinuclear actin cap. Scale bar,10 μm for the first three sections, and 5 μm for the last one. Graph of quantification of number of perinuclear actin cables of wild-type and KO myoblasts on hard and soft substrates, values are mean ± standard deviation. (mean number of perinuclear actin cables for wild-type and KO on hard substrate were 7 ± 2, 4 ± 2 respectively, ****P<0.0001; mean number of perinuclear actin cables for wild-type and KO on soft substrate were 7 ± 2 and 7 ± 2 on soft one; n > 30 cells for each group from three independent experiments). ns, not significant. (B) Representative confocal microscopy images of wild-type and ΔK37 fibroblasts stained for F-actin (phalloidin, red), non-muscle myosin IIa (NM2a, green) and nuclei (Hoescht, blue). Sections showing the actin filament network at apical and basal surfaces.

2.3 Emerin enrichment at the outer nuclear envelope membrane upon mechanical stretch in ΔK37 fibroblasts

Our results demonstrated in Figure 10 are in line with previous published results[152] that showed reduction in emerin expression in ΔK37 fibroblasts. We wondered whether mutant emerin, even at lower level, will be enriched at the outer nuclear membrane upon mechanical stretch in agreement with what was shown for wild-type emerin recently[69]. We used digitonin which selectively permeabilizes the plasma membrane yet leaves the intracelluar membrane intact. Compared to static conditions, emerin was enriched at the outer nuclear envelope membrane in both wild-type and ΔK37 fibroblasts (Figure 15).

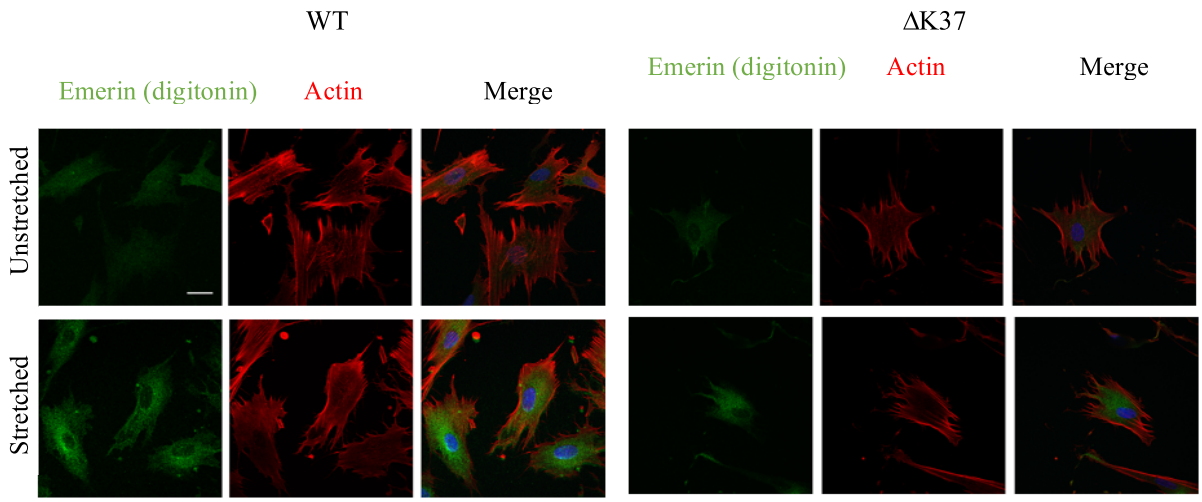

Figure 15. Emerin enrichment at the outer nuclear envelope membrane upon mechanical stretch in ΔK37 fibroblasts. Confocal Immunofluorescence analysis showing strain-induced enrichment of emerin at the outer nuclear membrane in digitonin-permeabilized wild-type and ΔK37 fibroblasts in which the inner nuclear membrane is inaccessible to the antibodies (Upper panel, unstretched; lower panel, stretched conditions). Cells were subjected to 10% cyclic stretch at 0.5 Hz for 4h. Scale bar, 10 µm. Emerin was enriched in ΔK37 fibroblasts upon mechanical stress similar to wild-type.

3 ΔK37 phosphorylation in vitro by Src

Phosphorylation is the first molecular event that occurs in the nuclei upon application of mechanical force. Indeed, the inner nuclear envelope membrane protein, emerin is phosphorylated by several kinases: Src, Abl, FAK, PKACA and Her2. However, in response to mechanical force application, emerin is phosphorylated by Src kinase. In this line, the phosphorylation of tyrosine 95 and 99 is of particular importance[175]. We thereby questioned the phosphorylation capacity of ΔK37 by Src kinase *in vitro*. We managed to phosphorylate ΔK37 *in vitro* by Src (Figure 16) but we could not deduce based on the mass spectrometry (MS) analysis whether all ΔK37 tyrosine residues are 100% phosphorylated. However, we concluded that the majority of tyrosines in ΔK37 are phosphorylated similar to EmN (Figure 16). In the MS analysis, tyrosine 105 and 161 were highly abundant, whereas, due to technical

reasons, the fragment 175-187 was difficult to be detected. Consequently, tyrosine 181 and 182 are not reported. The next question in future experiments will be whether ΔK37 can by phosphorylated upon force application.

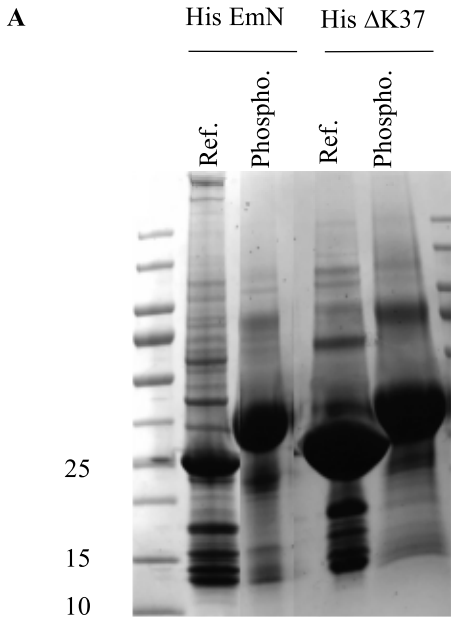

B MDNYADLSDTELTTLLRRY[19]NIPHGPVVGSTRRLYEKKIFEY[41]ETQRRRLSPPSSSAASSY[59]
SFSDLNSTRGDADMY[74]DLPKKEDALLY[85]QSKGYNDDY[94]Y[95]EESY[99]FTTRTY[105]GEPESAGP
SRAVRQSVTSFPDADAFHHQVHDDDLLSSSEEECKDRERPMYGRDSAY[161]QSITHY[167]RPV
SASRSSLDLS *Y[181]Y[182]*PTSSS

Figure 16. Phosphorylation of EmN and ΔK37 by Src kinase. Phosphorylation of His-EmN and His ΔK37 (0.9 mg) by Src kinase (0.9 µg) in presence of phosphorylation buffer (2 mM ATP, 0.5 mM $MgCl_2$, 5 mM DTT, 20 mM Tris HCl pH 7.5, 1X protease inhibitor) overnight at 30°C. (A) SDS-PAGE gels His-EmN reference (Ref.), phosphorylated His-EmN (Phospho.), His-ΔK37 reference and phosphorylated His-ΔK37. (B) Emerin amino acid sequence (1-187) demonstrating phosphorylation modified residues by mass spectrometry in red. Italic Y181 and Y182 were difficult to detect, whereas underlined Y105, Y161 were highly abundant in the mass spectrometry analysis.

All in all, emerin KO myoblasts and ΔK37 fibroblasts were able to respond to changes in substrate stiffness adapting their spreading area accordingly. Further, we did not detect

defects in nuclei roundness or perinuclear actin network in KO myoblasts and ΔK37 fibroblasts. Similar to wild-type fibroblasts, ΔK37 emerin was enriched in the outer nuclear envelope membrane upon mechanical stretch. Finally, ΔK37 emerin was successfully phosphorylated by Src *in vitro*. In light of the obtained data for the two mutations in our experimental setting (cell type and approaches adopted), we didn't detect a mechanosensing defect.

4 Effect of mutations on Wnt pathway

It was reported that emerin is important for restricting β-catenin levels and, be consequence, the Wnt/β-catenin signaling pathway[97]. For this reason, we asked whether there is defect in such function in the ΔK37 fibroblasts. As a preliminary result, we found higher nuclear β-catenin staining in ΔK37 compared to wild-type fibroblasts (Figure 17). However, we cannot yet conclude as it is a single experiment, besides we cannot extrapolate if this defect is triggered by the reduced emerin levels in the ΔK37 fibroblasts or provoked by the presence of the mutation in the ΔK37 emerin.

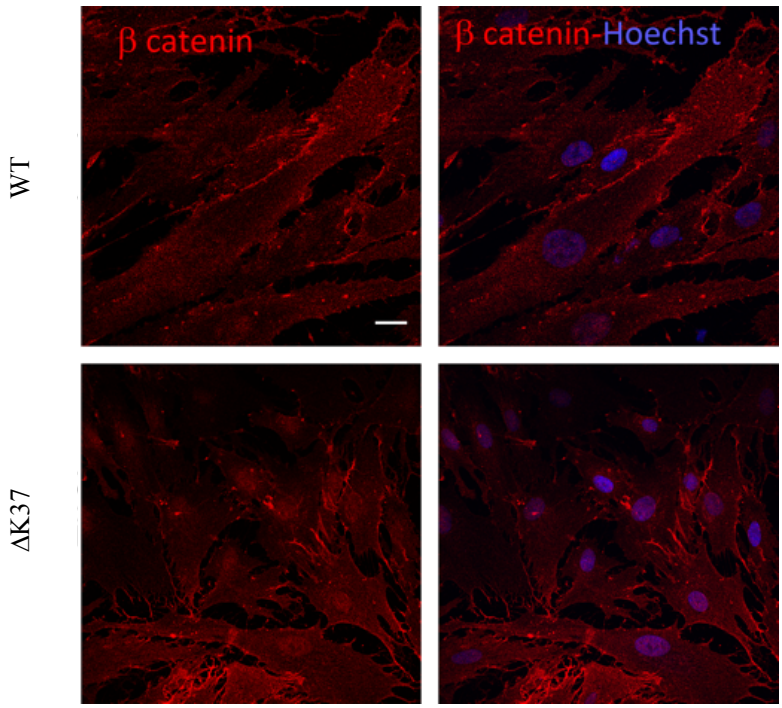

Figure 17. β-catenin expression in ΔK37. Representative confocal microscopy images of wild-type and ΔK37 fibroblasts stained for β-catenin. Nuclei were counterstained with hoescht. Scale bar, 10 μm**.**

5 Denaturation profiles of EmN using thermofluor assay

As shown in Essawy et al., we opted for the FBTSA assay for the purpose of studying the folding state of the mutant ΔK37. As preliminary experiments, we searched for buffer conditions that will be optimal for following denaturation. EmN denaturation profiles were obtained using different buffers, in absence and presence of salt or glycerol and using a pH screen (Figure 18). The Tm (average Tm= 47°C) generated was similar in the different tested conditions, except for the Mes buffer when EmN destabilized. That's probably because the Mes buffer pH (6) is close to the EmN isoelectric point pH (5.29).

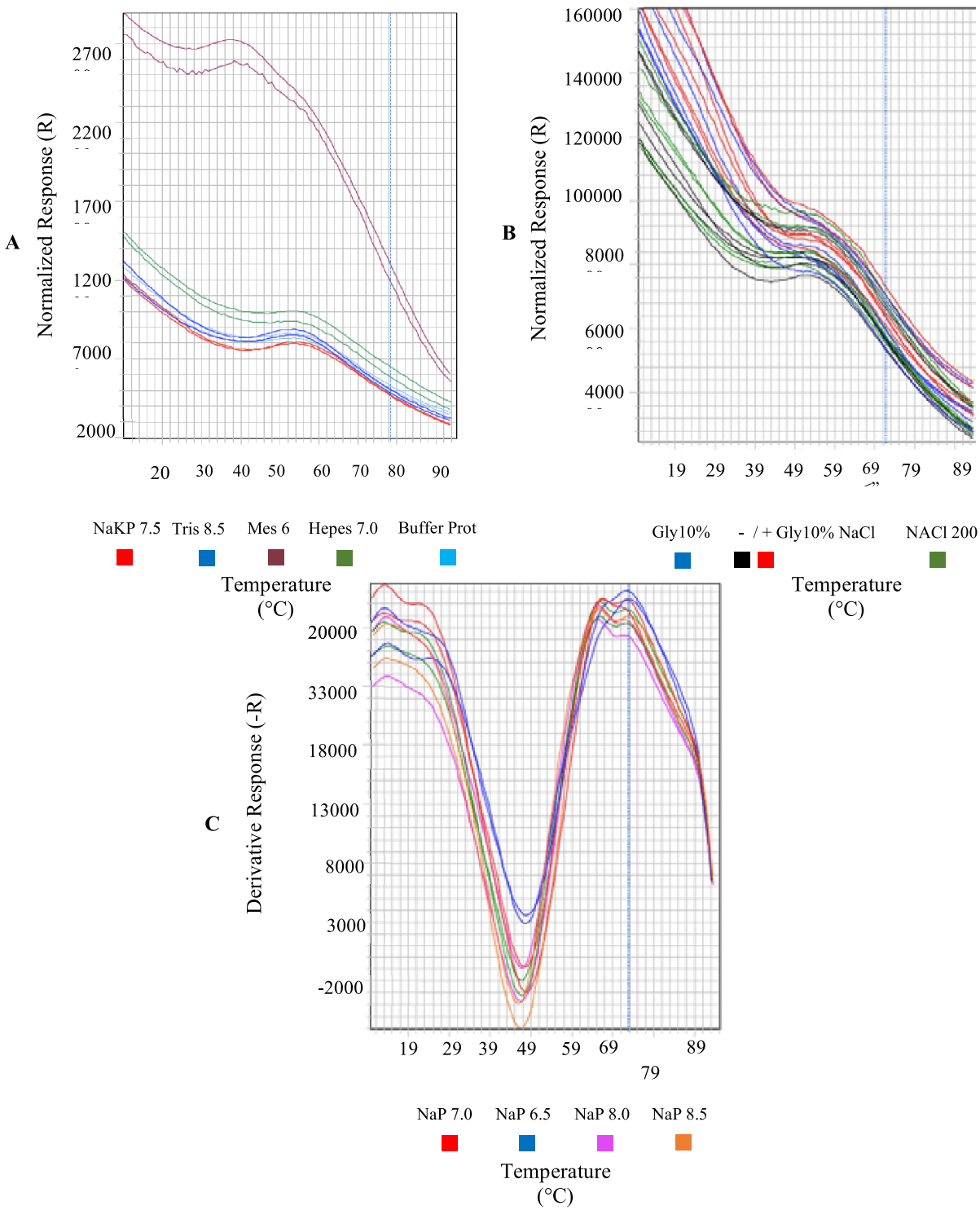

Figure 18. Denaturation profiles of EmN using thermofluor assay. (A) Denaturation tests were performed in five buffer conditions: Mes 6, Hepes pH 7, NaKP pH 7.5, Tris pH 8.5 and protein buffer (Tris HCl pH 8). Each test was done twice using two qPCR machines. The denaturation profiles of EmN were similar in the different buffers, except for Mes pH 6 when the protein destabilized. (B) The buffer screen was carried out in twelve conditions: Hepes pH 7, NaKP pH 7.5, Tris pH 8.5 in absence and presence of 200 mm NaCl with or without 10% glycerol or only glycerol. No significant effect was detected on the denaturation temperatures in these conditions. (C) The pH screen was done in a range of concentration of sodium

phosphate buffer (pH 6.5, 7, 7.5, 8, 8,5). There was no significant effect on the denaturation profile of EmN under these conditions.

6 EmN mutants-BAF interaction parameters determination

Despite the presence of the LEM-domain mutations in the site of interaction with BAF, we, unexpectedly, observed their interactions with BAF (Nada et al. draft). Subsequently, we wondered whether the mutations had attenuated the BAF binding parameters. We selected two commonly used biophysical techniques in order to determine the different interaction parameters: enthalpy change, stoichiometry, K_{on}, K_{off} and K_D.

6.1 Surface Plasmon Resonance (SPR)

We opted for a ProteOn HTG sensor chip suitable for capturing histidine-tagged proteins and studying protein-protein interactions in order to determine the K_{on}, K_{off} and K_D of BAF–mutants' interactions. All experiments were run at 20°C. Firstly, we immobilized histidine tagged EmN and the three mutants as ligands and injected a serial dilution of BAF dimer as analyte. The threshold of the chosen twofold dilution series was based on 10x the affinity of EmN to BAF (10 x 0.5 μM= 5 μM). Disappointingly, BAF exhibited nonspecific binding to the sensor chip surface characterized by significant binding responses that did not return to baseline at the end of the injection (only EmN data are shown in Figure 19 since the problem was consistent with the mutants). We tried subtracting the interspot signal from the reaction spot signal, however results were not satisfactory. Secondly, we immobilized BAF dimer as ligand with and without activating the chip with nickel and injected a serial dilution of EmN as analyte (date not shown). Similarly, we obtained nonspecific BAF binding to the sensor chip surface even in absence of nickel. We deduced that BAF favors binding to the alginate polymer bound to the gold surface of the sensor prism. Lastly, we immobilized histidine tagged BAF dimer as ligand (0.02 and 0.1mg/ml) and injected a serial dilution of

EmN as analyte. Equally, EmN binds nonspecifically to the sensor chip surface (data not shown). Given these points, we ditched the SPR for its unsuitability for the nature of our proteins and we tried the ITC technique.

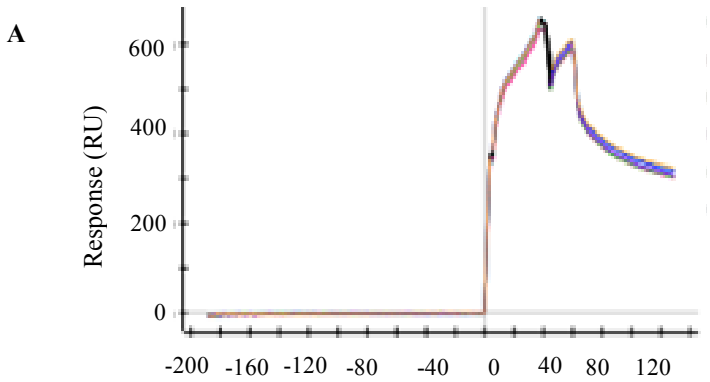

Figure 19. SPR analysis of EmN interaction with BAF. Sensorgram achieved using as ligand EmN at 0.05 mg/ml and a range of concentration of BAF as analyte (0, 0.375, 0.75, 1.25, 2.5, 5 μM) immobilized on a HTG sensor chip. Responses obtained 331.43 RU for EmN.

6.2 Isothermal Titration Calorimetry (ITC)

Our team had previously determined the binding affinity of BAF to EmN using ITC (K_D= 0.5 μM) (Samson et al. under review). For this reason, we chose this method to determine the stoichiometry and affinity (K_D) of the BAF binding to EmN mutants. All experiments were run at 10°C. References for EmN, P22L, ΔK37 and T43I were first run. Then each EmN mutant was syringe injected in the sample cell containing BAF dimer (Figure 20). Thermogram of ΔK37 is not shown due to lack of signal. Regarding P22L and T43I, we found a very low stoichiometry, which suggests that most EmN mutants is not available for binding. In particular the stoichiometry deduced from the preliminary fitting is very low, suggesting that a large proportion of the mutants is unable to bind BAF. It's possible that the mutants aggregated either during the injection or in the cell in view of their faster polymerization rate when compared to

EmN. We excluded the possibility that the problem is in the BAF inactivity as it was used for the same experiment but using another partner (lamin A/C) and it was active.

(a)

EmN reference

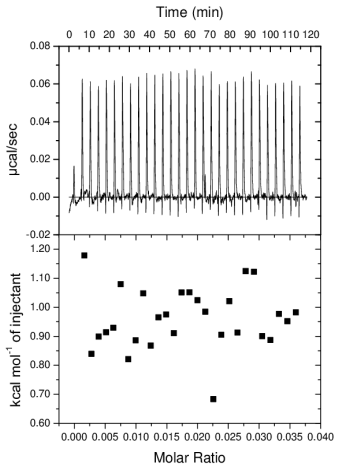

EmN-BAF

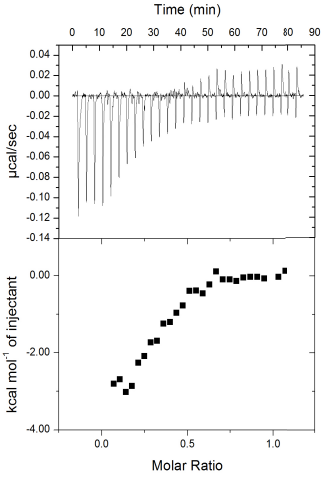

Kd= 0.6 ± 0.03 µM
N= 0.3 ± 0.01 sites

(b)

P22L reference

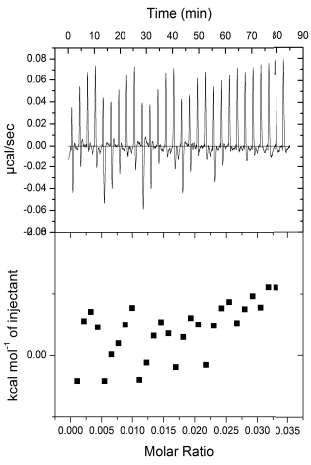

P22L-BAF

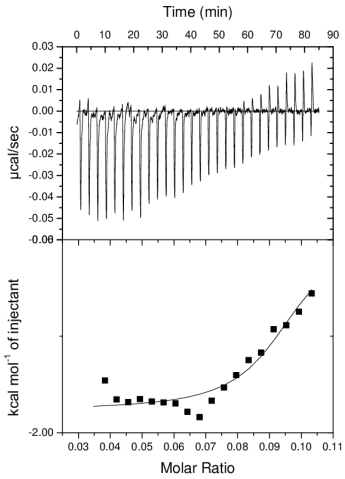

Kd= 0.014 ± 0.014 µM
N= 0.1 ± 0.01 sites

(c)

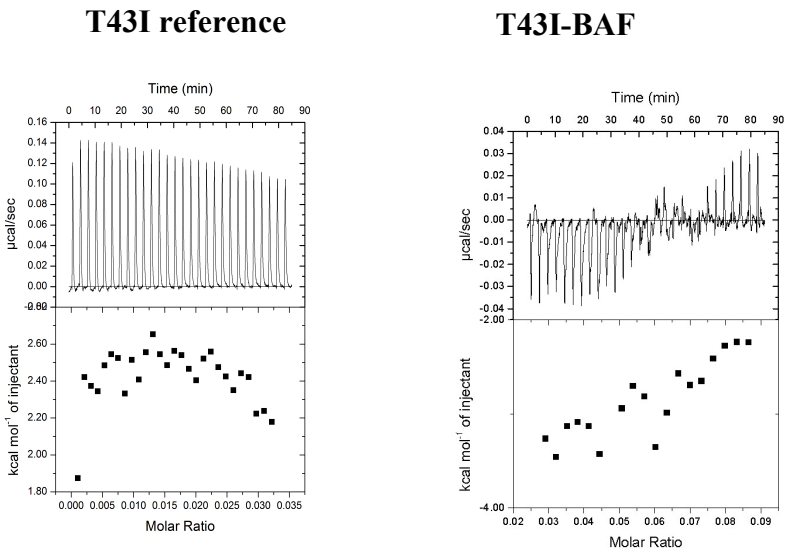

(e)

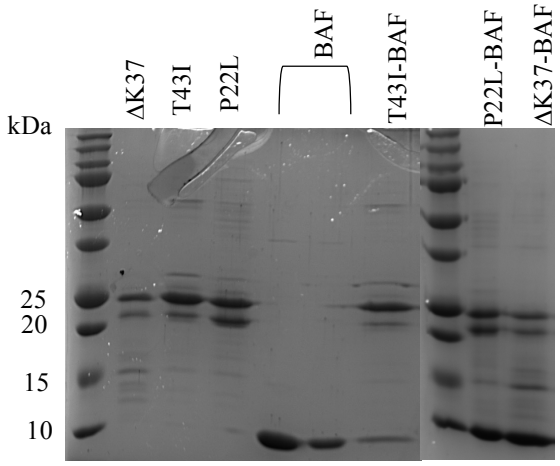

Figure 20. ITC of EmN, P22L ΔK37, and T43I interaction with BAF. Raw data of the ITC titrations of BAF onto (a)EmN (b)P22L (c) ΔK37 and (d)T43I is shown in the upper panels. Transformation of the data using Origin software yielded the titration curves is shown in the lower panels. 32 μM BAF was injected in a cell containing 110 μM, 154 μM, 130 μM, and 129 μM of EmN, P22L, ΔK37, and T43I respectively at 10°C. Reference curves were obtained by injecting binding buffer onto the same concentrations of the proteins at the same temperature. Presumably, the P22L and T43I interactions with BAF are both enthalpy and entropy driven. No apparent difference between the reference and interaction curves of ΔK37 was detected. No conclusions were made on stoichiometry or binding affinities due to the lack of well-behaved titration thermograms. (e) SDS-PAGE gels of BAF in absence and presence of ΔK37, T43I and P22L loaded after the ITC experiments runs.

Given all these points, we failed to determine the parameters of BAF-emerin binding *in vitro* using either SPR or ITC techniques due to non-specific binding in the former or aggregation of our tested proteins in the latter.

7 Titration of BAF and ΔK37

Since ΔK37 interacts with BAF despite the destabilization of its LEM domain, we hypothesized that (1) there is a small proportion of folded ΔK37 in solution, (2) the binding of BAF to ΔK37 might re-stabilize the LEM domain of the latter, thus favoring the folded state of ΔK37. It was decided that the best method to confirm this hypothesis was to record 2D NMR HSQC spectra of a BAF titration with ^{1}H ^{15}N ΔK37 at different molar ratios (1:10, 2:10, 5:10, 10:10) in order to trace the appearance of the folded LEM domain peaks after the interaction. Unfortunately, it wasn't possible to detect the peaks of folded LEM domain on the spectrum even by using saturating concentration of the ligand (10:10 ratio; 55 μM ΔK37: 110 BAF monomer) (Figure 21). Hence, we hypothesized that we have a fast change in conformation in the ΔK37 between the folded and unfolded LEM domain states, even in the presence of the BAF protein.

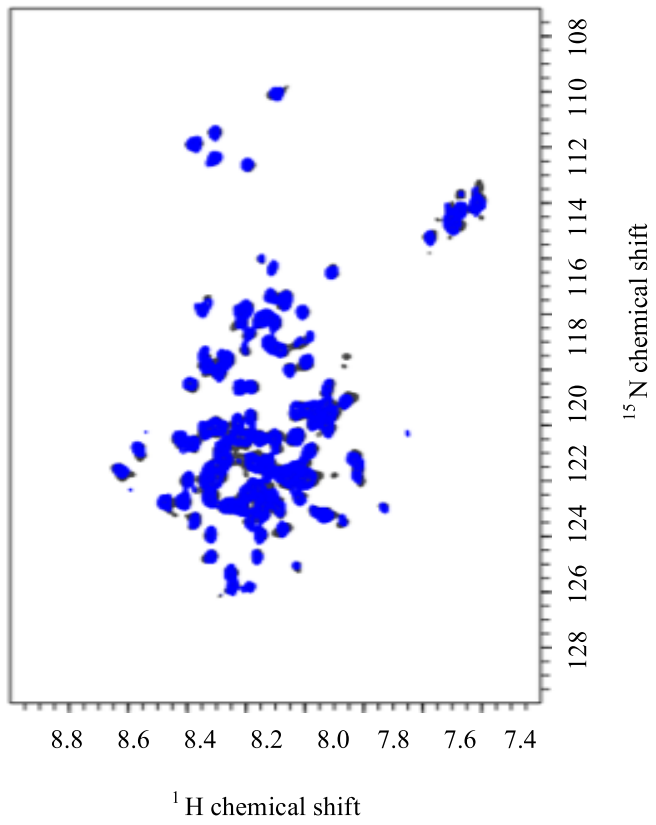

Figure 21. 2D NMR ΔK37-BAF interaction spectrum. To enable us to detect the stabilization of the ΔK37 LEM domain after binding to BAF, we recorded a reference 2D NMR ^{1}H ^{15}N ΔK37 HSQC spectrum (25 µM) and a ^{1}H ^{15}N ΔK37 HSQC spectrum in presence of equimolar concentration of BAF monomer (55 and 110 µM respectively) at 30°C. We didn't detect the peaks corresponding to the folded LEM domain after addition of BAF.

8 Crystallography trials of ΔK37-BAF, P22L-BAF-Ig fold, ΔK37-BAF-Ig fold complexes

In a further attempt to validate our hypothesis, which is the re-stabilization of ΔK37 LEM domain upon BAF binding, we opted for crystallizing the ΔK37-BAF complex. Having EmN-BAF-Ig Fold and T43I-BAF-Ig fold complexes crystallization conditions, we tried to crystalize P22L-BAF-Ig fold and ΔK37-BAF-Ig fold complexes as well. We succeeded to obtain few small P22L-BAF-Ig fold and ΔK37-BAF complexes crystals using high-throughput crystallization screening at EMBL Grenoble facility (Figure 22). Nevertheless, we

failed to reproduce the crystals using various protein concentrations and crystallization conditions. Tables 5, 6 and 7 summarize the different crystallography trials.

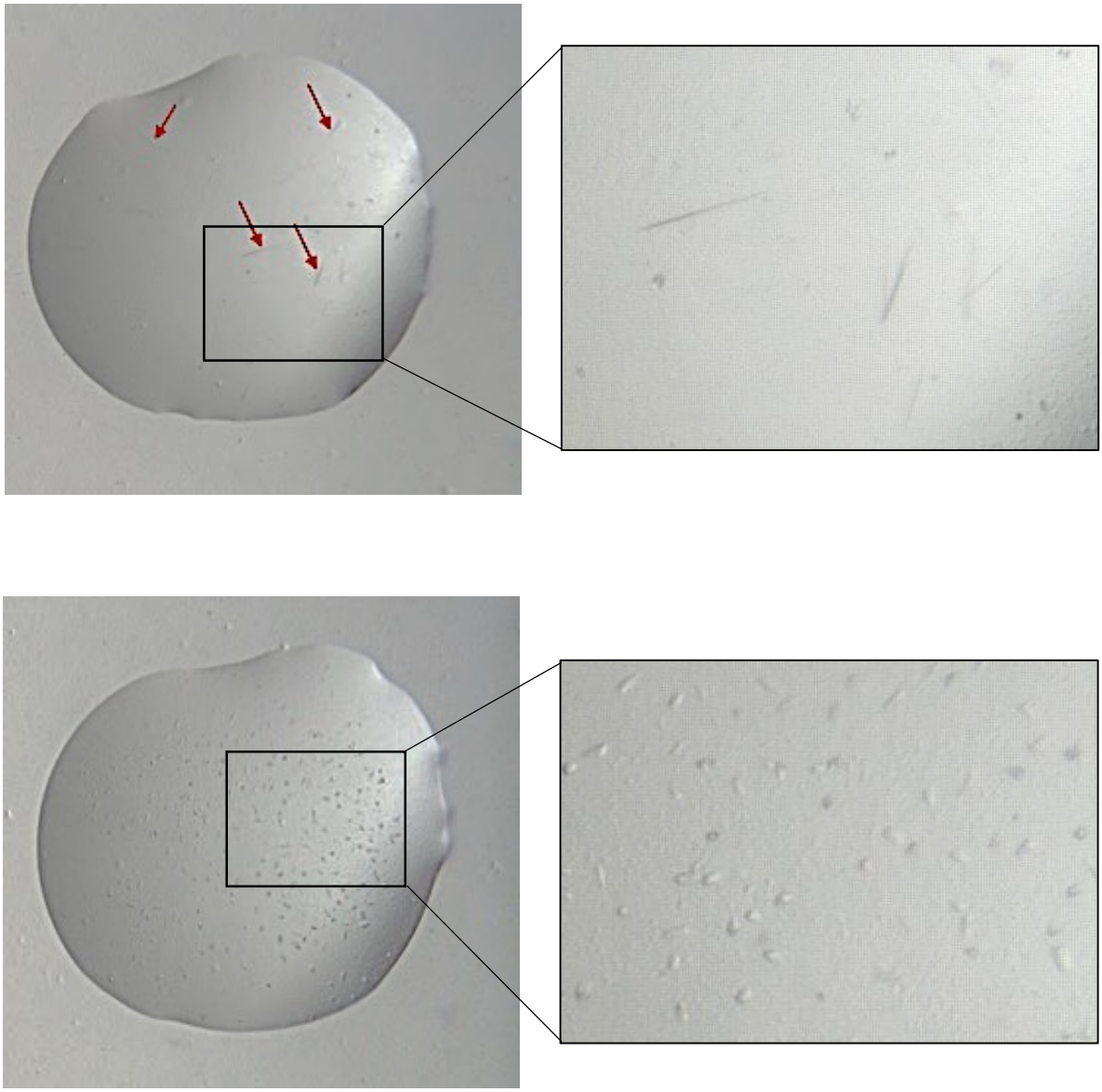

Figure 22. Initial crystals obtained for ΔK37-BAF (left) and P22L-BAF-Igfold (right) complexes by high throughput screening. ΔK37-BAF, 2 mg/ml at 4°C **(**Classics suite kit**:** 0.2M Magnesuim Chloride, 0.1M Tris HCl pH 8.5, 30% (w/v) PEG 4000). P22L-BAF-Igfold, 5mg/ml at 4°C **(**JCSG kit**:** 0.2M Magnesuim Sulphate, 0.1M Bis Tris pH 5.5, 25% (w/v) PEG 3350).

Table 5. ΔK37-BAF complex crystallography trials

Concentration	Size of drop	Conditions	Results	Place	Tempe-rature
2 mg/ml	N/A	**Classics suite 130901 H4**: 0,2M Magnesuim Chloride 0,1M TrisHCl pH 8,5 30% (w/v) PEG 4000	after 35 days → elongated crystals	Crystals obtained at Grenoble	4°C
		Classics suite 130901 G11: 0,2M AmmonuimSulphate 0,1M Soduim acetate pH 4,6 30% (w/v) PEG 2000	after 35 days → elongated crystals	Crystals obtained at Grenoble	4°C
0,7 mg/ml	0,1**μ**l protein 0,1**μ**l reservoir	**Classics suite 130901**	84% of wells → clear rest → precipitated	Plate prepared using mosquito at Synchontron-Soleil	4°C
2,4 mg/ml	0,1**μ**l protein 0,1**μ**l reservoir	**Classics suite 130901**	65% of wells → clear rest → precipitated	Plate prepared using mosquito at Synchontron-Soleil	4°C
5 mg/ml	0,1**μ**l protein 0,1**μ**l reservoir	**Classics suite 130901**	58% of wells → clear rest → precipitated	Plate prepared using mosquito at Synchontron-Soleil	4°C
8 mg/ml	0,1**μ**l protein 0,1**μ**l reservoir	**Classics suite 130901**	70% of wells → precipitated rest → clear	Plate prepared using mosquito at Synchontron-Soleil	4°C
2 mg/ml	1**μ**l protein 1**μ**l reservoir	Gradient: 95%, 90%, 85%, 80%, 75% of **H4 Classics suite**	Either precipitation or clear	CEA	4°C
	1**μ**l protein 1**μ**l reservoir	Gradient: 95%, 90%, 85%, 80%, 75% of **G11 Classics suite**	Either precipitation or clear	CEA	4°C
6 mg/ml	1**μ**l protein 1**μ**l reservoir	Gradient: 95%, 90%, 85%,80%,75% of **H4 Classics suite**	Either precipitation or clear	CEA	4°C
	1**μ**l protein 1**μ**l reservoir	Gradient: 95%, 90%, 85%, 80%, 75% of **G11 Classics suite**	Either precipitation or clear	CEA	4°C

Table 6. P22L-BAF-Ig fold complex crystallography trials

Concentration	Size of drop	Conditions	Results	Place	Temperature
5 mg/ml	N/A	**JCSG** 0,2M Magnesuim Sulphate 0,1M Bis Tris pH 5,5 25% (w/v) PEG 3350	after 3 days → crystals	Crystals obtained at Grenoble	4°C
		JCSG 0,17M Ammonuim Sulphate 15% (v/v) Glycerol 25.5% (w/v) PEG 4000	after 5 days → crystals	Crystals obtained at Grenoble	4°C

6,3 mg/ml	1μl protein 1μl reservoir	0,2M Ammonuim Sulphate 0,1 M Bis Tris pH 5,5 10, 15, 20, 25, 30, 35% (w/v) PEG 3350	Either precipitation or clear	CEA	4°C
		0,1M Ammonuim Sulphate 0,1M Bis Tris pH 5,5 10, 15, 20, 25, 30, 35% (w/v) PEG 3350	Either precipitation or clear	CEA	4°C

Table 7. ΔK37 -BAF-Ig fold complex crystallography trials

Concentration	Size of drop	Conditions	Results	Place	Temperature
7,7 mg/ml	1μl protein 1μl reservoir	0,2M Ammonuim Sulphate 0,1M Bis Tris pH 5,5 10, 15, 20, 25, 30, 35% (w/v) PEG 3350	precipitation	CEA	4°C
		2M Soduim formate 0,1M pH 4.5, 5, 5.5, 6, 6.5, 7, 7.5, 8, 8.5	Salt crystals	CEA	4°C

9 Determination of novel ΔK37 partners

Our structural biology experiments investigated the consequences of the LEM domain mutations on two emerin binding partners (BAF, lamin A/C) that could be involved in either the gene regulation or structural defect hypotheses of X-EDMD pathogenesis. However, we didn't detect major defects in either interactions. Similarly, cell biology experiments did not reveal defects in the studied nuclear envelope, microtubule, cytoskeletal, and focal adhesion proteins. Subsequently, we attempted to unveil defects in ΔK37 interactions with other binding partners present in immortalized human fibroblasts. First, we immunoprecipitated endogenous wild-type and ΔK37 emerin and studied alterations in their binding partners using mass spectrometry (MS). Main emerin partners identified in this analysis were: actin (cytoplasmic 1 and alpha cardiac muscle), myosin 9 (also named non-muscle myosin heavy chain IIa), myosin light polypeptide 6, myosin regulatory light chain 12A, vimentin, histone H4, histone H2A type 1D, histone H2B type 1B/C/E/F/G/I. However, emerin peptide count was very low in the wild-type samples and much lower in ΔK37 ones. Consequently, it was difficult to draw a conclusion from this analysis.

To overcome this limitation, we purified *in vitro* EmN and ΔK37 then we incubated them with whole cell wild-type human myoblast extracts. Affinity purification was next used in order to pull-down their partners (Figure 23), and we finally studied differences in binding partners using MS. This approach has two advantages: first, we have enough emerin amount (which is not the case in cells) so as to pull-down its different partners; second we always used equal amounts of EmN and ΔK37, so that identified alterations in binding to partners would be due to the presence of the mutation in ΔK37 mutant and not due its lower level expression (which was the case in IP experiments). We carried out this experiment three times using different amounts of cell extracts and purified proteins in order to optimize our protocol (Table 8). Processing the data of the three experiments is till on going, yet our primary observations are: 1) *experiment 1*, in which we used the highest amount of emerin, detected the highest differences between EmN and ΔK37 (Table 8). These differences were in proteins known as strong emerin partners (Table 9); 2) according to the three experiments collectively, the main binding partners of emerin in myoblasts are: vimentin, histone H4, histone H2B type 1B/C/E/F/G/I, and prelamin A/C (Table 9); and 3) *experiment 1* suggests that ΔK37 binds tighter to chromatin and weaker to actin/vimentin/myosin/lamin A/C (Table 10). We will repeat this analysis using experiment 1 conditions in order to reproduce our results.

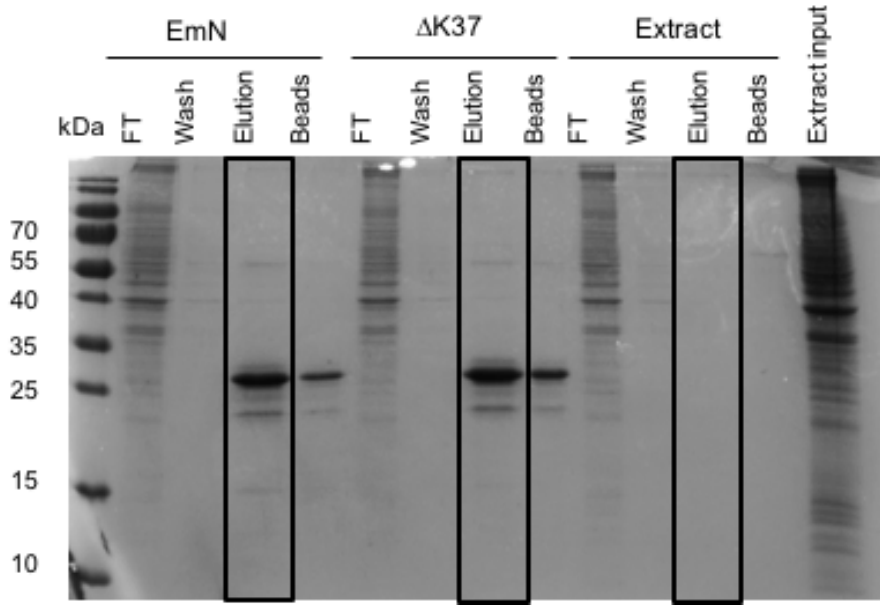

Figure 23. Identifying interactions between ΔK37 and its co-purifying partners from myoblast whole cell extract using affinity purification and mass spectrometry. (A) SDS-PAGE gel of affinity chromatography purification of purified EmN, ΔK37, and their co-purified partners from myoblast whole cell extract. Purified proteins (0.5 mg) incubated overnight with cell extract (1 mg) then interacting protein complexes eluted using Ni-beads and imidazole. Cell extracts were incubated with the Ni-beads and eluted similarly as control.

Table 8. Comparison of the three MS experiments conditions and results

Point of comparison	First experiment	Second experiment	Third experiment
Extract amount	0,4 mg	0,5 mg	1 mg
Protein amount	1,35 mg	0,25	0,5 mg
Number of proteins identified with different abundance in EmN vs ΔK37	69	30	4

Table 9. Summary of proteins bound to EmN

Experiment 1	Experiment 2	Experiment 3
Histone H4	Vimentin	Vimentin
Vimentin	Actin, cytoplasmic 1	Histone H4
Histone H2B type-1-C/E/F/H/I	Histone H4	Actin, cytoplasmic 1
Actin, cytoplasmic 1	Annexin A2	Prelamin A/C
Pyruvate kinase PKM	Tubulin beta chain	Histone H2B type-1-C/E/F/H/I
Prelamin A/C (8^{th} place)	Histone H2B type-1-C/E/F/H/I (10^{th} place)	
	Prelamin A/C (12^{th} place)	

Table 10. Summary of the results of experiment 1 MS analysis

Higher affinity to EmN	Higher affinity to ΔK37
Actin (3 fold, but not significant)	Histone H2A type 1-B (absent in EmN)
Alpha-actinin-4 (9 fold)	Nucleoside diphosphate kinase B (2 fold)
Elongation factor 1-alpha 1	Histone H3.1t
Elongation factor 2	40s ribosomal proteins S13, S18 & S19, 60S ribosomal protein l31
Filamins A and C (24 and 98 fold, respectively)	Histone h2b type 2-e
Moesin	Histone H2A type 1-D (3 fold)
Myosin 9	Histone H2B type 1-C/E/F/G/I (4 fold)
Plectin	Histone H4 (3 fold)
Prelamin A/C (2 fold, but not significant)	
Pyruvate kinase	
Spectrin beta chain	
Talin 1	
Thrombospondin 1	
Vimentin	

Additional materials and methods

Cell culture and reagents

Immortalized myoblasts were cultured in a proliferation medium consisting of 199 Medium and DMEM in a 1:4 ratio (Life Technologies) supplemented with 20% fetal bovine serum (Life Technologies), 0.25 mg/ml gentamicin (Sigma-Aldrich), 5 ng/ml human epithelial growth factor (Life Technologies), 5 mg/ml insulin (Life Technologies), 0.5 ng/ml bFGF, (Sigma-Aldrich), 50 mg/ml fetuin (Life Technologies), 0.2 mM dexamethasone (Saint Quentin- Fallavier, France). Immortalized fibroblasts were maintained in DMEM supplemented with 20% fetal bovine serum and 0.25 mg/ml gentamicin. All cells were incubated in humidified cell culture incubator at 37°C and 5% CO_2.

Fabrication of substrates of different stiffness

Polydimethylsiloxane (PDMS) soft substrates were synthesized using commercially available silicone elastomer kit (Sylgard 184, DowSIL) comprised of a polysiloxane polymer (Part A) and a curing agent (Part B). 50:1 weight ratios of Part A and Part B were mixed, respectively in order to achieve 20 kPa stiffness. Commercially available soft substrates of 8kPa stiffness (Matrigen Softview, Matrigen Life Technologies) were used. For hard substrates, cells were plated on surfaces coated with fibronectin (Sigma-Aldrich).

Cyclic strain

Cells were plated on tissue train plates (Flexcell International) for 1 day and stretched (10% elongation, 0.5 Hz, 4hr). Next cells were collected for subsequent experiments. Unstretched control cells were collected under same experimental conditions, without stretching.

DNA extraction for genotyping

Cells were first trypsinized, then pelleted (at 14000 rpm, for 3 min, at 4°C), solubilized (in 10 mM Tris HCl ph7.5, 10 mM NaCl, 25 mM EDTA, 1% SDS) and treated with Proteinase K

overnight at 37°C. DNA was neutralized with 5M NaOH, extracted with isopropanol (1 volume of the sample), then washed with 70% ethanol and finally resuspended in water. DNA yield was measured at 230 nm using Nanodrop.

Antibodies

Fixed cells were stained using the antibodies summarized in Table 11 and the following reagents: F-actin was stained with Alexa Fluor 568 Phalloidin (Thermofisher) and nuclei were counter-stained with Hoechst 33342 (H3570, Thermofisher). Secondary antibodies for immunoblotting were HRP-conjugated goat anti rabbit, rabbit anti-mouse, donkey anti-goat IgGs (Jackson ImmunoResearch). Secondary antibodies for immunofluorescence were Alexa Fluor-488 or 568 conjugated goat anti-rabbit IgG, Alexa-Fluor-568-conjugated donkey anti-goat IgG, Alexa Fluor 488 or 568-conjugated goat anti-mouse IgG (Life Technologies).

Table 11 Summary of antibodies

Antibody	Antigen	Note	Host	IF dilution	IB dilution	Reference/ Source
Anti-emerin NCL	Emerin	Used for emerin wild-type since its epitope include emerin residues 1-222	Mouse	1:20	1:500	Novocastra laboratories
Anti-emerin Manem8 7B9	Emerin	Used for emerin ΔK37 since its epitope includes emerin residues 7-17	Mouse	1:50	1:50	Glenn Morris
Anti-emerin Ab40688	Emerin	Used for emerin ΔK37 since its epitope includes emerin residues 100-200	Rabbit	1 µg/ml	-	Abcam
Anti-lamin A/C N-18	Lamin A/C	Used for emerin KO				Santa cruz
Anti-lamin A/C ab8984	Lamin A/C	Used for emerin ΔK37				
Anti-phosphophorylated (S22) lamin A Ab138450	Phosphophorylated (S22) lamin A		Rabbit	-	1:500	Abcam

Anti- SUN2 A9180	SUN2	Used for KO myobasts	Rabbit	1:500	-	In-house
Anti- SUN2 Ab124916	SUN2	Used for ΔK37 fibroblasts	Rabbit	1:500	-	Abcam
Anti-Vinculin V9131	Vinculin		Mouse	1:400	1:500	sigma
Anti-GAPDH Sc-25778	GAPDH		Rabbit		1:1000	Santa cruz
Anti-β-tubulin Ab6046	β-tubulin		Rabbit	1:200		Abcam
Anti-non muscular myosin IIa	Non muscular myosin IIa NMIIa		Rabbit	1 :200		Abcam
Anti-β-catenin	β-catenin		Rabbit	1 :200		Abcam

Immunohistochemistry and immunofluorescence microscopy

Cells were first fixed (4% paraformaldehyde in phosphate-buffer saline [PBS], for 15 min at room temperature [RT]), then permeabilized (with 0.2% Triton X-100 in PBS, for 10 min, at RT), before blocked (with 10% BSA in PBS, for 2h, at 4°C) and washed in PBS. Cells were incubated with primary antibodies (in PBS with 3%BSA, 2 hr, RT) and washed next in PBS. All secondary antibodies were first incubated for 1 hr at RT in PBS, then washed, after that nuclei were counterstained with Hoechst, and lastly slides were mounted in Mowiol mounting medium. Immunofluorescence microscopy was carried using an Olympus FV1000 (Olympus) and a Leica SP2 (Leica Microsystems) for confocal images.

Protein extraction and immunoblotting

Total proteins were extracted in cell lysis buffer (2% SDS, 250 mM sucrose, 75 mM urea, 50 mM Tris HCl pH 7.5, 1 mM DTT) with the addition of 1x Complete® protease inhibitors (Roche). Lysates were sonicated (3 pulses of 10 s at 30% amplitude), spin extracted (at 14,000 rcf, for 10 minutes, at 4°C) and quantified using BiCinchoninic acid Assay [BCA] (Thermo Scientific). Extracts were separated by 10% SDS-PAGE and transferred onto 0.45 μm

nitrocellulose membranes (Invitrogen). Membranes were blocked in 5% low-fat milk in TBS-Tween20 (for 1 hr, at RT), then incubated with the selected primary antibody (overnight at 4°C or for 4 hr at RT). Membranes were first washed with TBS-Tween20 before incubated with secondary horseradish peroxidase (HRP)-conjugated anti-rabbit or anti-mouse or anti-goat antibodies (for 1 hr, at RT). Signals were revealed using Immobilon Western Chemiluminescent HRP Substrate (Millipore) on a G-Box system with GeneSnap software (Ozyme). ImageJ software was used for band intensities quantification.

Surface Plasmon Resonance (SPR)

SPR measurements were performed on a ProteOn™ Surface Plasmon Resonance Detection System (Biorad) at 10°C in SPR buffer (50 mM TrisHCl pH8, 100 mM NaCl, 0,05% Tween20, 5 mM β-mercaptoethanol). Histidine tagged EmN mutants were immobilized on a nickel sulfate activated ProteOn HTG sensor chip (Biorad). Prior to immobilization, the sensor chip was conditioned as described by the manufacturer. Ligands (30 µl) were injected at 30 µl/min flow rate for 60 s contact time, whereas the analytes (150 µl) were injected at 50 µl/min flow rate for 180 s contact time.

Isothermal Titration Calorimetry (ITC)

ITC measurements were performed on a VP-ITC calorimeter (Malvern) at 10°C in binding buffer (50 mM Tris- HCl pH8, 100 mM NaCl, 10 mM β-mercaptoethanol and 1 tablet Complete® protease inhibitors). Reaction heats were recorded by a series of 10 injections of BAF (32 µM) into EmN mutants (T43I at 129 µM and P22L at 154 µM). Data analyses were performed using the Origin Software.

Affinity purification-Mass spectrometry (AF-MS)

Histidine tagged EmN and ΔK37 proteins were *in vitro* purified (previously described in Essawy et al., draft), concentrated (at 4°C) and dialyzed (in 100 mM NaCl, 50 mM Tris HCl

pH 7.5 buffer, at 4°C). A mixture of lysates from three different cell culture dishes of immortalized human wild-type myoblasts was obtained using the previously described cell lysis buffer, lysed (using 25 G syringe, then incubated for 30 min at 4°C on a roller, lastly centrifuged at 14000 rcf, for 15 min, at 4°C), and quantified using BCA assay. Purified proteins were incubated with cell lysates (overnight, at 4°C, on a roller) in ratio 1:2. No lysates were added to control samples. Next day the interacting protein complexes were immobilized on Ni-NTA Agarose beads (Qiagen) (for 4hr, at 4°C). Non-specific binding was removed with washing buffer (30 mM NaCl, 20 mM Tris HCL pH 8, 20 mM Imidazole). Emerin together with co-eluting proteins were eluted for mass spectrometry with elution buffer (30 mM NaCl, 20 mM Tris HCL pH 8, 1 M Imidazole). TCA precipitation of all samples was carried out and then the pellets were reconstituted in 1X loading buffer + β-mercaptoethanol. Samples were subsequently loaded for short migration on 4-12% Bis-Tris gel electrophoresis in MES/SDS buffer. Bands representing wild-type, ΔK37 and control complexes were cut for nanoLC-MS/MS analysis. The cut bands were digested using trypsin. NanoLC-MS/MS analysis was carried out after repeating the injection twice to obtain technical replicates. Trypsin digested peptide pools were analyzed using a 60 min gradient on a Q-Exactive HF mass spectrometer coupled to a nano HPLC. Patternlab software (version 4.0.0.76) was used for comparing peptide spectral counts, fold changes, and statistical significance.

Immunoprecipitation (IP)

Wild-type and ΔK37 fibroblasts were lysed in 40 µl RIPA lysis buffer (50 mM Tris-Hcl pH 7.4, 1% NP-40, 150 mM NaCl, 1 mM EDTA, 2 mM Na3VO4, 0.5% sodium deoxycholate, 0.1% SDS, 1x Complete® protease inhibitors [Roche], 1x PhosSTOP™ [Roche], and 1 mM DTT) for 5 min on ice, then incubated for 30 min at 4°C on a rotator, and centrifuged at 14 000 rcf for 10 in at 4°C. The supernatants were pre-cleared by incubation with 20 µl washed protein G–Sepharose 4 fast-flow (GE Healthcare) for 1 hr at 4°C on a

rotator, then centrifuged at 5000 rcf for 1 min at 4°C. Pre-cleared supernatants were then incubated with 10 µl Manem8 emerin antibody (Glenn Morris) overnight at 4°C on a rotator. No antibody was added to control samples. Next day, 14 µl washed beads were added and incubated for 2hr at 4°C on a rotator. Beads were pelleted (14 000 rcf, 1 min, 4°C), washed 5x using 15 µl RIPA buffer (14 000 rcf, 1 min, 4°C), collected in loading buffer (0.25M Tris-HCl, 8% SDS, 40% glycerol, 20% β-mercaptoethanol), and subjected to SDS-PAGE and immunoblotting.

Emerin *in vitro* phosphorylation and identification of phosphopeptides by mass spectrometry (MS)

Histidine tagged EmN and ΔK37 proteins were *in vitro* purified, concentrated (at 4°C) and dialyzed (in 30 mM NaCl, 50 mM Tris HCl pH 7.5 buffer, at 4°C). Reference (0.9 mg purified protein, 2mM ATP, 0.5 mM $MgCl_2$, 5 mM DTT) and phosphorylation (0.9 mg purified protein, 2mM ATP, 0.5 mM $MgCl_2$, 5 mM DTT, 0,9 µg Src kinase [Thermofisher]) samples were incubated overnight at 30°C. Phosphorylation was stopped next day by adding Laemmli sample buffer and heating the samples at 95°C for 5 min. All samples were then resolved by SDS-PAGE for mass spectrometry analysis. MS data analysis was perfomed using SwissProt human database

Image analysis

All image analyses were performed using ImageJ software. Actin fiber numbers were determined by drawing a 10-micron line perpendicular to the long axis of the nucleus. Then plot profiles were analyzed by find peaks command where the number of peaks represented the number of actin fibers. To quantify the deviation in nuclear circularity, the nuclear area and perimeter were measured in Hoechst stained nuclei using ImageJ software. From these date, contour ratio or nuclear roundness was computed (4π area/perimeter^2).

Statistics

Statistical analyses were done using GraphPad Prism software. Whenever needed, a two-tailed unpaired Student's t test was run. P values <0.05 were considered significant.

Chapter IV: Discussion

The main aim of my PhD project was to decipher the consequences of "unique" emerin LEM-domain missense mutations, namely P22L, ΔK37, and T43I, present in patients with isolated atrial cardiac defects (ACD), using different structural and cell biology techniques. The appellation of these three mutations as "unique" is because 1) they are the only mutations identified to date in the LEM domain, (2) mutated emerin is detected in cells, opposite to the majority of *EMD* mutants, 3) the mutations are present in patients with only atrial cardiac defects and not accompanied by any skeletal muscle defect or joint contractures[149,152,153] ,R. Ben Yaou personal communication.

Herrada et al. have demonstrated the structural consequences of some missense X-EDMD-causing mutations and how they affect the self-assembly capacity of emerin, together with its binding to lamin A/C in vitro and in cells[55]. We questioned whether our mutations of interest affect the global mutants structure, self-assembly capacity, interactions with emerin partners that are implicated in either gene regulation (BAF) or structural organization (lamin A/C).

Regarding the overall structure of P22L and T43I mutants, we did not reveal changes, whereas we identified destabilization of the LEM-domain of ΔK37. We also observed faster self-assembly of the EmN mutants *in vitro*. Concerning binding to partners, we detected defects neither in the binding of the mutants to BAF nor the Ig-fold domain of lamin A/C *in vitro*. However, we detected a decrease in the binding affinity for BAF, especially in the case of ΔK37, which should be confirmed. The most striking observation from the data is the fact that the mostly unstructured LEM domain of ΔK37 is still capable of binding to BAF, even if less efficiently. This suggests that a proportion of the LEM-domain of ΔK37 exists in a transient, poorly populated, yet folded, and binding competent, state in solution. The conformational

state of this proportion is in exchange with an unfolded one, which represents rather most of the species present in solution. This major unfolded population was the one is detected in our FBTSA.

It must be remembered that there is a possibility that we missed a binding defect to other partners that were not tested in our analysis. However, our cell biology experiments did not reveal a specific defect, that could have guided us to investigate additional partners. Indeed, the characterization of ΔK37 immortalized human fibroblasts did not uncover defects in nuclear envelope proteins (such as lamin A/C), focal adhesions proteins (vinculin) or microtubules (β-tubulin). At this point it was decided to employ proteomics so as to unveil defects in other emerin partners. Analysis of the proteomics results is now ongoing.

Fibroblasts from patient carrying *EMD* p.delK37 mutation did not display overt mechanobiology defects in our experiments, however we cannot totally exclude the possibility of a mechanical defect in these cells. There is some likelihood that the mechanical cues used in the experiments were not adequate enough to reveal a subtle defect in mechanotransduction. Hence, it could be useful to subject cells to exacerbated stress conditions in order to detect or provoke the manifestation of mechanical defects. Further, we observed in our spreading area analysis a decrease in the size of ΔK37 fibroblasts compared to wild-type ones. It can, thus, be conceivably hypothesized that in order to generate equal forces, cells might exhibit stiffer focal adhesions when responding to mechanical forces. Stiff focal adhesions could affect the adhesive capacity, mobility, and traction forces exerted by the cells on extracellular matrix.

Signaling defects coupling loss of emerin: relationship with cardiac defects?

Cardiac MAPK signalling pathway defect?

Analysing genome-wide expression profiles in hearts from *Emd* knockout mice, a model for X-linked EDMD, identified pathways altered in these mice including: JNK, MAPK,

Wnt, I-kappaB kinase/NF-kappaB, and TGF-β[117]. This analysis revealed hyper-activation of the ERK1/2 branch of the MAPK pathway, as well as activation of downstream targets implicated in the pathogenesis of cardiomyopathy[117]. Such activation is also observed in hearts obtained from *LMNA*$^{H222/H222P}$ knock-in mice, a model of AD-EDMD[117]. Moreover, delivering a drug, that inhibits ERK1/2 activation, improves the cardiac function in these mice[176]. Given that ERK1/2 activation contributes to myocardial fibrosis in the mouse model of *LMNA* cardiomyopathy and patients hearts with lamin A/C gene mutation[177]; it can thus be reasonably assumed that there is an involvement of ERK1/2 activation in the cardiac defect present in our mutations of interest.

ERK1/2, when activated, has a very large set of targets. One of these targets is cofilin-1, which is phosphorylated by ERK1/2 on Thr25. This phosphorylation event leads to the depolymerisation of sarcomeric F-actin; impairing the cardiac function[178]. Given these points, it would be interesting to investigate ERK1/2 activation and cofilin-1 phosphorylation state in cardiomyocytes expressing our missense mutations.

Cardiac Wnt/β-catenin signalling pathway defect?

It has been shown that emerin binds to β-catenin forming a complex at the intercalated disc of cardiomyocytes[98]. The loss of emerin results in the release of β-catenin from this complex[98]; activating the Wnt/β-catenin signalling pathway[97]. Accordingly, in emerin-null mice, the impairment in Wnt/β-catenin signalling pathway leads to an increase in the number, along with decrease in size of cardiomyocytes, and cardiac dysfunction[97].

Moreover, emerin binds to Wnt/β-catenin in early development of embryonic mouse hearts and suppresses Wnt/β-catenin[97]. The increase in emerin during the differentiation of embryonic mouse stem cells limits their proliferation and ensures their differentiation into

cardiomyocytes[97]. It follows that the emerin null mouse embryonic stem cells suffer from hyperproliferation and delayed cardiac differentiation[97].

Our preliminary data in ΔK37 fibroblasts showed increase in nucleoplasmic β-catenin staining. Thereupon, it would be interesting to test the activity of the Wnt/β-catenin in cardiomyocytes expressing our emerin missense mutations.

Cardiac autophagy defect?

It has been demonstrated that the nuclear-associated vacuoles present in *EMD*[163] and *LMNA*[179] mouse models are perinuclear autophagosomes/ autolysosomes containing nuclear components[180]. The inhibition of autophagy in the *Lmna*$^{H222P/H222P}$ fibroblasts increases the nuclear abnormalities and decreases cell viability[180], supporting a beneficial role for autophagy in these cells.

It has been shown that emerin has role in autophagy in human colon cancer cells[181]. The activation of C-16 ceramide-dependent-autophagy pathway resulted in emerin phosphorylation by protein kinase, cAMP-dependent, catalytic, α (PRKACA), and possibly other kinases as well, on its LEM-domain[181]. Phosphorylated emerin directly binds microtubule-associated protein 1 light chain 3 beta (MAP1LC3B) increasing phagosome formation and inducing autophagy[181].

Given that autophagy has crucial roles in the heart under both physiological and pathological conditions[182], emerin autophagic role should be investigated in our mutations of interest.

Quest for potential candidate proteins involved in the cardiac defect

A potential candidate protein is 4.1R, which localizes at the nuclear envelope and cytoplasm. It is a principal member of the cell division machinery and spotted in centrosomes, and mitotic spindles[183]. It was demonstrated that protein 4.1R co-precipitates with emerin and

lamin A/C, and has chief functional interactions with both proteins. To elaborate, the depletion of 4.1R in human cells results in the mislocalization of emerin to the cytoplasm, disorganization of lamin A/C at the nuclear rim, increased nucleus-centrosome distances, increased accumulation of β-catenin in the nucleus, and increased β-catenin signaling[184]. Moreover, emerin and lamin A/C null cells have less nuclear 4.1R[184]. Interestingly, it was demonstrated how 4.1R deficiency affects mouse embryonic fibroblasts cardiac electrophysiology, and it was similarly linked to progressive heart failure in humans[185]. Additionally, 4.1 has also developmental and tissue-specific isoform expression manner in mice, which can explain the tissue-specific symptoms accompanying EDMD[185]. Given these points, 4.1R is presented as potential candidate whose dysregulation might affect the distribution of emerin and the cardiac electrophysiology, explaining the etiology of the disease[186].

Emerin mutations associated with exclusive cardiac defects: no direct pathophysiological link

The prime interest in our "unique" mutations was based on a hypothesis, that links the common localisation of the mutations to a defect in a particular molecular mechanism, which is of significant importance for the cardiac function. In particular, they could disfavour interactions with the LEM-domain binding partner BAF, which could in turn play role in cardiac development and maintenance. However, the fact that other nuclear envelope proteins might play redundant roles with emerin suggests another hypothesis, in which the determinant of whether emerin mutations provoke skeletal muscle defects, is the co-existence of mutations in these proteins.

To further explain, mutations in several nuclear proteins are associated with skeletal myopathies combined with cardiac defects. For example, torsin 1-interacting protein 1 (TOR1AIP1), also named LAP1B, is mutated in patients with such disease phenotype, and

results in the loss of LAP1B in patient skeletal muscle fibres[187]. It was reported that this pathology is worsened in the absence of emerin, suggesting that both proteins contribute to muscle maintenance and might compensate for one another[188]. That's to say, the lack of skeletal muscle defect in our mutations could be due to compensatory mechanisms by proteins of redundant roles with emerin.

In addition, the *LMNA* gene is mutated in both EDMD and an exclusive cardiac pathology, the dilated cardiomyopathy (DCM)[189,190]. There is no specific localization-phenotype association with respect to the distribution of the disease-causing mutations along the *LMNA* gene[191]. In other words, no hotspot for DCM or diseases affecting the striated muscles have been identified (UMD-*LMNA* mutation database available at http://www.umd.be/LMNA)[192]. All points considered, the claim that there is a specific localization-related mechanism related to cardiac defects is refuted.

Future perspectives

We faced technical difficulties when we were attempting to determine the binding affinities of EmN variants for BAF, partly because these variants have a strong tendency to rapidly oligomerize. However, our results suggested a slight binding defect. As this might be a crucial event in the disease mechanism, we will next focus on determining the binding parameters using the new switchSENSE technology. The latter measures the binding rate constants and dissociation constants of an analyte when bound to short DNA nanolevers attached to the gold surface of a chip. Ideally, we will attach BAF covalently (directly or through its histidine tag) to the DNA, and then we will measure the binding affinity for emerin mutants as analytes, which will be injected in relatively low amount/concentrations and with an adapted flow rate.

Also, analysis of the proteomics data obtained using our EmN variants revealed first partners. However, we now have to reproduce this experiment using the best protocol deduced from our first analyses, in order to confirm our results. First data highlight the importance of emerin binding to actin and histones. The role of BAF in mediating these interactions is currently unknown and should be studied.

We also already demonstrated that phosphorylation of EmN by Src is not impaired by mutation ΔK37. However, emerin is phosphorylated by a large set of other kinases. Mass spectrometry analyses have shown that its LEM domain is also phosphorylated[120]. Given that little is known about kinases that phosphorylate this LEM-domain, and how phosphorylation of emerin LEM domain can play vital roles in cells; we are in Zinn-Justin group attempting to follow the phosphorylation kinetics of emerin by variety of kinases, such as: CK2, GSK3β, PKA, Src, and polo-like kinase 1 (PLK1). Using liquid-state NMR we will try to identify the kinases involved in LEM-domain phosphorylation. We will focus particularly on kinases that are predicted or were reported to phosphorylate the LEM domain, such as: CK2, GSK3ß, and PKA. We are interested in PLK1 because this kinase is important for the regulation of mitosis, particularly during DNA checkpoint and mitotic exit[193,194,195], and the predicted phosphorylation sites are mutated in classical EDMD.

Another faced problem was that EmN (1-187) fragment, used in all structural biology experiments described, may not entirely reflect the behavior of the full length emerin *in vivo*. The presence of the transmembrane domain and being membrane-bound in cells, both can potentially impede emerin's ability to freely self-assemble and affect emerin interactions with its various binding partners. For these reasons, Zinn-Justin's group attempted to use a longer emerin construct (emerin 1-221), however it was constantly aggregating at concentrations higher than 20 μM. Therefore, it was not feasible to use it for NMR or gel-filtration experiments. Studying the whole emerin protein could reveal additional structural

consequences of the mutations, however it requires analysing emerin in micelles/liposomes, which has not been performed yet. Therefore, for the purpose of mimicking emerin interaction at plasma membrane, we successfully cloned and purified C-histidine tagged emerin using affinity-based liquid chromatography. Thereafter, we used nickel-tagged Folche liposomes (to mimic the plasma membrane), incubated the C-histidine emerin with the liposomes, and eventually scrutinized emerin binding to liposomes using electron microscopy. Although it is difficult to conclude because it was a first trial, yet we detected emerin-emerin interactions forming what looked like filaments on the surface of liposomes as well as in between them. In future experiments, we suggest using the full-length construct in presence of low concentration of urea. In that way, protein-protein interactions (emerin self-assembly or its aggregation) will be inhibited. Hence, when incubating emerin with liposomes, we will only acquire the protein-lipid (emerin-liposome) interactions. After urea removal, the self-assembly of full length emerin can, thus, be studied in conditions simulating in vivo ones.

Finally, in the discussion section, we proposed several experiments to be performed in cardiomyocytes expressing our emerin missense mutations. Cardiomyocytes (CM) derived from human induced pluripotent stem cells (hiPSC) express several cardiac ion channels present in intact human hearts and have been established as a tool to test drug-induced conduction defects[196]. Future studies on P22L, ΔK37, and T43I mutations should be directed towards unveiling defects in either emerin cardiac-specific partners, alterations of emerin at ICDs, dysregulation of signalling pathways or mechanotransduction in (HiPSC- CM) models.

Acknowledgments

I would like to extend my gratitude to the many people, in many countries, who contributed in different ways to the work presented in this thesis.

Firstly, I would like to thank the supervisors that mentored me during my PhD. I thank **Dr Catherine Coirault**, with whom I spent the first year and a half of my PhD journey at the Institute of Myology in Paris, for the help, support, and understanding. I would like to thank also **Prof Simone Spuler**, my thesis director in Berlin and PhD progress committee member, for her valuable insights on my work and motivation. My sincere thanks go to **Dr Philip Selenko** from fMP Berlin for his guidance in the beginning of my PhD and whenever I needed advice, he always made sure I was enjoying the ride. An immense and heartfelt gratitude is due to **Dr Sophie-Zinn Justin** with whom I started the PhD then re-joined her team in the second half of my PhD at the CEA. You have had a constant faith in me and taught me a lot with your endless support and unequivocal enthusiasm. I am also hugely appreciative to **Dr Gisele Bonne** who was always there from the beginning till the end, encouraging and supporting me.

Many thanks go to **Susanne Wissl**er, without her assistance I would have been stuck with all the hectic administrative work forever.

I gratefully acknowledge the members of my thesis committee for their participation and guidance: **Dr Vincent Gache**, **Dr Francois Lallemand**, and **Prof Sigmar Sticker** for reviewing this thesis; **Dr Katherine Wilson**, for her motivation to my work; **Dr Maria Reichenbach**, for accepting to be part of the committee; and **Dr Onnic Agbulut** for chairing the committee.

I was honoured with a tremendous opportunity during my PhD to work in three different labs, in two different countries. Hence, special mention goes to all those who trained me or tried to make my journey easier in **fMP berlin**, **Institute of Myology**, and **CEA-Saclay**.

Profound gratitude goes to my forever mentor, **Dr Ahmed Ihab**. You have been believing in me for so long, offering generously advice and pushing me to strive towards my goals.

I am grateful to the different members of the groups that I worked with, **Daniel Owens**, **Martina Fischer**, and **Ambre Petitalot**, who contributed immensely to my professional and personal development.

My PhD journey was made enjoyable due to the many friends that I gained and became part of my life. Thanks **Blanca** for the fun times we had everywhere we travelled together. Thank you, **Camille**, the first one I ever worked with during my PhD and who had taught me almost everything I know in Biochemistry. **Fouad**, mon petit fils, and **Florian**, the gentleman, thank you for making sure I was always happy and surviving.

A huge shout out goes to the highlight of my PhD, which is as important as and more everlasting than my PhD results, the awesome team. **Coline**, the affectionate; **Maria**, the wise; **Apostolos**, the bro, if there is anything I would never regret in the last three years, it would be having gained you as a second family. Stress, research ups and downs, and the sleepless nights, all that was negligible next to our memories, laughers, and world-wide adventures. May we always have each other's back as we always do.

Because he understands my twisted mind the best, I owe a huge thank you to **Tonsy**. Thank you for understanding this soul, that I barely understand and living my dreams as much as you live yours.

My constants, the people that have been always there for me despite being miles apart, **Nouran**, **Engy**, and **Reem**. Thank you for being who you are and holding tight on what we have between us. May the far distance do nothing but bring us closer.

I owe my deepest gratitude to my backbone, **my dad, mum, brother, and sister**. Words cannot express how grateful I am to each one of them. This thesis would not have been possible, had it not been to their prayers, selflessness, and love. They are the reason for being who I am now.

A last special love note goes to the closest person to my heart, my sister **Hadeer**. You're my soul living in another-crazier- body.

Reference list

1. Hetzer, M. W. The nuclear envelope. *Cold Spring Harb. Perspect. Biol.* **2,** 1–16 (2010).
2. Schooley, A., Vollmer, B. & Antonin, W. Building a nuclear envelope at the end of mitosis : coordinating membrane reorganization , nuclear pore complex assembly , and chromatin de-condensation. 539–554 (2012). doi:10.1007/s00412-012-0388-3
3. Hetzer, M. W., Walther, T. C. & Mattaj, I. W. PUSHING THE ENVELOPE: Structure, Function, and Dynamics of the Nuclear Periphery. *Annu. Rev. Cell Dev. Biol.* **21,** 347–380 (2005).
4. D'Angelo, M. a. & Hetzer, M. W. Structure, dynamics and function of nuclear pore complexes. *Trends Cell Biol* **18,** 456–466 (2008).
5. Terry LJ Wente SR, S. E. B. Crossing the nuclear envelope: Hierarchical regulation of nucleocytoplasmic transport. *Science (80-.).* **318,** 1412–1416 (2007).
6. Wilhelmsen, K., Ketema, M., Truong, H. & Sonnenberg, A. KASH-domain proteins in nuclear migration, anchorage and other processes. *J. Cell Sci.* **119,** 5021 LP-5029 (2006).
7. Akhtar, A. & Gasser, S. M. The nuclear envelope and transcriptional control. *Nat. Rev. Genet.* **8,** 507–517 (2007).
8. Dorner, D., Gotzmann, J. & Foisner, R. Nucleoplasmic lamins and their interaction partners, LAP2α, Rb, and BAF, in transcriptional regulation. *FEBS J.* **274,** 1362–1373 (2007).
9. Schirmer, E. C. & Foisner, R. Proteins that associate with lamins: Many faces, many functions. *Exp. Cell Res.* **313,** 2167–2179 (2007).
10. Starr, D. A. ANChors away: an actin based mechanism of nuclear positioning. *J. Cell Sci.* **116,** 211–216 (2003).
11. Gruenbaum Y, Wilson KL, Harel A, Goldberg M, C. M. Review: nuclear lamins–structural proteins with fundamental functions. *J Struct Biol* **129,** 313–323 (2000).
12. Gruenbaum Y Goldman RD, Shumaker DK, Wilson KL, M. A. The nuclear lamina comes of age. *Nat Rev Mol Cell Biol* **6,** 21–31 (2005).
13. Reddy, K. L., Zullo, J. M., Bertolino, E. & Singh, H. Transcriptional repression mediated by repositioning of genes to the nuclear lamina. *Nature* **452,** 243–247 (2008).
14. Wilson, K. L. & Berk, M. The nuclear envelope at a glance. (2010). doi:10.1242/jcs.019042

15. Wong, X., Luperchio, T. R. & Reddy, K. L. NET gains and losses: the role of changing nuclear envelope proteomes in genome regulation This review comes from a themed issue on Cell nucleus. *Curr. Opin. Chem. Biol.* **28,** 105–120 (2014).
16. Schirmer, E. C., Florens, L., Guan, T., Yates, J. R. & Gerace, L. Nuclear membrane proteins with potential disease links found by subtractive proteomics. *Science* **301,** 1380–2 (2003).
17. Chen, I.-H., Huber, M., Guan, T., Bubeck, A. & Gerace, L. Nuclear envelope transmembrane proteins (NETs) that are up-regulated during myogenesis. *BMC Cell Biol.* **7,** 38 (2006).
18. Gomes, E. R., Jani, S. & Gundersen, G. G. Nuclear movement regulated by Cdc42, MRCK, myosin, and actin flow establishes MTOC polarization in migrating cells. *Cell* **121,** 451–63 (2005).
19. Pan, D. *et al.* The integral inner nuclear membrane protein MAN1 physically interacts with the R-Smad proteins to repress signaling by the transforming growth factor-{beta} superfamily of cytokines. *J. Biol. Chem.* **280,** 15992–6001 (2005).
20. Cohen, T. V., Kosti, O. & Stewart, C. L. The nuclear envelope protein MAN1 regulates TGF signaling and vasculogenesis in the embryonic yolk sac. *Development* **134,** 1385–1395 (2007).
21. Liu, G.-H. *et al.* Regulation of Myoblast Differentiation by the Nuclear Envelope Protein NET39. *Mol. Cell. Biol.* **29,** 5800–5812 (2009).
22. Datta, K., Guan, T. & Gerace, L. NET37, a nuclear envelope transmembrane protein with glycosidase homology, is involved in myoblast differentiation. *J. Biol. Chem.* **284,** 29666–76 (2009).
23. Shumaker, D. K. *et al.* The highly conserved nuclear lamin Ig-fold binds to PCNA: its role in DNA replication. *J. Cell Biol.* **181,** 269–80 (2008).
24. Janin, A., Bauer, D., Ratti, F., Millat, G. & Méjat, A. Nuclear envelopathies : a complex LINC between nuclear envelope and pathology. 1–16 (2017). doi:10.1186/s13023-017-0698-x
25. Worman, H. J. & Bonne, G. 'Laminopathies': A wide spectrum of human diseases. *Exp. Cell Res.* **313,** 2121–2133 (2007).
26. Scaffidi, P. & Misteli, T. Lamin A-dependent misregulation of adult stem cells associated with accelerated ageing. *Nat. Cell Biol.* **10,** 452–9 (2008).
27. Herrada, I. *et al.* Purification and Structural Analysis of LEM-Domain Proteins. *Methods Enzymol.* **569,** 43–61 (2016).

28. Wagner, N. & Krohne, G. LEM-Domain Proteins: New Insights into Lamin-Interacting Proteins. *Int. Rev. Cytol.* **261,** 1–46 (2007).
29. Lee K., K. . W. All in the family: evidence for four new LEM-domain proteins Lem2 (NET-25), Lem3, Lem4 and Lem5 in the human genome. *Oxford, UK BIOS Sci. Publ. LTD* (2004).
30. Wilson, K. L. & Dawson, S. C. Evolution: functional evolution of nuclear structure. *J. Cell Biol.* **195,** 171–81 (2011).
31. Lee, K. K., Gruenbaum, Y., Spann, P., Liu, J. & Wilson, K. L. C. elegans nuclear envelope proteins emerin, MAN1, lamin, and nucleoporins reveal unique timing of nuclear envelope breakdown during mitosis. *Mol. Biol. Cell* **11,** 3089–99 (2000).
32. Berger, R. *et al.* The characterization and localization of the mouse thymopoietin/lamina-associated polypeptide 2 gene and its alternatively spliced products. *Genome Res.* **6,** 361–70 (1996).
33. Herrada, I. *et al.* Purification and Structural Analysis of LEM-Domain Proteins. in 43–61 (2016). doi:10.1016/bs.mie.2015.07.008
34. Cai, M. *et al.* Solution structure of the constant region of nuclear envelope protein LAP2 reveals two LEM-domain structures: One binds BAF and the other binds DNA. *EMBO J.* **20,** 4399–4407 (2001).
35. Mansharamani, M. & Wilson, K. L. Direct binding of nuclear membrane protein MAN1 to emerin in vitro and two modes of binding to barrier-to-autointegration factor. *J. Biol. Chem.* **280,** 13863–70 (2005).
36. Lee, K. K. *et al.* Distinct functional domains in emerin bind lamin A and DNA-bridging protein BAF. *J. Cell Sci.* **114,** 4567–4573 (2001).
37. Brachner, A. *et al.* The endonuclease Ankle1 requires its LEM and GIY-YIG motifs for DNA cleavage in vivo. *J. Cell Sci.* **125,** 1048–57 (2012).
38. Cai, M. *et al.* Solution NMR structure of the barrier-to-autointegration factor-emerin complex. *J. Biol. Chem.* **282,** 14525–14535 (2007).
39. Wolff, N. *et al.* Structural analysis of emerin, an inner nuclear membrane protein mutated in X-linked Emery-Dreifuss muscular dystrophy. *FEBS Lett.* **501,** 171–6 (2001).
40. Bradley, C. M., Ronning, D. R., Ghirlando, R., Craigie, R. & Dyda, F. Structural basis for DNA bridging by barrier-to-autointegration factor. *Nat. Struct. Mol. Biol.* **12,** 935–936 (2005).

41. Wilson, K. L. & Berk, J. M. The nuclear envelope at a glance. *J. Cell Sci.* **123,** 1973–1978 (2010).
42. Snyers, L. *et al.* Lamina-associated polypeptide 2-alpha forms homo-trimers via its C terminus, and oligomerization is unaffected by a disease-causing mutation. *J. Biol. Chem.* **282,** 6308–15 (2007).
43. Gotic, I. & Foisner, R. Multiple novel functions of lamina associated polypeptide 2α in striated muscle. *Nucleus* **1,** 397–401 (2010).
44. Dechat, T., Gesson, K. & Foisner, R. Lamina-independent lamins in the nuclear interior serve important functions. *Cold Spring Harb. Symp. Quant. Biol.* **75,** 533–43 (2010).
45. Mans, B., Anantharaman, V., Aravind, L. & Koonin, E. Comparative genomics, evolution and origins of the nuclear envelope and nuclear pore complex. *Cell Cycle* **3,** 1612–1637 (2004).
46. Lusk, C. P., Blobel, G. & King, M. C. Highway to the inner nuclear membrane: rules for the road. *Nat. Rev. Mol. Cell Biol.* **8,** 414–420 (2007).
47. Grund, S. E. *et al.* The inner nuclear membrane protein Src1 associates with subtelomeric genes and alters their regulated gene expression. *J. Cell Biol.* **182,** 897–910 (2008).
48. Gonzalez, Y., Saito, A. & Sazer, S. Fission yeast Lem2 and Man1 perform fundamental functions of the animal cell nuclear lamina. *Nucleus* **3,** 60–76 (2012).
49. Steglich, B., Filion, G. J., van Steensel, B. & Ekwall, K. The inner nuclear membrane proteins Man1 and Ima1 link to two different types of chromatin at the nuclear periphery in S. pombe. *Nucleus* **3,** 77–87
50. Boone, P. M. *et al.* Hutterite-type cataract maps to chromosome 6p21.32-p21.31, cosegregates with a homozygous mutation in LEMD2, and is associated with sudden cardiac death. *Mol. Genet. genomic Med.* **4,** 77–94 (2016).
51. Hellemans, J. *et al.* Loss-of-function mutations in LEMD3 result in osteopoikilosis, Buschke-Ollendorff syndrome and melorheostosis. *Nat. Genet.* **36,** 1213–1218 (2004).
52. Orpha.net. Available at: www.orpha.net. (Accessed: 24th May 2018)
53. Yamamoto, S. *et al.* A drosophila genetic resource of mutants to study mechanisms underlying human genetic diseases. *Cell* **159,** 200–214 (2014).
54. Bione, S. *et al.* Identification of a novel X-linked gene responsible for Emery-Dreifuss muscular dystrophy. *Nat. Genet.* **8,** 323–7 (1994).
55. Herrada, I. *et al.* Muscular Dystrophy Mutations Impair the Nuclear Envelope Emerin

Self-assembly Properties. *ACS Chem. Biol.* **10,** 2733–2742 (2015).

56. Sakaki, M. *et al.* Interaction between emerin and nuclear lamins. *J. Biochem.* **129,** 321–7 (2001).
57. Jason M. Berk Clifton R. Jenkins-Houk, Jason W. Westerbeck, Line M. Grønning-Wang, Cathrine R. Carlson, and Katherine L. Wilson, D. N. S. The molecular basis of emerin–emerin and emerin–BAF interactions. *J. Cell Sci.* **127,** 3956–3969 (2014).
58. Samson, C. *et al.* Emerin self-assembly mechanism: role of the LEM domain. *FEBS J.* **284,** 338–352 (2017).
59. Cartegni, L. *et al.* Heart-specific localization of emerin: new insights into Emery–Dreifuss muscular dystrophy. *Hum. Mol. Genet.* **6,** 2257–2264 (1997).
60. Östlund, C., Ellenberg, J., Hallberg, E., Lippincott-Schwartz, J. & Worman, H. J. Intracellular trafficking of emerin, the Emery-Dreifuss muscular dystrophy protein. *J. Cell Sci.* **112 (Pt 1,** 1709–19 (1999).
61. Soullam, B. & Worman, H. J. Signals and structural features involved in integral membrane protein targeting to the inner nuclear membrane. *J. Cell Biol.* **130,** 15–27 (1995).
62. Ellenberg, J. *et al.* Nuclear membrane dynamics and reassembly in living cells: targeting of an inner nuclear membrane protein in interphase and mitosis. *J. Cell Biol.* **138,** 1193–206 (1997).
63. Ellis, J. A., Craxton, M., Yates, J. R. & Kendrick-Jones, J. Aberrant intracellular targeting and cell cycle-dependent phosphorylation of emerin contribute to the Emery-Dreifuss muscular dystrophy phenotype. *J. Cell Sci.* **111 (Pt 6,** 781–792 (1998).
64. Schuldiner, M. *et al.* The GET complex mediates insertion of tail-anchored proteins into the ER membrane. *Cell* **134,** 634–45 (2008).
65. Holaska, J. M., Wilson, K. L. & Mansharamani, M. The nuclear envelope, lamins and nuclear assembly. *Curr. Opin. Cell Biol.* **14,** 357–64 (2002).
66. Östlund, C., Sullivan, T., Stewart, C. L. & Worman, H. J. Dependence of Diffusional Mobility of Integral Inner Nuclear Membrane Proteins on A-Type Lamins †. *Biochemistry* **45,** 1374–1382 (2006).
67. Sullivan T, Escalente-Alcalde D, Bhatt H, Anver M, Naryan B, Nagashima K, Stewart CL, B. B. Loss of A-type lamin expression compromises nuclear envelope integrity leading to muscular dystrophy. *J. Cell Biol.* **147,** 913–920 (1999).
68. Berk, J. M., Tifft, K. E. and Wilson, K. L. The nuclear envelope LEMdomain protein emerin. *Nucleus* **4,** 298–314 (2013).

69. Le, H. Q. *et al.* Mechanical regulation of transcription controls Polycomb-mediated gene silencing during lineage commitment. *Nat. Cell Biol.* **18,** 864–875 (2016).
70. Berk Tifft, K. E. and Wilson, K. L, J. M. The nuclear envelope LEMdomain protein emerin. *Nucleus* **4,** 298–314 (2013).
71. Dabauvalle, M.-C. *et al.* Distribution of emerin during the cell cycle. *Eur. J. Cell Biol.* **78,** 749–756 (1999).
72. Fincham, J. R. S. Centromere. *Encycl. Genet.* 320–323 (2001). doi:10.1006/RWGN.2001.0179
73. Holaska, J. M., Kowalski, A. K. & Wilson, K. L. Emerin caps the pointed end of actin filaments: Evidence for an actin cortical network at the nuclear inner membrane. *PLoS Biol.* **2,** (2004).
74. Wilkinson, F. L. *et al.* Emerin interacts in vitro with the splicing-associated factor, YT521-B. *Eur. J. Biochem.* **270,** 2459–66 (2003).
75. Holaska, J. M., Lee, K. K., Kowalski, A. K. & Wilson, K. L. Transcriptional repressor germ cell-less (GCL) and barrier to autointegration factor (BAF) compete for binding to emerin in vitro. *J. Biol. Chem.* **278,** 6969–75 (2003).
76. Chang, W., Folker, E. S., Worman, H. J. & Gundersen, G. G. Emerin organizes actin flow for nuclear movement and centrosome orientation in migrating fibroblasts. *Mol. Biol. Cell* **24,** 3869–80 (2013).
77. Obrdlik, A. *et al.* Nuclear myosin 1 is in complex with mature rRNA transcripts and associates with the nuclear pore basket. *FASEB J.* **24,** 146–157 (2010).
78. Lambert, M. W. Nuclear alpha spectrin: Critical roles in DNA interstrand cross-link repair and genomic stability. *Exp. Biol. Med. (Maywood).* **241,** 1621–38 (2016).
79. Graham, D. M. & Burridge, K. Mechanotransduction and nuclear function. *Curr. Opin. Cell Biol.* **40,** 98–105 (2016).
80. Lombardi, M. L. & Lammerding, J. Keeping the LINC: the importance of nucleocytoskeletal coupling in intracellular force transmission and cellular function. *Biochem. Soc. Trans.* **39,** 1729–34 (2011).
81. Christophe Guilluy, Lukas D. Osborne, Laurianne Van Landeghem, L. S. & Richard Superfine, Rafael Garcia-Mata, and K. B. Isolated nuclei adapt to force and reveal a mechanotransduction pathway within the nucleus. *Nat Cell Biol* **16,** 376–381 (2014).
82. Lammerding, J. *et al.* Abnormal nuclear shape and impaired mechanotransduction in emerin-deficient cells. *J. Cell Biol.* **170,** 781–791 (2005).
83. Rowat, A. C., Lammerding, J. & Ipsen, J. H. Mechanical Properties of the Cell

Nucleus and the Effect of Emerin Deficiency. *Biophys. J.* **91,** 4649–4664 (2006).

84. Cen, B. *et al.* Megakaryoblastic leukemia 1, a potent transcriptional coactivator for serum response factor (SRF), is required for serum induction of SRF target genes. *Mol. Cell. Biol.* **23,** 6597–608 (2003).
85. Ho, C. Y., Jaalouk, D. E., Vartiainen, M. K. & Lammerding, J. Lamin A/C and emerin regulate MKL1-SRF activity by modulating actin dynamics. *Nature* **497,** 507–11 (2013).
86. Haraguchi, T. *et al.* Live fluorescence imaging reveals early recruitment of emerin, LBR, RanBP2, and Nup153 to reforming functional nuclear envelopes. *J. Cell Sci.* **113,** 779 LP-794 (2000).
87. Salpingidou, G., Smertenko, A., Hausmanowa-Petrucewicz, I., Hussey, P. J. & Hutchison, C. J. A novel role for the nuclear membrane protein emerin in association of the centrosome to the outer nuclear membrane. *J. Cell Biol.* **178,** 897–904 (2007).
88. Guelen, L. *et al.* Domain organization of human chromosomes revealed by mapping of nuclear lamina interactions. *Nature* **453,** 948–951 (2008).
89. Demmerle, J., Koch, A. J. & Holaska, J. M. The nuclear envelope protein emerin binds directly to histone deacetylase 3 (HDAC3) and activates HDAC3 activity. *J. Biol. Chem.* **287,** 22080–22088 (2012).
90. Somech, R. *et al.* The nuclear-envelope protein and transcriptional repressor LAP2beta interacts with HDAC3 at the nuclear periphery, and induces histone H4 deacetylation. *J. Cell Sci.* **118,** 4017–25 (2005).
91. Nili, E. *et al.* Nuclear membrane protein LAP2beta mediates transcriptional repression alone and together with its binding partner GCL (germ-cell-less). *J. Cell Sci.* **114,** 3297–3307 (2001).
92. Haraguchi, T. *et al.* Emerin binding to Btf, a death-promoting transcriptional repressor, is disrupted by a missense mutation that causes Emery-Dreifuss muscular dystrophy. *Eur. J. Biochem.* **271,** 1035–1045 (2004).
93. Holaska, J. M., Rais-Bahrami, S. & Wilson, K. L. Lmo7 is an emerin-binding protein that regulates the transcription of emerin and many other muscle-relevant genes. *Hum. Mol. Genet.* **15,** 3459–3472 (2006).
94. Markiewicz, E. *et al.* The inner nuclear membrane protein Emerin regulates β-catenin activity by restricting its accumulation in the nucleus. *EMBO J.* **25,** 3275–3285 (2006).
95. Lickert, H. *et al.* Formation of multiple hearts in mice following deletion of β-catenin in the embryonic endoderm. *Dev. Cell* **3,** 171–181 (2002).

96. Chen, X. *et al.* The -Catenin/T-Cell Factor/Lymphocyte Enhancer Factor Signaling Pathway Is Required for Normal and Stress-Induced Cardiac Hypertrophy. *Mol. Cell. Biol.* **26,** 4462–4473 (2006).
97. Stubenvoll, A., Rice, M., Wietelmann, A., Wheeler, M. & Braun, T. Attenuation of wnt/β-catenin activity reverses enhanced generation of cardiomyocytes and cardiac defects caused by the loss of emerin. *Hum. Mol. Genet.* **24,** 802–813 (2015).
98. Wheeler, M. A., Warley, A., Roberts, R. G., Ehler, E. & Ellis, J. A. Identification of an emerin-βcatenin complex in the heart important for intercalated disc architecture and β-catenin localisation. *Cell. Mol. Life Sci.* **67,** 781–796 (2010).
99. Ishimura, A. Man1, an inner nuclear membrane protein, regulates vascular remodeling by modulating transforming growth factor signaling. *Development* **133,** 3919–3928 (2006).
100. Margalit, A., Brachner, A., Gotzmann, J., Foisner, R. & Gruenbaum, Y. Barrier-to-autointegration factor - a BAFfling little protein. *Trends Cell Biol.* **17,** 202–208 (2007).
101. Montes de Oca, R., Shoemaker, C. J., Gucek, M., Cole, R. N. & Wilson, K. L. Barrier-to-autointegration factor proteome reveals chromatin-regulatory partners. *PLoS One* **4,** (2009).
102. Montes de Oca, R., Shoemaker, C. J., Gucek, M., Cole, R. N. & Wilson, K. L. Barrier-to-autointegration factor proteome reveals chromatin-regulatory partners. *PLoS One* **4,** e7050 (2009).
103. Wang, X. *et al.* Barrier to Autointegration Factor Interacts with the Cone-Rod Homeobox and Represses Its Transactivation Function. *J. Biol. Chem.* **277,** 43288–43300 (2002).
104. Nichols, R. J., Wiebe, M. S. & Traktman, P. The vaccinia-related kinases phosphorylate the N' terminus of BAF, regulating its interaction with DNA and its retention in the nucleus. *Mol. Biol. Cell* **17,** 2451–64 (2006).
105. Haraguchi, T. *et al.* BAF is required for emerin assembly into the reforming nuclear envelope. *J. Cell Sci.* **114,** 4575–4585 (2001).
106. Segura-Totten, M., Kowalski, A. K., Craigie, R. & Wilson, K. L. Barrier-to-autointegration factor: major roles in chromatin decondensation and nuclear assembly. *J. Cell Biol.* **158,** 475–85 (2002).
107. Hirano, Y., Segawa, M., Ouchi, F.S., Yamakawa, Y., Furukawa, K., T. & K., and Horigome, T. Dissociation of emerin from barrier-to-autointegration factor is regulated

through mitotic phosphorylation of emerin in a xenopus egg cell-free system. *J. Biol. Chem* **280,** 39925–39933 (2005).

108. Bengtsson, L. & Wilson, K. L. Barrier-to-autointegration factor phosphorylation on Ser-4 regulates emerin binding to lamin A in vitro and emerin localization in vivo. *Mol. Biol. Cell* **17,** 1154–63 (2006).
109. Cabanillas, R. *et al.* Néstor-Guillermo progeria syndrome: A novel premature aging condition with early onset and chronic development caused by BANF1 mutations. *Am. J. Med. Genet. Part A* **155,** 2617–2625 (2011).
110. Puente, X. S. *et al.* Exome sequencing and functional analysis identifies BANF1 mutation as the cause of a hereditary progeroid syndrome. *Am. J. Hum. Genet.* **88,** 650–6 (2011).
111. Holaska, J. M. & Wilson, K. L. An emerin "proteome": purification of distinct emerin-containing complexes from HeLa cells suggests molecular basis for diverse roles including gene regulation, mRNA splicing, signaling, mechanosensing, and nuclear architecture. *Biochemistry* **46,** 8897–908 (2007).
112. Lu, C. *et al.* Cell apoptosis: requirement of H2AX in DNA ladder formation, but not for the activation of caspase-3. *Mol. Cell* **23,** 121–32 (2006).
113. Manju, K., Muralikrishna, B. & Parnaik, V. K. Expression of disease-causing lamin A mutants impairs the formation of DNA repair foci. *J. Cell Sci.* **119,** 2704–2714 (2006).
114. Jacque, J.-M. & Stevenson, M. The inner-nuclear-envelope protein emerin regulates HIV-1 infectivity. *Nature* **441,** 641–645 (2006).
115. Melcon, G. *et al.* Loss of emerin at the nuclear envelope disrupts the Rb1/E2F and MyoD pathways during muscle regeneration. *Hum. Mol. Genet.* **15,** 637–651 (2006).
116. Bakay, M. *et al.* Nuclear envelope dystrophies show a transcriptional fingerprint suggesting disruption of Rb–MyoD pathways in muscle regeneration. *Brain* **129,** 996–1013 (2006).
117. Muchir, A., Pavlidis, P., Bonne, G., Hayashi, Y. K. & Worman, H. J. Activation of MAPK in hearts of EMD null mice: similarities between mouse models of X-linked and autosomal dominant Emery–Dreifuss muscular dystrophy. *Hum. Mol. Genet.* **16,** 1884–1895 (2007).
118. Iyer, A., Koch, A. J. & Holaska, J. M. Expression Profiling of Differentiating Emerin-Null Myogenic Progenitor Identifies Molecular Pathways Implicated in Their Impaired Differentiation. *Cells* **6,** 38 (2017).
119. Roberts, R. C. *et al.* The Emery?Dreifuss muscular dystrophy associated-protein

emerin is phosphorylated on serine 49 by protein kinase A. *FEBS J.* **273,** 4562–4575 (2006).

120. Tifft, K. E., Bradbury, K. a & Wilson, K. L. Tyrosine phosphorylation of nuclear-membrane protein emerin by Src, Abl and other kinases. *J. Cell Sci.* **122,** 3780–90 (2009).
121. Ozcelik, C. *et al.* Conditional mutation of the ErbB2 (HER2) receptor in cardiomyocytes leads to dilated cardiomyopathy. *Proc. Natl. Acad. Sci. U. S. A.* **99,** 8880–5 (2002).
122. Pradhan, R., Ranade, D. & Sengupta, K. Emerin modulates spatial organization of chromosome territories in cells on softer matrices. *Nucleic Acids Res.* **46,** 1–26 (2018).
123. Lattanzi, G. *et al.* Association of emerin with nuclear and cytoplasmic actin is regulated in differentiating myoblasts. *Biochem. Biophys. Res. Commun.* **303,** 764–70 (2003).
124. Ellis, J. A., Craxton, M., Yates, J. R. and Kendrick-Jones, J. Aberrant intracellular targeting and cell cycle-dependent phosphorylation of emerin contribute to the Emery-Dreifuss muscular dystrophy phenotype. *J. Cell Sci* **111,** 781–792 (1998).
125. Yang, X. & Qian, K. Protein O-GlcNAcylation: emerging mechanisms and functions. *Nat. Rev. Mol. Cell Biol.* **18,** 452–465 (2017).
126. Berk, J. M. *et al.* O-Linked β-N-acetylglucosamine (O-GlcNAc) regulates emerin binding to barrier to autointegration factor (BAF) in a chromatin- and lamin B-enriched "niche". *J. Biol. Chem.* **288,** 30192–209 (2013).
127. Morris, G. E. & Manilal, S. Heart to heart: From nuclear proteins to Emery-Dreifuss muscular dystrophy. *Hum. Mol. Genet.* **8,** 1847–1851 (1999).
128. Hopkins, L. & Warren, S. Emery-Dreifuss muscular dystrophy. in *Handbook of Clinical Neurology: Myopathies* (eds. Rowland, L. & DiMauro, D.) 145–160 (Elsevier Science, 1992).
129. Norwood, F. L. M. *et al.* Prevalence of genetic muscle disease in Northern England: in-depth analysis of a muscle clinic population. *Brain* **132,** 3175–86 (2009).
130. Khadilkar, S. V., Yadav, R. S. & Patel, B. A. Emery–Dreifuss Muscular Dystrophy. in *Neuromuscular Disorders* 183–187 (Springer Singapore, 2018). doi:10.1007/978-981-10-5361-0_16
131. Cestan R, L. Une myopathie avec retractions familiales. *Nouv. Iconogr. Salpetriere* **15,** 38–52 (1902).
132. Schnek, P. & Mathias, E. Zur Kasuistik der Dystrophia musculorum progressiva

retrahens. *Klin Wochenschr* **57,** 557–8 (1920).

133. Dreifuss, F. E. & Hogan, G. R. Survival in X-chromosomal muscular dystrophy. *Neurology* **11,** 734 LP-734 (1961).
134. Emery, a E. & Dreifuss, F. E. Unusual type of benign x-linked muscular dystrophy. *J. Neurol. Neurosurg. Psychiatry* **29,** 338–342 (1966).
135. Hunter, T. & Eckhart, W. The Discovery of Tyrosine Phosphorylation: It's All in the Buffer! Commentary. *Cell* **116,** 35–39 (2004).
136. Waters, D. D., Nutter, D. O., Hopkins, L. C. & Dorney, E. R. Cardiac Features of an Unusual X-Linked Humeroperoneal Neuromuscular Disease. *N. Engl. J. Med.* **293,** 1017–1022 (1975).
137. Rowland, L. *et al.* Emery-dreifuss muscular dystrophy. *Ann. Neurol.* **5,** 111–117 (1979).
138. Emery, A. E. H. Syndrome of the month Emery-Dreifuss syndrome. *J. Med. Genet.* **26,** 637–641 (1989).
139. Straub, V. & Campbell, K. P. Muscular dystrophies and the dystrophin-glycoprotein complex. *Curr. Opin. Neurol.* **10,** 168–75 (1997).
140. Nagano, A. *et al.* Emerin deficiency at the nuclear membrane in patients with Emery-Dreif uss muscular dystrophy. *Nat. Genet.* **12,** 254–259 (1996).
141. Manilal, S., Nguyen, T. M., Sewry, C. A. & Morris, G. E. The Emery-Dreifuss muscular dystrophy protein, emerin, is a nuclear membrane protein. *Hum. Mol. Genet.* **5,** 801–8 (1996).
142. Bonne, G. *et al.* Mutations in the gene encoding lamin A/C cause autosomal dominant Emery-Dreifuss muscular dystrophy. *Nat. Genet.* **21,** 285–288 (1999).
143. Mora, M. *et al.* X-linked Emery-Dreifuss muscular dystrophy can be diagnosed from skin biopsy or blood sample. *Ann. Neurol.* **42,** 249–253 (1997).
144. Fairley, E. A., Kendrick-Jones, J. & Ellis, J. A. The Emery-Dreifuss muscular dystrophy phenotype arises from aberrant targeting and binding of emerin at the inner nuclear membrane. *J. Cell Sci.* **112 (Pt 15),** 2571–82 (1999).
145. Rudenskaia, G. E. *et al.* [Clinical, genealogical and molecular genetic study of Emery-Dreifuss muscular dystrophy]. *Zhurnal Nevrol. i psikhiatrii Im. S.S. Korsakova* **106,** 58–65 (2006).
146. Yates, J. R. W. *et al.* Genotype-phenotype analysis in X-linked Emery-Dreifuss muscular dystrophy and identification of a missense mutation associated with a milder

phenotype. *Neuromuscul. Disord.* **9,** 159–165 (1999).

147. Funakoshi, M., Tsuchiya, Y. & Arahata, K. Emerin and cardiomyopathy in Emery-Dreifuss muscular dystrophy. *Neuromuscul. Disord.* **9,** 108–14 (1999).
148. Manilal, S. *et al.* Mutations in Emery – Dreifuss muscular dystrophy and their effects on emerin protein expression. **7,** 855–864 (1998).
149. UMD-EMD. Available at: http://www.umd.be/EMD/.
150. Yaou, R. Ben, Gerard, M., Chami, K., Sehier, A. & Belin, A. A new EMD gene missense mutation in exon 1 leads to absence of emerin and is responsible for X-linked dilated cardiomyopathy with conduction defects and arrhythmias and almost elusive skeletal muscle features. in *Neuromuscular Disorders 24* 843–844 (2014).
151. KARST, M. L., HERRON, K. J. & OLSON, T. M. X-Linked Nonsyndromic Sinus Node Dysfunction and Atrial Fibrillation Caused by Emerin Mutation. *J. Cardiovasc. Electrophysiol.* **19,** 510–515 (2008).
152. Yaou, R. Ben *et al.* Multitissular involvement in a family with LMNA and EMD mutations: Role of digenic mechanism? *Neurology* **68,** 1883–1894 (2007).
153. Ben Yaou, R. *et al.* G.P.142. *Neuromuscul. Disord.* **24,** 843–844 (2014).
154. Gisèle Bonne and Rabah Ben Yaou, F. L. Emery-Dreifuss Muscular Dystrophy. *GeneReviews* (2015).
155. Ray E Hershberger and Ana Morales. LMNA-Related Dilated Cardiomyopathy. *GeneReviews* (2008).
156. Manuscript, A. & Dysfunction, E. NIH Public Access. **25,** 713–724 (2015).
157. Brown, C. a *et al.* Novel and recurrent EMD mutations in patients with Emery-Dreifuss muscular dystrophy, identify exon 2 as a mutation hot spot. *J. Hum. Genet.* **56,** 589–94 (2011).
158. Bonne, G. *et al.* Clinical and molecular genetic spectrum of autosomal dominant Emery-Dreifuss muscular dystrophy due to mutations of the lamin A/C gene. *Ann. Neurol.* **48,** 170–80 (2000).
159. Sanna, T. *et al.* Cardiac features of Emery-Dreifuss muscular dystrophy caused by lamin A/C gene mutations. *Eur. Heart J.* **24,** 2227–36 (2003).
160. Mercuri, E. *et al.* Early and severe presentation of autosomal dominant Emery-Dreifuss muscular dystrophy (EMD2). *Neurology* **54,** 1704–5 (2000).
161. ClinicalTrials.gov. Available at: www.clinicaltrials.gov. (Accessed: 3rd June 2018)
162. Pillers, D.-A. M. & Von Bergen, N. H. Emery-Dreifuss muscular dystrophy: a test case for precision medicine. *Appl. Clin. Genet.* **9,** 27–32 (2016).

163. Ozawa, R. *et al.* Emerin-lacking mice show minimal motor and cardiac dysfunctions with nuclear-associated vacuoles. *Am. J. Pathol.* **168,** 907–17 (2006).
164. Melcon, G. *et al.* Loss of emerin at the nuclear envelope disrupts the Rb1/E2F and MyoD pathways during muscle regeneration. *Hum. Mol. Genet.* **15,** 637–651 (2006).
165. Arimura, T. *et al.* Mouse model carrying H222P-Lmna mutation develops muscular dystrophy and dilated cardiomyopathy similar to human striated muscle laminopathies. *Hum. Mol. Genet.* **14,** 155–169 (2005).
166. Mounkes, L. C., Kozlov, S. V., Rottman, J. N. & Stewart, C. L. Expression of an LMNA-N195K variant of A-type lamins results in cardiac conduction defects and death in mice. *Hum. Mol. Genet.* **14,** 2167–2180 (2005).
167. Huber, M. D., Guan, T. & Gerace, L. Overlapping functions of nuclear envelope proteins NET25 (Lem2) and emerin in regulation of extracellular signal-regulated kinase signaling in myoblast differentiation. *Mol. Cell. Biol.* **29,** 5718–28 (2009).
168. Taylor, M. R. G. *et al.* Thymopoietin (lamina-associated polypeptide 2) gene mutation associated with dilated cardiomyopathy. *Hum. Mutat.* **26,** 566–574 (2005).
169. Mamchaoui, K. *et al.* Immortalized pathological human myoblasts: Towards a universal tool for the study of neuromuscular disorders. *Skelet. Muscle* **1,** (2011).
170. Buxboim, A. *et al.* Matrix elasticity regulates lamin-A,C phosphorylation and turnover with feedback to actomyosin. *Curr. Biol.* **24,** 1909–1917 (2014).
171. Manuscript, A. Forcing tumor Progresion. **9,** 108–122 (2009).
172. Khatau, S. B. *et al.* A perinuclear actin cap regulates nuclear shape. *Proc. Natl. Acad. Sci.* **106,** 19017–19022 (2009).
173. Chang, W., Folker, E. S., Worman, H. J. & Gundersen, G. G. Emerin organizes actin flow for nuclear movement and centrosome orientation in migrating fibroblasts. *Mol. Biol. Cell* **24,** 3869–80 (2013).
174. Kim, D.-H., Chambliss, A. B. & Wirtz, D. The multi-faceted role of the actin cap in cellular mechanosensation and mechanotransduction. *Soft Matter* **9,** 5516–5523 (2013).
175. Christophe Guilluy Laurianne Van Landeghem, Lisa Sharek, L. D. O. & Richard Superfine and Keith Burridge, R. G.-M. Isolated nuclei adapt to force and reveal a mechanotransduction pathway within the nucleus. *Nat Cell Biol* **16,** 376–381 (2014).
176. Muchir, A. *et al.* Abnormal p38α mitogen-activated protein kinase signaling in dilated cardiomyopathy caused by lamin A/C gene mutation. *Hum. Mol. Genet.* **21,** 4325–33 (2012).

177. Chatzifrangkeskou, M. *et al.* ERK1/2 directly acts on CTGF/CCN2 expression to mediate myocardial fibrosis in cardiomyopathy caused by mutations in the lamin A/C gene. *Hum. Mol. Genet.* **25,** 2220–2233 (2016).
178. Chatzifrangkeskou, M. *et al.* Cofilin-1 phosphorylation catalyzed by ERK1/2 alters cardiac actin dynamics in dilated cardiomyopathy caused by lamin A/C gene mutation. *Hum. Mol. Genet.* (2018). doi:10.1093/hmg/ddy215
179. Park, Y.-E. *et al.* Nuclear changes in skeletal muscle extend to satellite cells in autosomal dominant Emery-Dreifuss muscular dystrophy/limb-girdle muscular dystrophy 1B. *Neuromuscul. Disord.* **19,** 29–36 (2009).
180. Park, Y.-E. *et al.* Autophagic degradation of nuclear components in mammalian cells. *Autophagy* **5,** 795–804 (2009).
181. Deroyer, C., R??nert, A. F., Merville, M. P. & Fillet, M. New role for EMD (emerin), a key inner nuclear membrane protein, as an enhancer of autophagosome formation in the C16-ceramide autophagy pathway. *Autophagy* **10,** 1229–1240 (2014).
182. Nishida, K., Kyoi, S., Yamaguchi, O., Sadoshima, J. & Otsu, K. The role of autophagy in the heart. *Cell Death Differ.* **16,** 31–38 (2009).
183. Krauss, S. W. *et al.* Downregulation of protein 4.1R, a mature centriole protein, disrupts centrosomes, alters cell cycle progression, and perturbs mitotic spindles and anaphase. *Mol. Cell. Biol.* **28,** 2283–94 (2008).
184. Meyer, A. J., Almendrala, D. K., Go, M. M. & Krauss, S. W. Structural protein 4.1R is integrally involved in nuclear envelope protein localization, centrosome-nucleus association and transcriptional signaling. *J. Cell Sci.* **124,** 1433–1444 (2011).
185. Stagg, M. A. *et al.* Cytoskeletal Protein 4.1R Affects Repolarization and Regulates Calcium Handling in the Heart. *Circ. Res.* **103,** 855–863 (2008).
186. Meyer, A. J., Almendrala, D. K., Go, M. M. & Krauss, S. W. Structural protein 4.1R is integrally involved in nuclear envelope protein localization, centrosome-nucleus association and transcriptional signaling. *J. Cell Sci.* **124,** 1433–44 (2011).
187. Kayman-Kurekci, G. *et al.* Mutation in TOR1AIP1 encoding LAP1B in a form of muscular dystrophy: A novel gene related to nuclear envelopathies. *Neuromuscul. Disord.* **24,** 624–633 (2014).
188. Shin, J.-Y. *et al.* Lamina-associated polypeptide-1 interacts with the muscular dystrophy protein emerin and is essential for skeletal muscle maintenance. *Dev. Cell* **26,** 591–603 (2013).
189. Bertrand, A. T., Chikhaoui, K., Yaou, R. Ben & Bonne, G. Clinical and genetic

heterogeneity in laminopathies. *Biochem. Soc. Trans.* **39,** 1687–92 (2011).

190. Worman, H. J. Nuclear lamins and laminopathies. *J. Pathol.* **226,** 316–325 (2012).
191. Tesson, F. *et al.* Lamin A/C mutations in dilated cardiomyopathy. *Cardiol. J.* **21,** 331–342 (2014).
192. Bonne, G. & Yaou, R. Ben. UMD-LMNA. Available at: http://www.umd.be/LMNA/.
193. Archambault, V., Lépine, G. & Kachaner, D. Understanding the Polo Kinase machine. *Oncogene* **34,** 4799–4807 (2015).
194. Wang, G., Jiang, Q. & Zhang, C. The role of mitotic kinases in coupling the centrosome cycle with the assembly of the mitotic spindle. *J. Cell Sci.* **127,** 4111–4122 (2014).
195. Iyer, A., Koch, A. J. & Holaska, J. M. Expression Profiling of Differentiating Emerin-Null Myogenic Progenitor Identifies Molecular Pathways Implicated in Their Impaired Differentiation. *Cells* **6,** 38 (2017).
196. Izumi-Nakaseko, H. *et al.* Characterization of human iPS cell-derived cardiomyocyte sheets as a model to detect drug-induced conduction disturbance.
197. Chow, Kin-Hoe; Factor, E. Rachel; Ullman, S. K. NIH Public Access. *Nat Rev Cancer* **12,** 196–209 (2012).
198. Koch, A. J. & Holaska, J. M. Emerin in health and disease. *Semin. Cell Dev. Biol.* **29,** 95–106 (2014).
199. Madej-Pilarczyk, A. Clinical aspects of Emery-Dreifuss muscular dystrophy. *Nucleus* **9,** 268–274 (2018).